On the emergence and molecular characteristics of LRR-RLKs and LRR-RLPs in plant immunity

Dissertation

der Mathematisch-Naturwissenschaftlichen Fakultät

der Eberhard Karls Universität Tübingen

zur Erlangung des Grades eines

Doktors der Naturwissenschaften

(Dr. rer. nat.)

vorgelegt von

Philippe Guillaume Chatelain

aus Lausanne (Schweiz)

Tübingen

2017

Gedruckt mit Genehmigung der Mathematisch-Naturwissenschaftlichen Fakultät der Eberhard Karls Universität Tübingen.

Tag der mündlichen Qualifikation:	15.12.2017
Dekan:	Prof. Dr. Wolfgang Rosenstiel
1. Berichterstatter:	Prof. Dr. Georg Felix
2. Berichterstatter:	Prof. Dr. Thorsten Nürnberger

Summary

Plant immunity is commonly mediated by pattern-recognition receptors (PRRs), located at the cell-surface, which can recognise a broad spectrum of pathogen-associated molecular patterns (PAMPs). The main classes of PRRs in *Arabidopsis thaliana* contain leucine-rich repeat (LRR) domains for ligand binding and can be subdivided in receptor-like kinases (LRR-RLKs) and receptor-like proteins (LRR-RLPs). LRR-RLKs consist of a signal peptide, extracellular LRRs, a single transmembrane domain (TMD) and a cytoplasmic Ser/Thr kinase domain. LRR-RLPs have the same architecture, but lack the kinase domain. Instead, they associate constitutively with the LRR-RLK adaptor kinase SOBIR1. In the present work, we identified 24'234 sequences from 51 plant proteomes which relate to either type of LRR-receptors and present an evolutionary perspective on the emergence of LRR-containing PRRs. In a second part, we investigate the molecular differences between LRR-RLKs and LRR-RLPs with respect to their dependence on SOBIR1. Using domain swaps between various LRR-RLKs and LRR-RLPs, we demonstrate how to interconvert these two types of receptors. We show that the interaction with SOBIR1 and the functionality as RLP depends on a "flat" surface in the α-helix of the TMDs of the LRR-RLPs. We also conduct the reverse approach to convert a LRR-RLP into a LRR-RLK by fusing the TMD and kinase domain of SOBIR1 to RLP23 and prove that this chimeric construct behaves like a regular LRR-RLK. The conclusions of the present thesis are of broader interest since they demonstrate functional modularity of receptor domains, a feature that will allow future studies to address complex signalling pathways by dividing the problem in simpler tasks. Further studies should focus on applying the approach to solve the CLV3 perception system, to study non-LRR class of PRRs, to search for co-receptors of so-far uncharacterized receptors or to solve biotechnological problems.

Zusammenfassung

Pflanzenimmunität wird von mustererkennenden Rezeptoren (PRRs) vermittelt, die auf der Zelloberfläche lokalisiert sind und verschiedene "pathogen-associated molecular patterns" (PAMPs) erkennen können. Die Hauptklasse von PRRs in *Arabidopsis thaliana* enthält "leucine-rich repeats" (LRRs) und kann weiter in sogennante "receptor-like kinases" (LRR-RLKs) und "receptor-like proteins" (LRR-RLPs) unterteilt werden. LRR-RLKs bestehen typischerweise aus einem Signalpeptide, extrazellulären LRRs, einer einsträngigen Transmembrandomäne (TMD) und einer zytoplasmatischen Ser/Thr-Kinasedomäne. LRR-RLPs haben die selbe Struktur, jedoch ohne Kinasedomäne. Stattdessen interagieren sie mit der "adaptor kinase" SOBIR1, einer anderen LRR-RLK. In dieser Arbeit haben wir 24'234 Sequenzen von 51 pflanzlichen Proteomen identifiziert und präsentieren eine evolutionäre Perspektive der Entstehung von LRR-RLKs und LRR-RLPs. Im zweiten Teil untersuchen wir die molekularen Unterschiede zwischen diesen beiden Rezeptorentypen. Mit Domänentausch-Experimenten zeigen wir, wie man eine LRR-RLK in eine LRR-RLP (und anders herum) umwandeln kann. Wir zeigen darüber hinaus, dass die Spezifität von LRR-RLPs für SOBIR1 in der TMD durch eine "flache" Struktur der α-Helix der TMD kodiert ist. Zuletzt demonstrieren wir, wie man eine LRR-RLK aus einer LRR-RLP herstellen kann. Dafür vereinigen wir die TMD und Kinasedomäne von SOBIR1 mit RLP23 und zeigen, dass sich diese Chimäre wie eine SOBIR1-unabhängige LRR-RLK verhält. Die Schlussfolgerungen dieser Arbeit sind besonders interessant, weil sie eine Bandbreite von Möglichkeiten aufzeigen, um komplexe Signalwege zu studieren und biotechnologisch zu manipulieren.

Table of contents

1. Introduction 1

1.1 Immunity 1

1.2 Plant immunity 2

1.3 Same same, but different: LRR-RLKs and LRR-RLPs 5

1.4 Ligand perception and signal transduction across the membrane 11

1.5 PTI output 14

1.6 PTI regulation 18

1.7 What can we learn from LRR-RLPs and LRR-RLKs from other pathways? 21

2. Aim of the work 26

3. Materials and methods 27

3.1 Chemicals and solvents 27

3.2 Peptides and elicitors 27

3.3 Bacterial strains 27

3.4 Plant material 27

3.5 Protoplasts isolation and pFRK1::Luc assay 28

3.6 Agrobacterium-mediated transformation of *Nicotiana benthamiana* 28

3.7 Ethylene production 29

3.8 Oxidative burst 29

3.9 Molecular biology 29

3.9.1 PCRs, electrophoresis and DNA sequencing 29

3.9.3 Vectors 30

3.10 Protein biochemistry 30

3.11 Binding assay 31

3.12 Microscopy 31

3.13 Bioinformatics 31

3.13.1 Wet lab related 31

3.13.2 LRR receptor evolution 32

3.13.3 Analysis of TMD momentum and conservation 34

4. Results 35

4.1 Evolution of LRR-PRRs and approach to a better understanding of the SERK family 35

4.2 Molecular differences between LRR-RLKs and LRR-RLPs: converting a RLK into a RLP 42

4.2.1 Truncated EFR still undergoes complex formation with BAK1 but is not functional and does not recruit SOBIR1 42

4.2.2 EFRΔkin containing TMD and C-tail from RLP23 is functional and recruits SOBIR1 44
4.2.3 EFRΔkin containing the TMD alone from RLP23 can recruit SOBIR1 and is functional 48
4.2.4 What can we learn from the CLV3 pathway? 49
4.3 Molecular differences between LRR-RLKs and LRR-RLPs: converting a RLP into a RLK 54
4.4 Analysis of TMD sequences using Shannon's entropy 60
5. Discussion 62
6. Conclusion 76
Acknowledgments 77
References 78
List of figures and tables 93
List of abbreviations 94
Annex 98

The One who was sitting on the throne said,
“Look! I am making everything new!”
Then he said,
“Write this, because these words are true and can be trusted.”

[Book of Relevation 21:5]

1. Introduction

1.1 Immunity

The recognition of non-self and protection against potential damaging infections forms the core concept of immunity. It is present in all living organisms, from Archaea to Eukaryotes, and the innate immune networks of eukaryotes were most likely transmitted from their respective ancestral prokaryotic endosymbionts (Dunin-Horkawicz *et al.*, 2014). Immune responses are composed of three main phases: perception, signaling and output. Several physical barriers, such as cell walls, high hair density, epidermis or mucous membranes, allow animals and plants to prevent physical entry of pathogen. Yet, successful pathogenic organisms can penetrate the body of their hosts, feed and reproduce. Perception of pathogen associated-molecular patterns (PAMPs), such as bacterial flagellin, peptidoglycans, lipoproteins or viral ssRNA, is a key step of the initiation of the innate immunity. PAMPs are typically derived from essential microbial proteins or compounds which are often highly conserved across species (Boller and Felix, 2009), thus allowing hosts to detect a broad range of potential pathogens with a limited number of receptors. The animal toll-like receptors (TLRs) are pattern-recognition receptors (PRRs) that mediate the perception of an array of PAMPs. Together with adaptors and/or co-receptors they can transmit the signal from the extracellular side of the membrane to cytoplasmic signaling cascades. The signaling cascade ultimately leads to transcriptional changes which typically turn on defense-related genes and may lead to resistance to the infection (Nürnberger *et al.*, 2004; Ausubel, 2005).

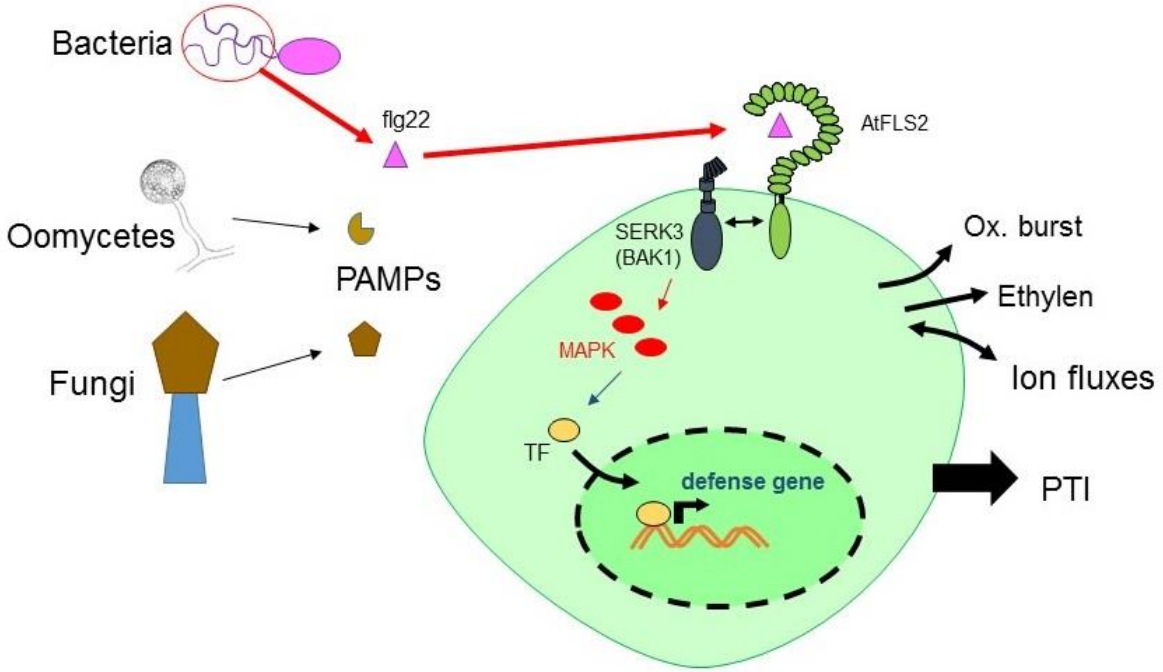

Figure 1.1 Overview of PAMP-triggered immunity (PTI) in plants
Plants can sense presence of microbial pathogens by recognising pathogen-associated molecular patterns (PAMPs) using cell-surface receptors. In *A. thaliana* and many other plants the receptor FLS2 can, for instance, recognise bacterial flagellin or its minimal motif flg22. Upon ligand recognition, FLS2, as many others LRR-RLKs involved in PTI, undergoes complex formation with SERK3. This closer proximity of both kinase moieties induce transphospholyration and activation of cytoplasmic signaling cascades. Ion fluxes, burst of reactive oxygen species (ROS) and ethylene production as well as induction of MAPK cascade are part of the early cell responses. MAPK cascade leads, in a different time frame, to transcriptional changes and allows the induction of defense-related genes and defense responses such as callose deposition or programmed cell-death. All the basal resistances triggered by PAMPs are grouped under the term PAMP-triggered immunity (PTI).

1.2 Plant immunity

Immune systems of animals and plants show many striking parallels and share structurally similar receptors (Bentham *et al.*, 2016; Duxbury *et al.*, 2016; Fliegmann and Felix, 2016; Ranf, 2016) and components in signaling (Clapham, 1995; Meng and Zhang, 2013). Bacterial flagellin, for instance, is recognized even at very low concentrations through different epitopes by the leucine-rich repeats (LRR) PRRs FLS2 and FLS3 in plants and TLR5 in animals (Fliegmann and Felix, 2016). Yet all three receptors seem to have evolved independently (Ausubel, 2005; Caplan *et al.*, 2008). Plants make up their lack of mobility by a

broad biochemical weaponry to resist pathogens. Plant molecular immunity knows a two-layers immune system. The first layer is called PAMP-triggered immunity (PTI) and starts in a similar fashion as in animal immune system with the perception of PAMPs by cell-surface receptors. After PAMP perception, PRRs quickly undergo heterodimer formation which allow signal transduction across the plasma membrane and initiation of the cytoplasmic signaling cascade, including ion fluxes, burst of reactive oxygen species, ethylene production, activation of mitogen-activated protein kinase (MAPK) cascade, callose deposition and transcriptional changes (Boller & Felix, 2009; Fig. 1.1). PTI is often enough for plants to deter non-specific pathogen invasions, but co-evolution brought many pathogens to evolve several distinct mechanisms to avoid PTI initiation, either by shutting it down via bacterial effectors that target specific PTI components, or by changing the epitopes that are usually recognized by PRRs. For instance, AvrPto and AvrPtoB are effectors from *Pseudomonas syringae* which are injected in the cytoplasm of the host via a type III secretion system and which can shut down plant immune responses upstream of the MAPK cascade (Abramovitch *et al.*, 2006; De Torres *et al.*, 2006; He *et al.*, 2007), most likely by targeting BAK1-like kinases (Shan *et al.*, 2008). Effector-triggered immunity (ETI) is then the second layer of immunity in plants, it starts with the recognition of certain effectors or changes in structure/phosphorylation status of NB-LRR (NLR) or R-gene proteins (Jones and Dangl, 2006; Dodds and Rathjen, 2010). RIN4, for instance, is a small protein found at the plasma membrane in association to PRR complexes, is guarded in the plant model organism *Arabidopsis thaliana* by two NLRs, RPM1 and RPS2, which initiate immune responses upon modification of RIN4 by microbial effectors (Khan *et al.*, 2016). The immune response in ETI is usually strong, plant cells undergo programmed cell death and this leads to necrosis around the infection site, the so-called hypersensitive response (HR), thus circumventing future expansion of the pathogen in the plant (Boller and Felix,

2009). Together with PTI, HR and ETI are all local responses to a specific infection site. Systemic acquired resistance (SAR) is usually initiated in parallel of HR and induces resistance also in the non-infected parts of the plant (Alvarez *et al.*, 1998; Meng and Zhang, 2013), also known as the so-called "priming" effect. The arms race being an ongoing process, certain pathogens are able to shut down the ETI and are become therefore virulent again. *Nota bene*, PTI and ETI are terms coined by scientists and are not clearly distinct: one pathogen can be detected by certain receptors which induce PTI and simultaneously can try to shut it down by injecting effectors, resulting in partial (a)virulence, depending on many other factors (e.g. plant hydration status; see Garrett *et al.*, 2006). Immunity triggering is therefore not a black-or-white process, as it has been noted for the Necrosis and ethylene-inducing peptide 1-like proteins (NLPs) which induce leaf necrosis but also contain a 20 amino acids core part which triggers PTI, thus showing that ETI is an extension of PTI *stricto senso* (Böhm *et al.*, 2014).

The current strategy for global food safety in crop production is gene-stacking, not only of R-genes, but PRRs too (Lacombe *et al.*, 2010; Zhu *et al.*, 2012; Schoonbeek *et al.*, 2015). Another approach is to edit crop genomes to silence or knock-out given susceptibility genes (S-genes), which can be used by pathogens to promote their own growth at the detriment of the host’s fitness (Chu *et al.*, 2006; Chen *et al.*, 2010; Zhou *et al.*, 2015; Sun *et al.*, 2016).

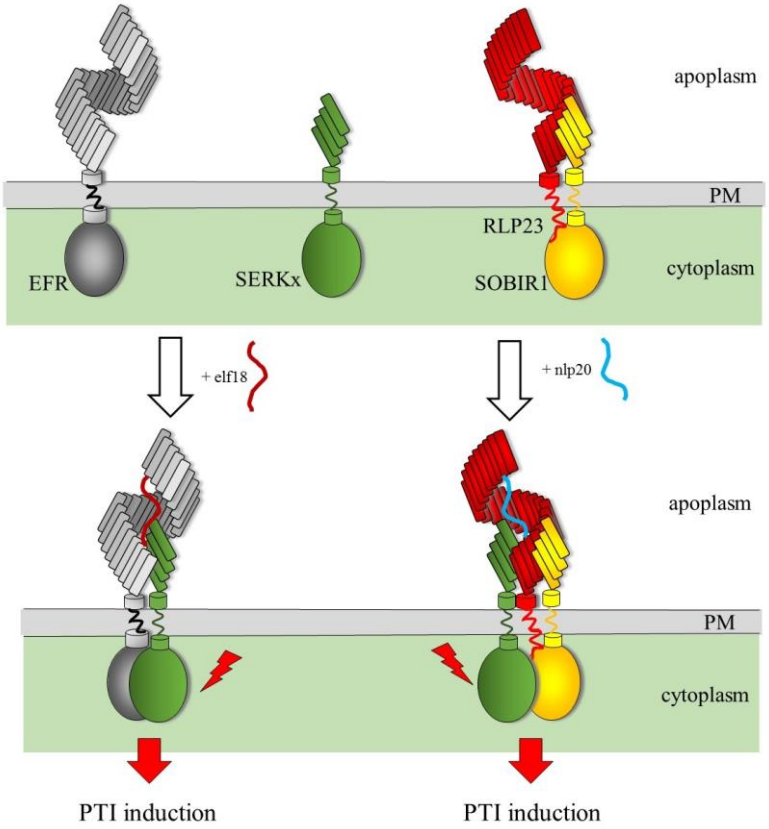

Figure 1.2 LRR-RLKs and LRR-RLPs with SOBIR1 look similar
LRR-RLKs, such as EFR, undergo complex formation with a SERK-type co-receptor upon ligand binding which allow signal transduction across the membrane. LRR-RLPs, such as RLP23, typically interact constitutively with an adaptor kinase, SOBIR1 in this example. Upon ligand binding, a SERK-type co-receptor joins the complex and allows signal transduction across the membrane. Both receptor types look too similar to have independently evolved. The molecular differences as well as the fine tuning of interaction specificity will be studied in the present work

1.3 Same same, but different: LRR-RLKs and LRR-RLPs

PRRs involved in PTI can be classified in two main classes: (i) receptor-like kinases (RLKs), consisting of an extracellular ligand-interacting part, typically a single transmembrane domain and a cytoplasmic Ser/Thr kinase domain, and (ii) receptor-like proteins (RLPs), which have a similar setup but lack a kinase domain (Fig. 1.2). The extracellular domains of either RLKs or RLPs can show different motifs, including LRR-motifs, lysine motifs (LysM), lectin domains or EGF-like domains (Böhm *et al.*, 2014*a*). There are over 600 RLKs in *Arabidopsis thaliana*, of which 233 are proteins containing extracellular LRR motifs (Shiu and Bleecker, 2003). There are also 57 additional LRR-RLPs

identified in *A. thaliana* (Wang *et al.*, 2008). LRR-containing PRRs are, therefore, the major class of plant receptors, which act in various pathways, including growth, organ development or defense (Zhang & Thomma, 2013). The direction of LRR receptor evolution in plants remains, however, an enigma, for certain receptors can recognize endogeneous signals and hormones while others recognize PAMPs. Additionally, there is still no consensus as to which of the RLPs or the RLKs evolved first. Some evolutionary hints have been found for given species or given genes, but there is no comprehensive study of plant LRR as a whole. This issue will be addressed in the first part of this thesis.

Leucine-rich repeats are 20-30 – residues long with a strong conservation of leucine (or isoleucine/valine) in a β-sheet, eventually followed by an α-helix and two free loops connecting both. There exists many LRR subfamilies and the consensus of typical plant LRR is IPxxLxxLxxLxxLxLxxNxL(T/S)Gx, where "x" can be any residues (Jones *et al.*, 1994; Kobe and Kajava, 2001; Mueller *et al.*, 2012*a*). The conserved residues with their side chains build the inner part of the solenoid and form the backbone of the LRR stackings. Crystal structures of LRR ectodomains showed that the stacking of LRRs knows a slight curvature between each repeat, resulting in a typical horse-shoe shape (Fig. 1.3; Kobe and Deisenhofer, 1993; Evdokimov *et al.*, 2001; Kobe and Kajava, 2001; Enkhbayar *et al.*, 2003; Di Matteo *et al.*, 2003; Bella *et al.*, 2008*a*; Hothorn *et al.*, 2011; Sun *et al.*, 2013*b*; Zhang and Thomma, 2013; Sun *et al.*, 2013*a*; Santiago *et al.*, 2013; McAndrew *et al.*, 2014; Tang *et al.*, 2015; Wang *et al.*, 2015). The concave side of the LRRs forms a binding surface, where the side-chains of the amino acid mediate ligand perception (Kobe and Kajava, 2001; Bella *et al.*, 2008; Zhang and Thomma, 2013). The LRRs are capped both at the N- and C-terminals by cysteine-rich motifs, so that the hydrophobic core of the structure is not exposed (Kobe and Kajava, 2001; Di Matteo *et al.*, 2003; Zhang and Thomma, 2013).

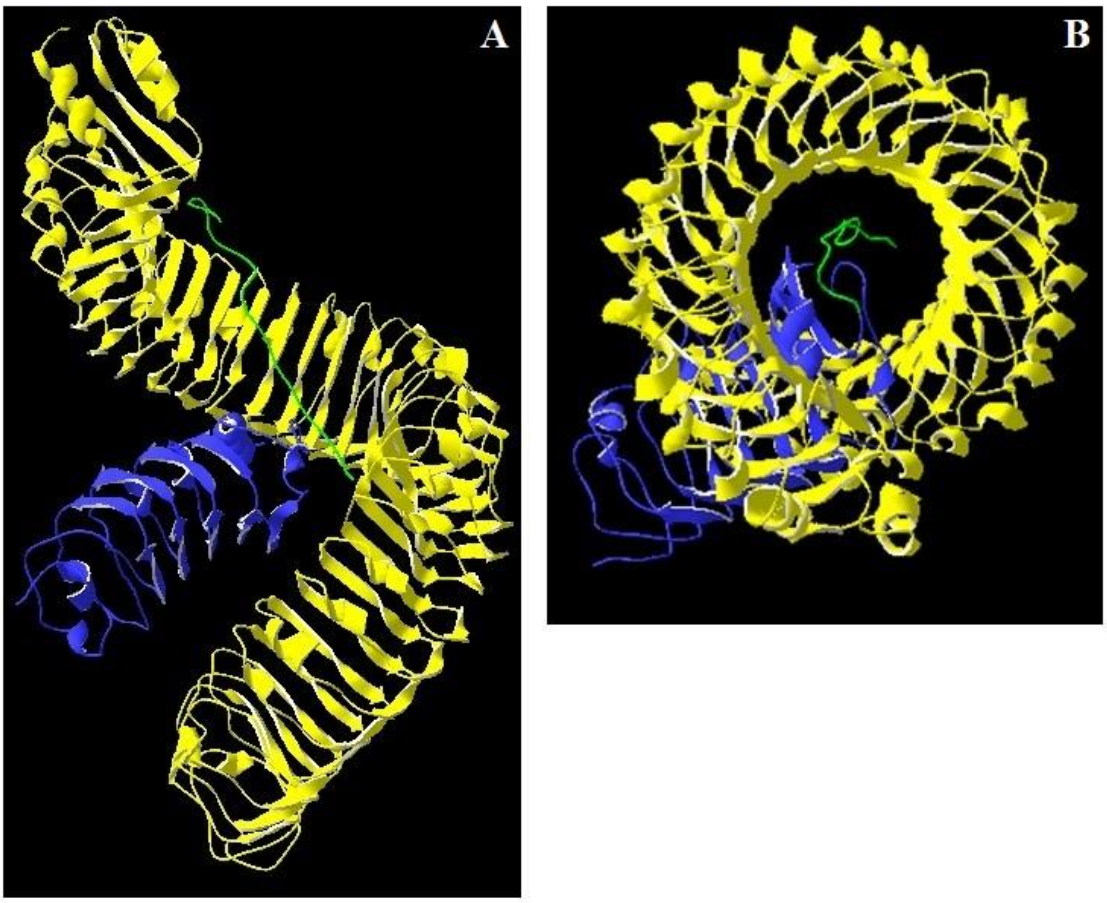

Figure 1.3 Crystal structure of FLS2-SERK3-flg22 complex (data from Sun et al., 2013)
Side (A) and top (B) view of the FLS2-SERK3-flg22 complex. The LRR stacking gives this typical horse-shoe shape (as seen from the top) to the protein, which is highly suitable for protein-protein interaction. Here, FLS2 (in yellow) can recognise flg22 (green). SERK3 (blue) joins the complex and interacts with FLS2 through multiple residues located on the surface of some leucine repeats. SERK3 additionally interacts directly with flg22 through a loose N-terminal loop. Data from Sun *et al.*, 2013; visualisation using the Swiss PDB-Viewer "DeepView" (Guex and Peitsch, 1997).

After ligand perception, both RLPs and RLKs must undergo a multimer complex formation for signal transduction across the plasma membrane and initiation of the signaling cascade (see Fig. 1.2; Gust and Felix, 2014). For all the PTI-involved LRR-RLKs studied so far, the BRI1-associated kinase 1 (BAK1, also known as SERK3) (Li *et al.*, 2002) acts as a co-receptor for PAMP signal transduction (Heese *et al.*, 2007; Chinchilla *et al.*, 2007; Schulze *et al.*, 2010; Koller and Bent, 2014; Holton *et al.*, 2015). SERK3 is a plasma

membrane-bound LRR-RLK protein with five LRRs. SERK3 was first identified as an interactor of BRI1, the receptor for brassinosteroids (BR) (Li *et al.*, 2002; Nam and Li, 2002) and SERK3 belongs to a small family of LRR-RLKs, containing four other members with highly redundant functionality (Li, 2010). The SERKs act in several pathways, such as BR signaling, PTI, organ growth, floral and stomatal development, pollen maturation or even cell death (Aan Den Toorn *et al.*, 2015; Schwessinger and Rathjen, 2015; Ma *et al.*, 2016). Interestingly, SERK1, SERK2, SERK3, SERK4 but not SERK5 have been found to function in PTI and to associate with PRRs after ligand perception (Roux *et al.*, 2011). SERK5 is thought to be kinase dead in Col-0 through a point mutation R→L in the critical kinase RD motif (He *et al.*, 2007), but was shown to be functional in BR signaling in L*er*-0, where this mutation is not present (Wu *et al.*, 2015). In the case of RLPs, the presence of the adaptor-kinase Suppressor of BIR1 (SOBIR1) is required for successful signaling (Gao *et al.*, 2009). As a general rule, it seems that all PTI-involved RLPs interact constitutively with SOBIR1, and in a second ligand-dependent step with the SERKs (Zhang and Thomma, 2013; Liebrand *et al.*, 2013, 2014; Albert *et al.*, 2015; Bi *et al.*, 2015; Postma *et al.*, 2015). Exceptions to this rule might be AtRLP42 and SlCuRe1 which associate with SOBIR1 but interaction with the SERKs could not be observed in coimmunoprecipitation assays (Zhang *et al.*, 2014; Hegenauer *et al.*, 2016). It has been suggested that RLPs behave like bi-molecular RLKs once they form a complex with SOBIR1 and the structural similarity between both is striking (Gust & Felix, 2014; see Fig. 1.2).

The recruitment of SOBIR1 by RLPs is thought to be mediated through a GxxxG motif (where “G” is glycine and “x” can be any other amino-acid) found in the transmembrane domain (TMD) of both RLPs and SOBIR1s (Fig. 1.4; Gust and Felix, 2014; Bi *et al.*, 2015*a*). Glycine zippers in form of the GxxxG motif are known to promote helix-helix interaction in the alpha helix of TMDs

(Russ and Engelman, 2000; Senes *et al.*, 2000; Curran and Engelman, 2003; Cymer *et al.*, 2012; Fink *et al.*, 2012; Li *et al.*, 2012). Bi et al., (2015) investigated the importance of the glycine residues from SOBIR1 TMD and showed that when multiple glycine residues are mutated to alanine at the same time, the interaction with RLPs is abolished. Recent evidence additionally showed that mutating the glycine residues on the TMD of RLP23 abolished the recruitment of SOBIR1 and impeded the signaling of nlp20 (I. Albert, personal communication). Yet some RLPs, e.g. SlEIX2 (Ron and Avni, 2004) or AtReMAX (Jehle *et al.*, 2013*b*), known to be functional in PTI and to interact with SOBIR1, lack the GxxxG motif (Fig. 1.4). Studies on the interactions of TMD-helices in bacteria led to the proposal of an extended interaction motif comprising "(small)xxx(small)", whereby small residues such as Ala, Ser or Thr can replace Gly (Russ and Engelman, 2000; Senes *et al.*, 2000).

The LRR-RLP CLV2 is involved in mersitem maintenance in plants and has been shown to interact with CORYNE (CRN), an adaptor kinase different from SOBIR1 (Muller *et al.*, 2008; Bleckmann *et al.*, 2010; Zhu *et al.*, 2010). Whereas CLV2 also has a GxxxG motif in its TMD, the adaptor kinase CRN has no such motif. Nevertheless, a minimal construct composed of the TMD and the outer and inner juxtamembrane domain of CRN was found to be sufficient for this interaction (Bleckmann *et al.*, 2010). Moreover, the GxxxG motif was shown to be present in TMDs of hundreds of bacterial proteins which do not necessarily interact together, thus suggesting that additional factors play a critical role in association specificity (Russ and Engelman, 2000). Indeed, although the (small)xxx(small) pattern seems to facilitate association of given TMDs, adjacent, more voluminous residues must be fitting on both helices to enable interaction according to the knobs-into-hole packing (Lupas and Bassler, 2017). Additionally, more distant residues have been identified as important in stabilizing the interaction (Melnyk *et al.*, 2004) and the sequence context has

been shown to be crucial for stabilizing a GxxxG-mediated interaction (Doura *et al.*, 2004; Schneider and Engelman, 2004). The presence of a glycine motif is thus a hint but not a proof for facilitated TMD-TMD interaction with high specificity. Its exact role in mediating SOBIR1-RLPs interaction should be therefore further studied.

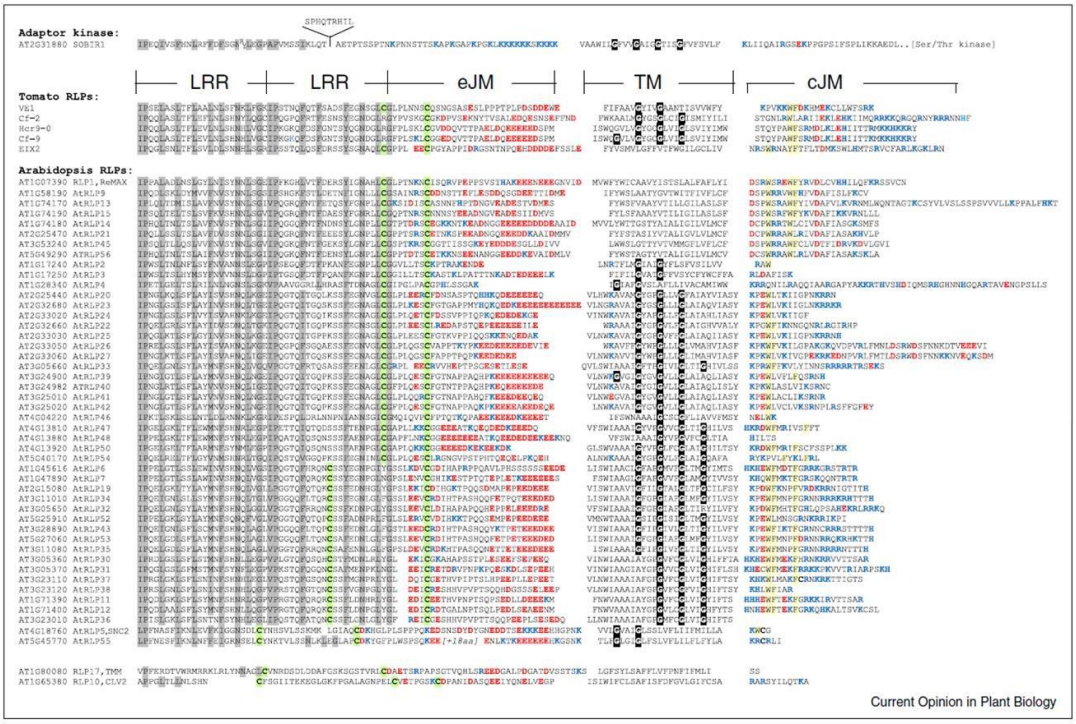

Figure 1.4 RLPs and SOBIR1s share a common motif in their transmembrane domain
(Figure from Gust & Felix, 2014)
The constitutive interaction between SOBIR1 and several LRR-RLPs is thought to be facilitated by a GxxxG motif which creates a flat surface in the α-helix of both transmembrane domains (TMD). Such a surface enables both proteins to be in close proximity, yet the interaction specificity must be encoded in other neighbouring residues.

Lastly, other regions than the TMD might help to mediate the RLP-SOBIR1 interaction. Ve1 and Ve2, two tomato RLPs, were recently used to study the function of the C-tails of RLPs; while Ve1 mediates resistance to *Verticillium* wilt, no function could be attributed to Ve2, yet both can interact with SOBIR1 through their C-tail (Fradin *et al.*, 2014). The significance of the small C-terminal cytoplasmic tail of RLPs remains thus elusive, for no strongly conserved patterns could be identified (Gust and Felix, 2014). Also, the C-tail of

AtRLP23 could be deleted without abolishing functionality nor interaction with SOBIR1 (I. Albert, personal communication). Cytoplasmic signaling specificity must be somehow encoded in this region and a chimeric use of immune vs developmental RLPs may shed more light on this enigma.

1.4 Ligand perception and signal transduction across the membrane

The LRR-RLKs EF-Tu receptor (EFR) (Zipfel *et al.*, 2006) and Flagellin-sensing 2 (FLS2) (Gómez-Gómez and Boller, 2000) recognize bacterial elongation factor (EF-Tu or minimal synthetic epitope elf18) (Zipfel *et al.*, 2006) and bacterial flagellin (or minimal synthetic epitope flg22) (Felix *et al.*, 1999; Gómez-Gómez and Boller, 2000; Gómez-Gómez *et al.*, 2001; Chinchilla *et al.*, 2006), respectively. Both associate with SERK3 after ligand-perception (Heese *et al.*, 2007; Chinchilla *et al.*, 2007) and are the most studied plant PRRs. The signaling of flagellin in plants knows quite some variation, depending on several factors, such as the expression level of FLS2 (Vetter *et al.*, 2012), the localization of FLS2 expression (Wyrsch *et al.*, 2015), the degree of conservation of the flagellin epitope (Naito *et al.*, 2008; Clarke *et al.*, 2013) or the efficiency of complex turnover (Smith *et al.*, 2014). For instance, some species, like *Agrobacterium tumefaciens*, managed to modulate their flg22 epitope to avoid FLS2 perception (Felix *et al.*, 1999). The tomato FLS2 (SlFLS2, for *Solanum lycopersicum)* was shown to be more sensitive to flg22 than AtFLS2 (Chinchilla *et al.*, 2006), and chimeric constructs of both versions allowed to narrow down the region responsible for the higher affinity of SlFLS2 to LRRs 7-10 (Mueller *et al.*, 2012*a*), while the LRRs 9-15 of AtFLS2 were identified as critical for flg22 perception (Dunning *et al.*, 2007). Later on, Sun et al., (2013b) published the crystal structures of FLS2 and FLS2 in complex with SERK3 and flg22 (see visualization in Fig. 1.3). It revealed that not only FLS2, but also SERK3 directly interacts with the ligand through a loose-loop located on the N-terminal part of its ectodomain, flg22 acting like a molecular glue to

stabilize the SERK3 – FLS2 interaction. It also showed that several exposed residues located in the β-sheet of SERK3's LRRs were important for interacting with FLS2. Interestingly, their results seem to show no ligand-dependent structural changes, which does not quite fit the current model of complex activation and might reflect an artifact of structure fixation in crystallography. This raised several questions as to how the recruitment of SERK3 is achieved. Indeed, the kinetics of the complex formation cannot be addressed through crystallography (see Koller and Bent, 2014; Aan Den Toorn *et al.*, 2015). Additional SERK crystal structures allowed to understand better their relationship to various PRRs (Sun *et al.*, 2013*a*; McAndrew *et al.*, 2014; Tang *et al.*, 2015; Wang *et al.*, 2015; Santiago *et al.*, 2016).

The recruitment of SERK3 by an activated FLS2 brings both of their kinases in close proximity, allowing transphosphorylation and activation of downstream signaling (Oh *et al.*, 2010; Schwessinger *et al.*, 2011), as described in more details in the next chapter. It is thought ligand-induced recruitment of a SERK co-receptor is the molecular mechanism of transmembrane activation for LRR-RLKs (Li *et al.*, 2002, 2014; Heese *et al.*, 2007; Chinchilla *et al.*, 2007; Albert *et al.*, 2010*a*; Lu *et al.*, 2010; Segonzac *et al.*, 2014; Aan Den Toorn *et al.*, 2015; Holton *et al.*, 2015; Monaghan *et al.*, 2015; Couto *et al.*, 2016).

Plants can directly recognize microbial pathogens through various receptors that specifically bind distinct PAMP ligands. Examples for such PRR/PAMP pairs are: FLS2 and SlFLS3 recognizing flg22 and flgII-28 from bacterial flagellin, respectively (Gómez-Gómez and Boller, 2000; Hind *et al.*, 2016); AtEFR binds the bacterial EF-Tu or its elf18 minimal binding motif (Zipfel *et al.*, 2006); CERK1/CeBIP pair recognizing chitin (Kaku *et al.*, 2006; Miya *et al.*, 2007; Petutschnig *et al.*, 2010; Shimizu *et al.*, 2010); AtLORE detecting lipopolysaccharides (LPS) of Gram-negative bacteria (Ranf *et al.*, 2015); AtLYM3/LYM1 pair sensing bacterial peptidoglycans (PGN) (Willmann *et al.*,

2011); CORE in tomato binding the csp22-epitope of the bacterial cold-shock protein (Wang *et al.*, 2016); EIX2 detecting fungal xylanase (Ron and Avni, 2004) and AtRLP23 detecting nlp20-epitope of fungal and bacterial NLPs (Böhm *et al.*, 2014*b*; Oome *et al.*, 2014; Albert *et al.*, 2015).

In both, animals and plants, pattern-triggered responses can also be induced after detection of host-derived damage-associated molecular patterns (DAMPs), which are cell debris or endogenous elicitors (Boller and Felix, 2009; Yamaguchi and Huffaker, 2011). Wounded tissue also provides access to pathogens. Damaged cells release proteins and compounds to the apoplasm and these can be recognized by neighbouring cells, e.g. extracellular ATP is recognised by the lectin receptor kinase DORN1 (Choi *et al.*, 2016), can induce defense response and was classified as a DAMP (Tanaka *et al.*, 2014). The Plant Elicitor Peptides (PEPs) are a class of DAMPs which are released downstream of PRRs activation such as EFR or FLS2 (Tintor *et al.*, 2013). PEPs are recognized by the LRR-RLKs PEPR1/PEPR2 (Yamaguchi *et al.*, 2006, 2010; Krol *et al.*, 2010; Tang *et al.*, 2015) and can initiate PTI on their own (Huffaker *et al.*, 2006; Ma *et al.*, 2012; Ross *et al.*, 2014), thus acting like PTI amplifiers. PROPEPs are cleaved after initiation of PTI signaling and activate PDF1.2 and PR1, two defense-related genes (Huffaker and Ryan, 2007). The AtPEP family comprises 8 members with functional redundancy, but with different spatial expression (Bartels *et al.*, 2013). PEPs are broadly present among higher plants, yet do not have interspecific recognition: e.g. ZmPEPs are not recognized in *Arabidopsis sp.*, while AtPEPs are not recognized by *Zea mays* (Lori *et al.*, 2015). Prosystemin in tomato is thought to be an equivalent to the PEPs and is cleaved after damage-perception (e.g. by insect herbivory), the resulting free systemin can be detected by the SYSRE which in turn initiates PTI (L. Wang, personal communication).

Thus, there are many ways of initiating PTI. Pathogen recognition and initiation of PTI is probably mediated by redundancy of several epitopes simultaneously, either via several PRRs having overlapping functionality and/or with the detection of protein modifications. This seemingly cost-intensive survival strategy ensures robust detection of pathogens, thus allowing an efficient initiation of plant defenses. Plants can cope with the loss of one or several PRRs and still be biologically fit to survive. Finally, some receptors have not yet been matched to a defined PAMP (e.g. AtRLP30-SCFE1, AtReMAX-eMAX) and some PAMPs have not yet been matched to receptors (e.g. HaX23, HpaG) (Boller and Felix, 2009; Jehle *et al.*, 2013*a*; Zhang *et al.*, 2013; Albert, 2013). Although finding the receptor for a defined PAMP became easier with the use of forward genetic screens or with use of natural variation among accessions (e.g. Jehle *et al.*, 2013*b*; Albert *et al.*, 2015), PAMP identification remains a long and tedious biochemical and analytical work in most of the cases and may take up to several years. However, the access to cheaper genome-sequencing technologies made data-mining in genomes of pathogens easier and led to the identification of several effectors from spider mites (Villarroel *et al.*, 2016). This approach was shown to be suitable for PAMP identification as well (Cai *et al.*, 2011; McCann *et al.*, 2012) and it might be a great help in specific cases.

1.5 PTI output

Opening of ion channels is among the very early responses, within 2 minutes, of PRR complex activation and lead to H^+ and Ca^{2+} influxes as well as K^+ and Cl^- effluxes among others (Mithöfer *et al.*, 2005; Boller and Felix, 2009). Ionic changes allow membrane depolarization and increase in extracellular pH, which can be easily used as semi-quantitative output assay with cell cultures (Blume *et al.*, 2000; Mithöfer *et al.*, 2005; Chinchilla *et al.*, 2006; Boller and Felix, 2009). A recent paper showed that *Fusarium oxysporum*, a pathogenic fungus, promotes its own growth by secreting homologues of the plant rapid

alkalinizaiton factor (RALF) peptides, which induce apoplastic alkalinization that in turn lead to the activation of a pathogenicity-related MAPK of *F. oxysporum* (Masachis *et al.*, 2016). RALFs are ubiquitous in plants and bind to the RLK Feronia, which initiates extracellular alkalinizaiton leading to an inhibition of cell elongation (Haruta *et al.*, 2014). On the cytoplasmic side of ion fluxes, calcium influx is a very generic response to a broad variety of stimulus, which specificity is thought to be encoded in the temporal frequency, amplitude and shape of the cytosolic Ca^{2+} increases (so called calcium signatures) (Dodd *et al.*, 2010). Calcium is thought to help mediate the activation of burst of reactive oxygen species (ROS) and ethylene production. Calcium influx was indeed shown to follow PAMP perception by PRRs (Blume *et al.*, 2000), to precede ROS production (Grant *et al.*, 2000) and to be a general secondary messenger in both plant and animal cells (Clapham, 1995; Dodd *et al.*, 2010). The ACA8 and ACA10 Ca^{2+}-ATPases were found in complex with FLS2 at the plasma membrane and were shown to be required for correct tuning of downstream signaling events and induction of PTI (Frei dit Frey *et al.*, 2012).

The reactive oxygen species (ROS) O_2^- or its relative H_2O_2 are important signals in PTI. They are continuously produced in plant cells as byproducts of various metabolic pathways (see review of Apel & Hirt, 2004) but were also shown to be massively produced, the so called oxidative burst, within minutes after PAMP perception by PRRs (Doke, 1985; Bradley *et al.*, 1992; Jabs *et al.*, 1997). AtRbohD and AtRbohF control the production of ROS in disease resistance and HR responses with partially overlapping functions (Torres *et al.*, 2002) and spatially different expression levels (Morales *et al.*, 2016). The RbohD-NADPH oxidase is a PM protein with multi-transmembranes and contains two EF-hands at the N-terminal which can perceive Ca^{2+} (Keller et al., 1998; Torres & Dangl, 2005). ROS production can be easily used as readout in a luminol-peroxidase based assay (Keppler, 1989; e.g. Albert et al., 2010).

Ethylene is one of several hormone gases which might be produced after PAMP perception, through a rapid activation of the ACC-synthase (Yang and Hoffman, 1984; Spanu *et al.*, 1994). Ethylene production typically reaches a peak 3-4 hours after PAMP perception. Ethylene is detected by ETR1 coupled to CTR1 which negatively regulates EIN2. After ethylene perception, EIN2 is cleaved at its COOH end (CEND, residues 459-1294) and the CEND is relocated to the nucleus where it activates the transcription factors EIN3 and EIL1 which, in turn, regulate the transcriptional changes of ethylene-induced genes (Alonso *et al.*, 1999; Zheng and Zhu, 2016). FLS2 seems to be one of the genes targeted by ethylene-induced gene regulation, leading to higher expression levels of FLS2 after ethylene perception (Boutrot *et al.*, 2010; Mersmann *et al.*, 2010), in a positive feedback-loop fashion to enforce detection of pathogens. Interestingly, the ethylene sensor ETR1 seems to also be able to sense H_2O_2 and mediate stomatal closure to prevent additional pathogen entry (Desikan *et al.*, 2005). Ethylene production is commonly measured by gas chromatography as readout for PTI induction (e.g. Felix et al., 1999; Jehle et al., 2013).

MAPK cascades are a complex signaling hub for various pathways, including growth, development and responses to biotic and abiotic stresses (Champion *et al.*, 2004; Meng and Zhang, 2013). In *A. thaliana*, there are about 20 MAPKs, which are regulated by 10 MAPK kinases (MAP2K), which in turn are themselves regulated by more than 80 MAPKK kinases (MAP3K) (Ichimura *et al.*, 2002; Dóczi *et al.*, 2007). MAPK cascades are also a central point of convergence for the different PAMP signaling pathways in plants and also a focal target for pathogen elicitors (Pitzschke *et al.*, 2009; Meng and Zhang, 2013). In *A. thaliana*, MAPK cascade activation starts 1-2 minutes and peaks 10-15 minutes after perception of flg22 (Nühse *et al.*, 2000). MAPK3 and MAPK6 activations are the most commonly tested for successful PAMP signaling, for they get phosphorylated after flg22 treatment and positively

regulate many downstream components of PTI (Asai *et al.*, 2002). MKKK7, a MAP3K, was recently shown to physically interact with FLS2 and to negatively regulate MAPK6 activation as well as ROS production, thus making the link between cell-surface receptors and MAPK cascade activation (Mithoe *et al.*, 2016). The MAPK cascade activation by PAMP perception leads to repression and/or activation of various transcription factors, which in turn dictate transcriptional gene reprogramming. WRKYs are a huge family of plant transcription factors that bind to W-box-containing promoters (Rushton et al., 2010), of which WRKY22 and WRKY29 were shown to be highly activated downstream of MAPK3/6 after flg22 treatment (Asai *et al.*, 2002). Additionally, the Flagellin-induced receptor kinase 1 (FRK1) is highly induced after flg22 treatment and its promoter fused to a luciferase gene pFRK1::Luc became a widely-used reporter gene for PTI induction in *A. thaliana* protoplasts (Asai *et al.*, 2002; Yoo *et al.*, 2007).

Salicylic acid (SA) and jasmonic acid (JA) are two other signal hormones, which are produced in reaction to biotrophic pathogens and herbivores/necrotrophic pathogens, respectively (Thomma *et al.*, 1998; Glazebrook, 2005). Interestingly, the SA- and JA-pathways are antagonistic (Thaler *et al.*, 1999) and NPR1 is a key regulator of SA-induced suppression of JA, which is not required when ethylene is present, suggesting that ethylene can bypass NPR1 to suppress JA (Leon-Reyes *et al.*, 2010). Several successful pathogens were shown to be able to manipulate the antagonism between these two pathways to their benefit (Thaler *et al.*, 2012). *Pseudomonas syringae* was, for instance, shown to be able to produce JA-coronatine, a JA-mimic that shuts down the SA-pathway and, consequently, the defense of the host plants (Cui *et al.*, 2005).

1.6 PTI regulation

PRR complexes at the plasma membrane are under tight regulation to avoid wasting energy on defense when it could be allocated to other processes (e.g. growth). For instance, SERK3 (and probably the other SERKs) is involved in various pathways, such as defense, cell death, growth, stomatal development or pollen maturation (Colcombet *et al.*, 2005; Li, 2010; Meng *et al.*, 2015; Schwessinger and Rathjen, 2015; Ma *et al.*, 2016). Because the SERKs play such a central signaling role in a variety of pathways, their interactions with different signaling partner must therefore tightly regulated so that undesired processes are not randomly activated. The BAK1-interacting receptor (BIR) family, composed of four members, interacts constitutively with the SERKs and PRRs to prevent heterodimer formation prior to ligand binding and is released after ligand binding (Fig. 1.5; Gao *et al.*, 2009; Halter *et al.*, 2014; Huang *et al.*, 2017; Imkampe *et al.*, 2017). BIR1 seems to be an active repressor of the SERKs activity in the cell death pathway (Gao *et al.*, 2009), while BIR2 was proposed to be involved in repressing the SERKs in immunity, for BIR2 overexpression reduced the complex formation of FLS2 – SERK3 after flg22 treatment (Halter *et al.*, 2014). BIR3 was also recently shown to be an active inhibitor of the SERKs and PRRs in immunity (Huang *et al.*, 2017; Imkampe *et al.*, 2017). BIR4 has not yet been functionally characterized for it is most likely kinase dead (T. Halter, personal communication).

Receptor-like cytoplasmic kinases (RLCKs), lacking extracellular and transmembrane domains, are getting growing attention, for they participate in regulation of signaling complexes and sometimes mediate the cytoplasmic propagation of signaling. For instance, the Botrytis-induced kinase 1 (BIK1), PBL1, PBL2 and PBS1, all members of the large PBL family, are positive regulators of PTI (Fig. 1.5; Zhang *et al.*, 2010; Lu *et al.*, 2010; Laluk *et al.*, 2011). BIK1 was shown to interact physically with both FLS2 and SERK3, to get phosphorylated after flg22 perception and to phosphorylate in return both FLS2 and SERK3 kinases, thus amplifying the flg22 signaling for successful downstream responses (Lu *et al.*, 2010). It also interacts with others PRRs, such

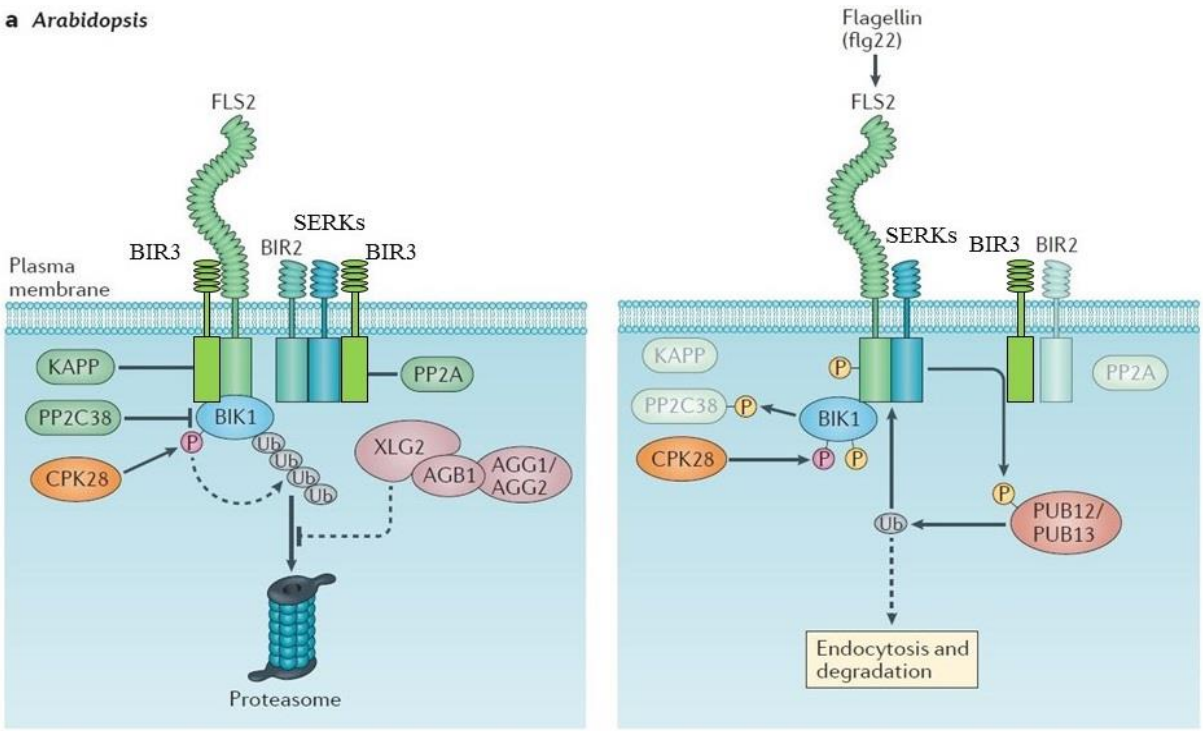

Figure 1.5 - Regulation of PRR at the plasma membrane
(Adapted from Couto et al., 2016)
PRR such as FLS2 are under tight regulation to avoid signaling mistakes. The BIR family represses the formation of signaling complexes by interacting with both the receptor and the co-receptor. Upon ligand recognition, the BIRs are released and signaling partners can interact to initiate signal transduction across the membrane. In the cytoplasm, several CPKs and RLCKs are involved in PRR complex regulation too.

as PEPR1/PEPR2 (Liu *et al.*, 2013; Tintor *et al.*, 2013) and CERK1 (Zhang and Zhou, 2010; Zhang *et al.*, 2010). Furthermore, BIK1 was shown to be a direct positive regulator of the NADPH – RbohD, thus making a further link between activated PRR complexes and oxidative burst (Kadota *et al.*, 2014; Li *et al.*, 2014).

The Ca^{2+}-dependent protein kinase (CPK) family is heavily involved in regulation of immunity and CPKs have a calmodulin-like calcium sensor as well as a kinase domain, making them good candidate for intermediate actors in PTI. CPK28 was shown to negatively regulate BIK1-mediated NADPH activation (Kadota *et al.*, 2015; Monaghan *et al.*, 2015), most likely by phosphorylating BIK1 to promote ubiquitination, thus favouring BIK1 turnover (Monaghan *et al.*, 2014, 2015). CPK5 was identified as a positive regulator of PTI, by mediating NADPH activation and being a sensor in SAR (Asai *et al.*, 2013; Dubiella *et al.*, 2013). There are also several phosphatases involved in PTI regulation (Felix *et al.*, 1994; Gómez-Gómez *et al.*, 2001; Segonzac *et al.*, 2014; Rahikainen *et al.*, 2016). Felix et al., (1994) showed that PTI could be induced not only after ligand binding and activation of signaling, but also by inhibiting the repression of PTI by certain phosphatases. PP2A, for instance, is a negative regulator of PTI located at the plasma membrane and can be found constitutively in complex with SERK3 (Segonzac *et al.*, 2014). It inhibits complex activation by modulating SERK3 phosphorylation status, and treatment with cantharidin, a PP2A-specific inhibitor, was sufficient to trigger BIK1 phosphorylation and oxidative burst production (Segonzac *et al.*, 2014). Recently, another phosphatase, PP2C38, was also shown to be a supplementary negative regulator of BIK1 and of BIK1-mediated immunity (Couto *et al.*, 2016).

Finally, protein maturation and recycling has a fundamental role in PTI regulation to ensure an efficient signaling by undamaged proteins and the turnover of activated signaling complexes. The E3-ubiquitin ligases PUB12 and

PUB13 were shown to mediate FLS2-SERK3 degradation and turnover after ligand perception (Lu *et al.*, 2011), most likely to avoid repetitive signaling of single infection event (Smith *et al.*, 2014). Correct glycolysation and folding was shown to be required for exportation of PRRs from the endoplasmic reticulum (ER) to Golgi apparatus and finally to the plasma membrane (Trempel *et al.*, 2016). Such trafficking regulations and quality control in the ER was shown to be primordial for successful PTI (Li *et al.*, 2009; Nekrasov *et al.*, 2009; Tintor and Saijo, 2014). Quality control thus prevents misfolded PRRs to be exported to the plasma membrane, which is a convenient qualitative assessment *in planta* of artificially designed receptors, such as chimeric receptors.

1.7 What can we learn from LRR-RLPs and LRR-RLKs from other pathways?

Interestingly, certain LRR-RLKs and LRR-RLPs are involved in other signaling programs than immune signaling, yet still share the same structure and sometimes even same co-receptors. The LRR-RLKs ERECTA (Torii *et al.*, 1996) and ERECTA-like (ERL) 1 and 2 (Shpak *et al.*, 2004, 2005) were shown to bind to ERF peptides and to act with the LRR-RLP Too many mouths (TMM) (Nadeau and Sack, 2002) in multiple pathways, such as stomatal development, transpiration regulation or lateral organ and floral shapes (Masle *et al.*, 2005; Shpak *et al.*, 2005; Shpak, 2013). More than a decade ago, Godiard et al., (2003) reported that ERECTA from Col-0 accession could rescue the Landberg *erecta* accession's susceptibility to bacterial wilt, thus suggesting a cross-talk between resistance and development pathway. It has been recently shown that the ERECTAs and TMM physically interacts with the SERKs (Meng *et al.*, 2015) and together they regulate PTI (Jordá *et al.*, 2016). HAE and HSL2, two other LRR-RLKs, are involved in perception of the IDA-derived peptides and mediate cell wall remodeling and lateral root growth (Butenko *et al.*, 2003; Kumpf *et al.*, 2013). Later on, it was shown that HAE and HSL2 also interact with the SERKs

in a ligand-dependent fashion (Meng *et al.*, 2016) and the HAE – IDA – SERK1 crystal structure was recently published (Santiago *et al.*, 2016), showing a similar interaction mechanism as in the FLS2 – flg22 – SERK3 crystal where the ligand acts as a molecular glue stabilizing the signaling complex. The LRR-RLK phytosulkine (PSK) receptors (PSKR), which belongs to the same family as BRI1, is involved in root growth and cell expansion and also interact with the SERKs (Wang *et al.*, 2015). Unlike the BRI1-SERK1, HAE-SERK1 and the FLS2-SERK3 crystal structures, the PSKR1-SERK1 and PSKR1-SERK2 crystals revealed that the PSK ligand does not interact with the SERKs ectodomains, but instead it stabilizes the island domain of PSKR1 which in turn allows the interaction with the SERKs (Wang *et al.*, 2015). This suggests that unlike the HAE, FLS2 and BRI1 ectodomains, PRRs containing an island domain undergo structural changes to allow a signaling co-receptor to approach its activated ectodomain. SERKs are involved in several signaling pathways, showing a high functional plasticity as well as a high redundancy among each other, yet the signal specificity remains high. Interestingly, for all IDA, PSK and ERF peptides signaling, as well as for flg22, elf18 and BR signaling, there exists differential affinity for SERK members as co-receptor (reviewed in Ma et al., 2016). This suggests that SERK ectodomains interact slightly differently with each PRR and that additional signaling specificity must also be encoded in the differential phosphorylation sites activated in distinct signaling pathways (Ma et al., 2016).

The LRR-RLK CLAVATA1 (CLV1) (Clark *et al.*, 1993, 1997) as well as the LRR-RLP CLV2 (Kayes and Clark, 1998; Jeong *et al.*, 1999) in complex with the pseudokinase CORYNE (CRN) (Muller *et al.*, 2008; Bleckmann *et al.*, 2010; Zhu *et al.*, 2010; Nimchuk *et al.*, 2011) and the LRR-RLK RPK2 (Kinoshita *et al.*, 2010) negatively regulate shoot apical meristem maintenance upon CLV3 treatment (Clark *et al.*, 1995; Ogawa *et al.*, 2008; Ohyama *et al.*, 2009), by

repressing the transcription factor WUSCHEL (Brand *et al.*, 2000). CLV3 is part of the CLE family, which encodes small hormone peptides involved in intercellular signaling events (Kiyohara and Sawa, 2012) and CLV3 peptides do not induce PTI responses (Segonzac *et al.*, 2012; Mueller *et al.*, 2012*b*). Binding of CLV3 has been shown for CLV1 (Ogawa *et al.*, 2008; Ohyama *et al.*, 2009), but its interaction with CLV2 and RPK2 remains indirect, through (lack of) responses of multiple mutants. This issue will be addressed in the present work. Certain pathogenic nematodes can produce and secrete CLE-like peptides (Wang *et al.*, 2005, 2011; Lu *et al.*, 2009), which were shown to promote parasitism (Replogle *et al.*, 2011, 2012; Wang *et al.*, 2011; Kiyohara and Sawa, 2012). Interestingly, to this day, no serious link could be found between the SERKs and/or SOBIR1 and the CLV1/CLV2/CRN pathway. The interaction of CLV2 with CRN seems to be mediated by a TMD-TMD interaction taking place in the ER prior to exportation to the plasma membrane (Bleckmann *et al.*, 2010) and which is apparently not dependent on a GxxxG motif, although CRN does contain a (small)xxx(small) motif at the beginning of its TMD, thus making these proteins particularly interesting controls.

The brassinosteroids receptor BRI1 is a LRR-RLK which mediates plant growth (Li & Chory, 1997). It also interacts with the SERKs (Li *et al.*, 2002; Nam and Li, 2002; Russinova *et al.*, 2004; Karlova *et al.*, 2006; He *et al.*, 2007; Gou *et al.*, 2012) and the crystal structures have been published for BRI1 ectodomain (Hothorn *et al.*, 2011), BRI1 – BR – SERK1 complex (Santiago *et al.*, 2013), BRI1 – BR – SERK3 complex (Sun *et al.*, 2013*a*) as well as the activated BRI1 kinase (Bojar *et al.*, 2014). These crystals revealed that the ectodomains of SERK3 and SERK1 behave very similarly when in complex with activated FLS2 and BRI1. In both instances, the interaction with the receptor is mediated through surface-exposed residues located in the β-sheet of the LRRs as well as with the ligand through the N-terminal cap of the SERKs (Sun *et al.*, 2013*a*,*b*;

Santiago *et al.*, 2013). The phosphorylation status of SERK3 kinase by FLS2 and BRI1, on the other hand, knows quite some variation, as the *A. thaliana* mutant *bak1-5* is strongly impaired in EFR- and FLS2-mediated PTI but is barely influenced for BR-signaling (Schwessinger *et al.*, 2011). It was suggested that the phosphorylation residues of SERK3 kinase might be differentially affected by BRI1, FLS2 and EFR, therefore having potentially an effect on regulators present in the signaling complex as well as on the specificity of the signal (Oh *et al.*, 2010; Schwessinger *et al.*, 2011; Macho *et al.*, 2014, 2015).

BR perception by the BRI1 – SERKs complex leads to the release of BIK1 from both kinases and allow phosphoactivation of the BR-specific cytoplasmic signaling cascade (Lin *et al.*, 2013). BIK1 release from the BRI1 – SERKs activated complex allows the repression of BIN2, which phosphorylates and represses BZR1/BES1 in absence of BR (Yin *et al.*, 2002; Vert and Chory, 2006). BZR1/BES1 are major regulators of BR-driven transcriptional changes (Wang *et al.*, 2002). In contrast to its negative regulatory effect in BR signaling, BIK1 was shown to be a positive regulator of PTI, as *bik1* mutant were more susceptible in bacterial growth assay (Lu *et al.*, 2010) and primed plants were not more resistant to PstDC3000 (Laluk *et al.*, 2011). BIK1 was also shown to interact with PEPR1/PEPR2 and PAMP-induced ethylene accumulation was shown to be compromised in *bik1* mutants (Liu *et al.*, 2013). The opposite regulation of BR and immune pathways by BIK1 revealed potential cross-talk between both pathways, which had already been reported (Albrecht *et al.*, 2012; Belkhadir *et al.*, 2012). The common co-receptor SERK3 was thought to be a potential point of trade-off between BR and immune pathways, but quantitative results then confirmed the role of the transcription factors BZR1/BES1 on repressing PTI (Lozano-Durán *et al.*, 2013). In plants expressing constitutively activated versions of BZR1/BES1, FLS2 – SERK3 complex formation, oxidative burst as well as MAPK phosphorylation were possible after flg22

treatment, but there were no expression of defense genes or seedling growth inhibition (Albrecht *et al.*, 2012; Lozano-Durán *et al.*, 2013). Not only does BZR1 regulates BR-involved genes, but it also upregulates several WRKY transcription factors, WRKY11/15/18/40/70, which are negative regulators of defense-related genes (Lozano-Durán *et al.*, 2013). SERK3 expression level was ruled out as trade-off point when the presence of nanoclusters for BRI1 and FLS2 multiplexes was shown to be spatially separated (Bücherl *et al.*, 2017). Finally, it was long thought that the BR versus immune pathways antagonism was unidirectional, but recent evidence showed that BR-related gene expression was down-regulated as soon as 15 minutes after flg22 treatment, even though BR signaling might not be affected (Jiménez-Góngora *et al.*, 2015).

Because of the structural similarities between BRI1 and LRR-RLKs involved in PTI, several groups suggested that domain swaps could allow a modulation of the functionality of a given LRR-RLK. The principle of chimeric receptors appeared when BRI1 functionality was not yet proven; He et al., (2000) swapped domains from OsXa21 and AtBRI1 to map the functionality of BRI1. The resulting eBRI1-tmXa21, with apoplastic ectodomain of BRI1 and TMD-kinase domain of Xa21, could trigger defense responses after BL treatment. This synthetic approach opened the way to several studies which addressed ligand-receptor pairs as well as receptor activation (Wulff *et al.*, 2009; Albert *et al.*, 2010*c*; Wang *et al.*, 2014), could help identify AtWAK1 as the receptor for oligogalacturonides, a DAMP derived from cell-wall proteins (Brutus *et al.*, 2010) and generally helped better understand signal transduction across the membrane (Wulff, 2001; Mueller *et al.*, 2012*a*).

Of particular interest is the work of Albert et al., (2010) where kinases of FLS2 and SERK3 were swapped to isolate both actors: they were exclusively able to signal when transiently expressed together. This is especially remarkable, for it allows to tackle the technical issue of lethality in multiple SERKs mutant plants

(He *et al.*, 2007). Working with chimeras of RLPs and RLKs should enable us to understand the exact role of the GxxxG motif in recruiting SOBIR1. Also, the use of chimeras of several structurally similar, but functionally different receptors, such as CLV1/2, should allow us to explore the molecular basis for their non-dependence on the SERKs.

2. Aim of the work

Pathogen perception by PRRs occurs in the extracellular space and crystal structures help us understand the mechanistics for ligand binding but not the specificity of the various receptors. Plants have very large families of LRR-receptors and most of the PRRs in plants contain LRRs. The LRR structure is present in all kingdoms of life and plant evolved a specific type of LRR subfamily, whose consensus sequence is IPxxLxxLxxLxxLxLxxNxL(T/S)Gx, where "x" can be any residues (Jones *et al.*, 1994; Kobe and Kajava, 2001; Mueller *et al.*, 2012*a*). LRR-containing proteins in plants are mainly distributed in either LRR-RLKs and LRR-RLPs. In the present work we will study the emergence of both receptor types, from a bioinformatic perspective. In a second part, we will study signal transduction by focusing on the molecular features that define LRR-RLKs and LRR-RLPs, and focus on how we can interconvert these two types of receptors by domain swapping approaches.

3. Materials and methods

3.1 Chemicals and solvents

Chemicals and solvents were ordered from Sigma-Aldrich (St. Louis, USA), Carl Roth (Karlsruhe), Merck (Darmstadt), VWR (Radnor, USA), Duchefa (Haarlem, NL) and Fluka (Buchs, CH).

3.2 Peptides and elicitors

Flg22, csp22, elf18, CLV3 and PEP1 were synthetized and provided by different suppliers. Stock solutions of peptides were prepared in H_2O and diluted in a solution medium with 1 mg/ml BSA and 100 mM NaCl.

3.3 Bacterial strains

XL1 blue *Escherichia coli* were used for vector production in bacteria (maxi- and mini-prep). TOP10 *E. coli* were used for pENTR TOPO cloning. *E. coli* were grown in liquid LB medium at 37°C and 200 rpm in a shaker or on LB-agarose plates at 37°C in stationary incubators. *Agrobacterium tumefaciens* GV3101 were used for plant transformation and transient expression in *Nicotiana benthamiana*. *A. tumefaciens* were transformed by electroporation and positive colonies were picked after 48h growth on LB-agarose plates at 30°C in stationary incubators. They were then grown overnight at 30°C and 250 rpm in a shaker in liquid LB medium.

3.4 Plant material

Seedlings of *Arabidopsis thaliana* were grown at 22°C under a 8:16 h light:dark photoperiod at 70 µE/m^2/s and 40-65% relative humidity in controlled environment (four weeks covered with a lid in a Percival growth chamber, followed by two weeks without lid in a Mobylux Grow Bank, CLF Plant-Climatics, Emersacker). Leaves of 4-6 weeks old *A. thaliana* sobir1-12 mutant plants were used for protoplasts isolation and transformation.

To study protein expression and functionality in a different plant background, 4-5 weeks old *Nicotiana benthamiana* were used for bioassays as well as for interaction studies. They were grown in the greenhouse at 22°C 16:8 h light:dark photoperiod.

3.5 Protoplasts isolation and pFRK1::Luc assay

Transient expression in mesophyll protoplasts from *Arabidopsis thaliana* sobir1-12 mutant leaves was performed as described in (Yoo *et al.*, 2007). Briefly, aliquots of 20 000 protoplasts were cotransformed with 5 µg plasmid with the reporter construct pFRK1::luciferase and 5 µg plasmid with the receptor construct to be tested. Protoplasts were resuspended in W5 solution with 0.2 mM luciferin. Aliquots were incubated overnight (max 12h) in a 96-well plate before treatment with the respective peptides (BSA-NaCl as control, elf18, pep1, BL, csp22, CLV3, flg22). Luciferase activity was monitored via light emission using a luminometer (Mithras LB 940).

3.6 Agrobacterium-mediated transformation of *Nicotiana benthamiana*

Nicotiana benthamiana is commonly used for transient expression assays (e.g. Albert *et al.*, 2015). Transformation was mediated by *Agrobacterium tumefaciens* (strain GV3101) carrying plasmids encoding the gene of interest. After overnight incubation of transformed bacteria in LB medium (at 30°C, 250 rpm), bacteria were collected by centrifugation (4000 *g*, 8 min) and resuspended to an OD of 1 in 10 mM $MgCl_2$ with 150 uM acetosyringone. After incubation at room-temperature for 90 min, bacteria were diluted to an OD of 0.4, mixed 1:1 with *A. tumefaciens* (C58C1) carrying the P19 suppressor of silencing (Voinnet *et al.*, 2003) and pressure-infiltrated in 4-5 week old *N. benthamiana* leaves. Leaves were cut in pieces for bioassays 24h after infiltration, or harvested 36h after infiltration and directly frozen in liquid nitrogen for protein expression analysis.

3.7 Ethylene production

Leaves of *N. benthamiana* were cut in small pieces and incubated on water overnight (at room temperature). To measure ethylene production, three leaf pieces were carefully placed in a 6 ml glass tube with 500 µl H_2O. Samples were treated with either water (negative control), 90 µg/ml *Penicillium sp.* extract (positive control, Thuerig *et al.*, 2006) or the peptides to be tested. Ethylene accumulating in the air space was measured 4h30 after treatment using gas chromatography as previously described (Albert *et al.*, 2010*c*).

3.8 Oxidative burst

Analysis of oxidative burst was performed on leaf pieces (see Ethylene production, above) of transiently transformed *N. benthamiana*. Leaf pieces were placed in individual wells of a 96-well plate with a 90:10 µl H_2O:mastermix solution (1 ml H_2O, 20 µl luminol, 3 µl peroxidase). After a 5-10 min pre-run to test for the background of ROS production, leaf pieces were induced with either the peptide to be tested, BSA/NaCl (neg. control) or flg22 100 nM (positive control) as previously described (Albert et al., 2010).

3.9 Molecular biology

3.9.1 PCRs, electrophoresis and DNA sequencing

Primers were designed with CLC Workbench 7, with an optimal length of 20-22 nt, ideally with 60% GC content and a melting temperature between 55-63°C. The forward primers had an additional "CACC" overhang for directional pENTR TOPO cloning. Chimeric receptors were created by binding two separate PCR products with overlapping ends as previously described (Albert *et al.*, 2010*c*; Mueller *et al.*, 2012*a*). Truncated constructs were generated using reverse primers at the desired target (no stop codon). Chimeric receptors were built with normal external primers and overlapping chimeric internal primers, which had half of each sequence and were 40-50 nt long (Annex Table 1, see

also Digital Table 1 for the full sequences of all constructs). All primers were ordered from Sigma-Aldrich.

Gel electrophoresis were all performed with 1% agarose-TAE gels and band purification was done with the GeneJET Gel Extraction kit from ThermoFisher Scientific. DNA sequencing was performed by GATC Biotech (Konstanz).

3.9.3 Vectors

After using pENTR/TEV/D-TOPO or pENTR/D-TOPO as entry vectors (pENTR directional TOPO kits, Invitrogen), constructs were exported to EcoRI-digested pK7FWG2 expression vectors (Spectinomycin resistance in bacteria), containing the cauliflower mosaic virus 35S overexpressing promoter and a C-terminal GFP tag. Alternatively, pGWB14 was used for HA-tagged constructs and pGWB17 for Myc-tagged constructs (both vectors have Hygromycin and Kanamycin resistances in bacteria).

3.10 Protein biochemistry

Protein separation from crude extract or immune-enriched fractions was achieved with 8% SDS-PAGE gels, unless indicated otherwise. Western blotting to nitrocellulose membrane (GE Healthcare) was performed using semi-dry western blotting technology from BioRad. Immunoprecipitation (IP) and co-IP was based on magnetic GFP-Trap_MA beads (unless indicated otherwise) from Chromotek, and performed as described in Jehle et al., (2013). Crude extract blotting used 30 mg of grinded leaf material resuspended in 2 volumes [w/v] of loading buffer mixed with β-mercaptoethanol. The following antibodies were used: anti-GFP produced in rabbit (Torrey Pines Biolabs Inc.), anti-Myc produced in rabbit (Sigma-Aldrich) and anti-HA produced in mouse (Sigma-Aldrich).

3.11 Binding assay

To assess whether CLV2 and RPK2 bind to CLV3, we ordered CLV3-acridinium labeled peptide to the Interfaculty Institute of Biochemistry (IFIB), Tuebingen University. The Kalbacher group could synthesize and purify a CLV3-acridinium peptide with a molecular weight of 2149.605 Da (Annex Fig. 1). Normal CLV3 peptide has a molecular weight of 1482.561 Da, as measured per HPLC (Annex Fig. 1). Plants were agro-transformed as described above to express CLV1-GFP, CLV1Δkinase-GFP, CLV2-GFP or CLV2-GFP with CRN-myc. After 48h hours, plant material was shock-freezed with liquid nitrogen and ground to a fine powder. The binding assay was performed as described in Wildhagen et al., (2015). Light emission was measured with a single-tube luminometer (Sirius Luminometer, Berthold Detection Systems Gmbh, Profzheim, Germany). Specific binding was calculated as integrated light emission over a 30 seconds period after contact with the H_2O_2 (induction of luminescence).

3.12 Microscopy

An Eclipse 80i microscope (Nikon, Düsseldorf) was used for bright field and fluorescence microscopy.

3.13 Bioinformatics

3.13.1 Wet lab related

DNA and protein sequences for chimera designs and ordering of primers were obtained from NCBI, TAIR (arabidopsis.org) and/or UniProt.

Structural data were obtained from PDB, protein modelisation was done using the Phyre2 and Swiss-model platforms. Protein visualization was performed in DeepView and Cn3. PolyPhobius and TMHMM were used to predict signal peptides and transmembrane domains.

The figures and results shown are representative of at least three independent repetitions. All statistical analyses were conducted on R (v. 3.2.2) using a significance threshold of P = 0.05.

3.13.2 LRR receptor evolution

To study the evolution of LRR receptors, we first had to establish a suitable dataset. For that, AtEFR (UniProt ID: C0LGT6) was BLASTed against all plant reference proteomes available on UniProt (www.uniprot.org). A CLANS map was generated using the best 1000 hits from every proteome. The 1000 hits per proteome mark was chosen to keep the following computing steps to a reasonable time. A pairwise comparison was launched using the global alignment STRETCHER from EMBOSS to generate the CLANS map. Length-adjusted scores were then used as cutoff in the CLANS map, as p-values were giving a suboptimal discriminating power within our dataset. For instance, when running a BLASTp search on NCBI for AtEFR against all Viridiplantae (taxonomy ID: 33090, max target output: 5000), the typical results would show over 2500 results having an E-value of 0.0, while their Max scores vary from 2099 to 546, giving a long range of differences which are not reflected in E-values. *Nota bene*, the analysis was performed on available sequences, which in some cases may contain sequencing errors or sequences that might have been mislabelled. The CLANS map ran at different cutoff values to identify the optimal cutoff: enough to separate clusters that they can be individually identified, but not so much that it becomes tedious work to decipher the map. For the rest of the analysis, the length-adjusted HSP score cutoff of 2.0 was chosen as indicative of cluster evolution. After manually annotating the map by accessing UniProt Reference Proteome annotations and checking back on the NR database for annotations not present in the Reference Proteomes, sequences of the main clusters were extracted on separate FASTA files and the phylogenetic tree of each cluster was established. Sequences from each cluster

were aligned using Clustal Omega (v. 1.2.1) and alignments were refined using MUSCLE (v. 3.8.31). TMD were identified with PolyPhobius (phobius.sbc.su.se/poly.html). An overview of the workflow is depicted in Fig. 3.1.

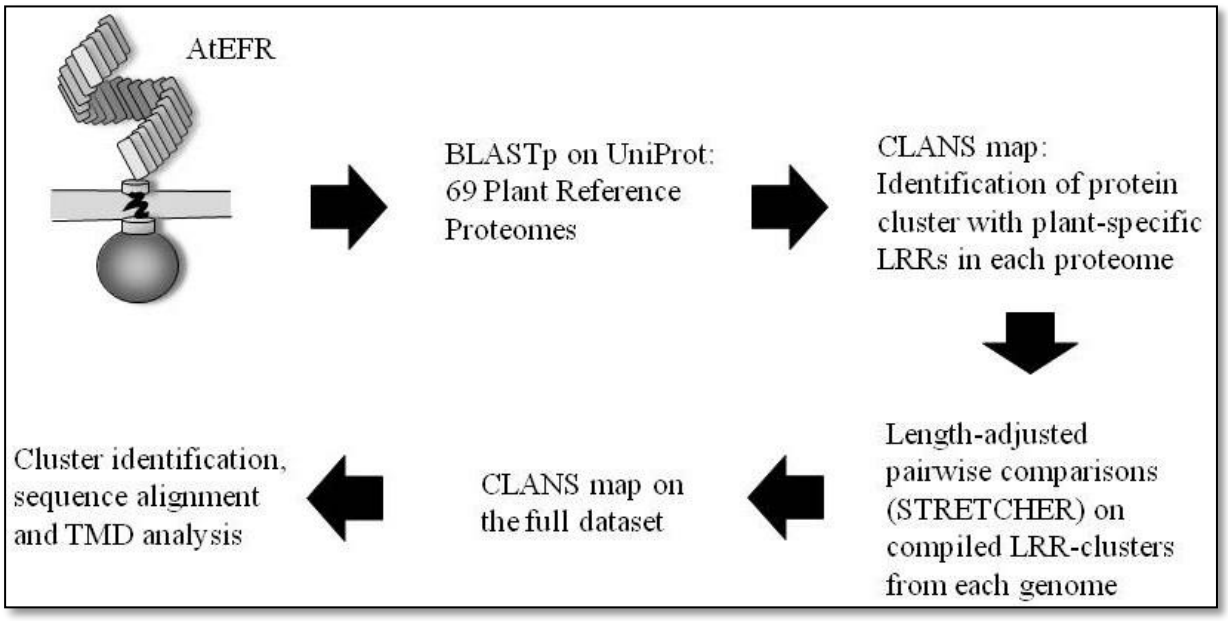

Figure 3.1 - Workflow for the analysis of LRR-protein evolution

We ran a BLASTp of AtEFR against all available Plant Reference Proteomes from UniProt and ran a CLANS on the 1000 best resulting hits to identify plant-specific LRR consensus within each proteome. Then we compiled the sequences from all proteomes and made pairwise-comparison and corrected the score according the length of the proteins. Using the scores from the pairwise-comparison matrix, we ran a CLANS on the full dataset and annotated manually cluster of interest to extract and align their sequences.

Table 3.1 - List of bioinformatic tools and their corresponding websites

Name of the tool	Website
BLAST	blast.ncbi.nlm.nih.gov/Blast.cgi
TAIR	www.arabidopsis.org
UniProt	www.uniprot.org
PDB	www.rcsb.org/pdb/home/home.do
PolyPhobius	phobius.sbc.su.se/poly.html
DeepView	spdbv.vital-it.ch
Phyre2	sbg.bio.ic.ac.uk/phyre2/
TMHMM	cbs.dtu.dk/services/TMHMM/
R-stats	www.r-project.org
CLANS	ftp://ftp.tuebingen.mpg.de/pub/protevo/CLANS/
STRETCHER	www.ebi.ac.uk/Tools/psa/emboss_stretcher/
Clustal Omega	www.clustal.org/omega/
MUSCLE	www.drive5.com/muscle/

3.13.3 Analysis of TMD momentum and conservation

The Shannon entropy was calculated on the alignment of canonical TMDs for selected cluster to analyze their conservation moment, meaning if a position is highly conserved, it will have a lower entropy (Shannon, 1948). Entropies were then fitted to the best helix model, as based on heptads or optimized for conservation momentum (Lupas and Bassler, 2017). This allowed us to identify the probable interaction surfaces of TMDs in different clusters and to emit hypothesis on how two α-helixes may be expected to interact.

4. Results

4.1 Evolution of LRR-PRRs and approach to a better understanding of the SERK family

The LRR structure with the tandemly arranged repeats forming stacks adopting the form of solenoids evolved independently at multiple occasion in all domains of life (Kobe and Kajava, 2001). The LRR structures can be classified in at least seven subfamilies (Kobe and Kajava, 2001; Kajava *et al.*, 2008), yet stacking from different LRR subfamilies is never occurring within one LRR protein (Kajava, 1998). Even though several LRR subfamilies are present in plants, the typical plant LRR structure is based on a 24 amino-acids repeat with a IPxxLxxLxxLxxLxLxxNxL(T/S)Gx consensus, where x can be any residue (Kobe and Kajava, 2001; Mueller *et al.*, 2012*a*). The most notable part of the plant-specific LRR is the NxxxG motif which is virtually 100% conserved (G. Felix, personal communication). To better understand the evolution of plant-specific LRR proteins and to facilitate the identification of important receptors, we used bioinformatics to scout for LRR-containing proteins. We performed a BLASTp against each of the 69 Plant Reference Proteomes available on UniProt to identify proteins similar to the LRR-RLK EFR from *A. thaliana*. We could identify significant CLANS cluster formation (cluster with more than 4 sequences) in 51 species, including 2 subspecies of *Oryza sativa* (Fig. 4.1)[1]. The central cluster of each proteome at a p-value cutoff of 1E-200 was retrieved (it contained all sequences phyologenetically related to LRR receptors). In Figure 4.2, an example of a CLANS map is shown for the *A. thaliana* proteome. The final dataset contained 24’234 protein sequences, representing all proteins with plant-type LRR domain. Notably, only few NB-LRRs could be found in our dataset which is expected since they belong to a different LRR subfamily (Kobe

[1] We had to exclude certain species from the *Oryza* genus since they presented an amount of gene copies far exceeding the 1000 hits upper limit of our selection process.

and Kajava, 2001). The only available reference proteome for a member of the gymnosperms is the one for *Picea glauca*, which was not available in an assembled proteome on UniProt and could not be included in this analysis. Besides angiosperms, we found plant-specific LRR proteins from the Lycophyte *Selaginella moellendorfii*, a non-seed vascular plant, the moss *Physcomitrella patens*, the liverwort *Marchantia polymorpha* as well as the unicellular algae *Micromonas commoda* and *Coccomyxa subellipsoidea*.

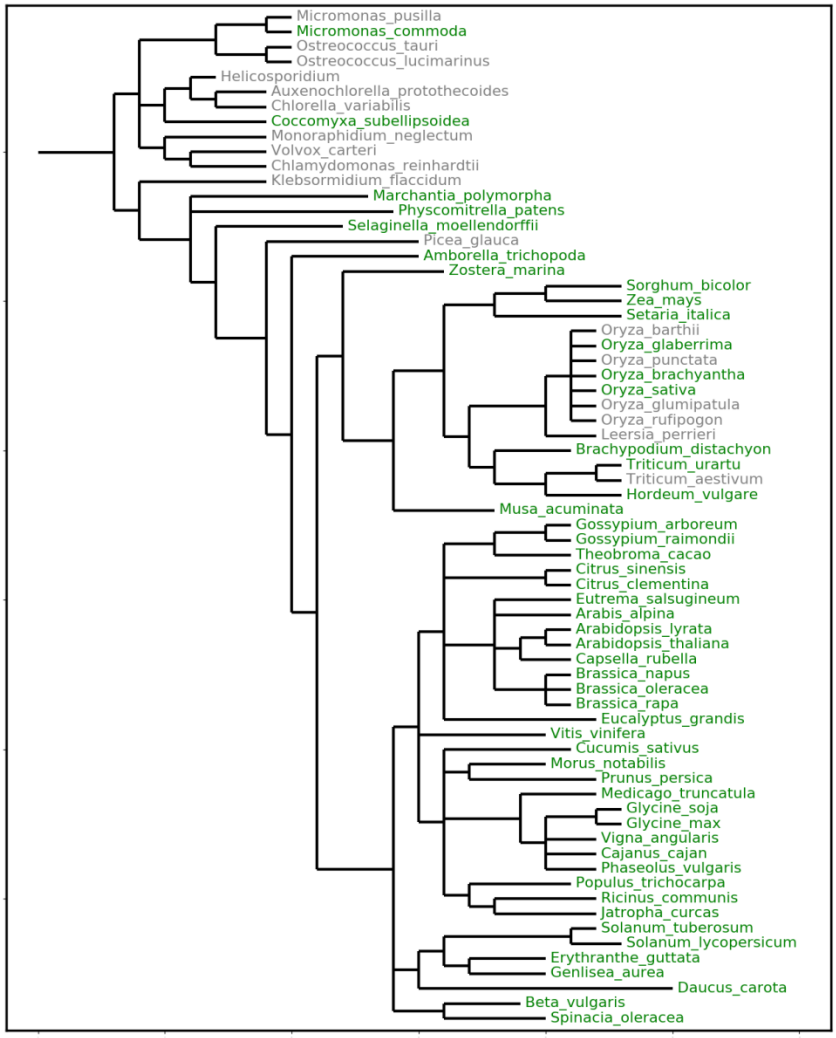

Figure 4.1 Taxonomic list of used plant reference proteomes from UniProt

From 69 plant reference proteomes available on UniProt, relevant hits could be found in 51 species (highlighted in green). The list spans from microcellular green algae up to higher plants. The unique gymnosperm proteome available, *Picea glauca*, was unfortunately not yet assembled and could not be used in the present work.

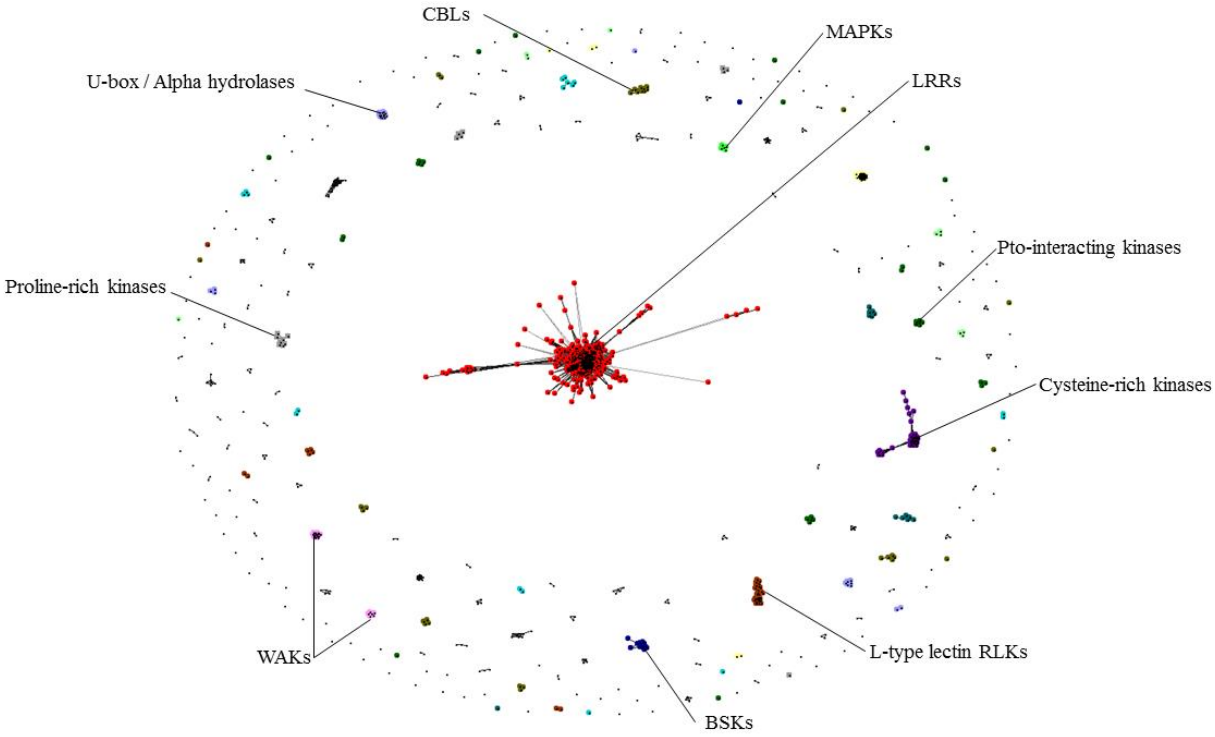

Figure 4.2 - CLANS map for the *A. thaliana* proteome

The cluster analysis of sequence (CLANS) is based on pairwise similarity scores. Here, the proteome of *A. thaliana*, with EFR as BLAST query, shows a central cluster containing all proteins containing plant-specific LRR which will be extracted and compiled with other LRR-containing clusters from other plant proteomes to create the starting dataset for further analyses. On this map, other similar, yet for us irrelevant proteins are found, such as CBLs, MAPKs, WAKs and other protein kinases.

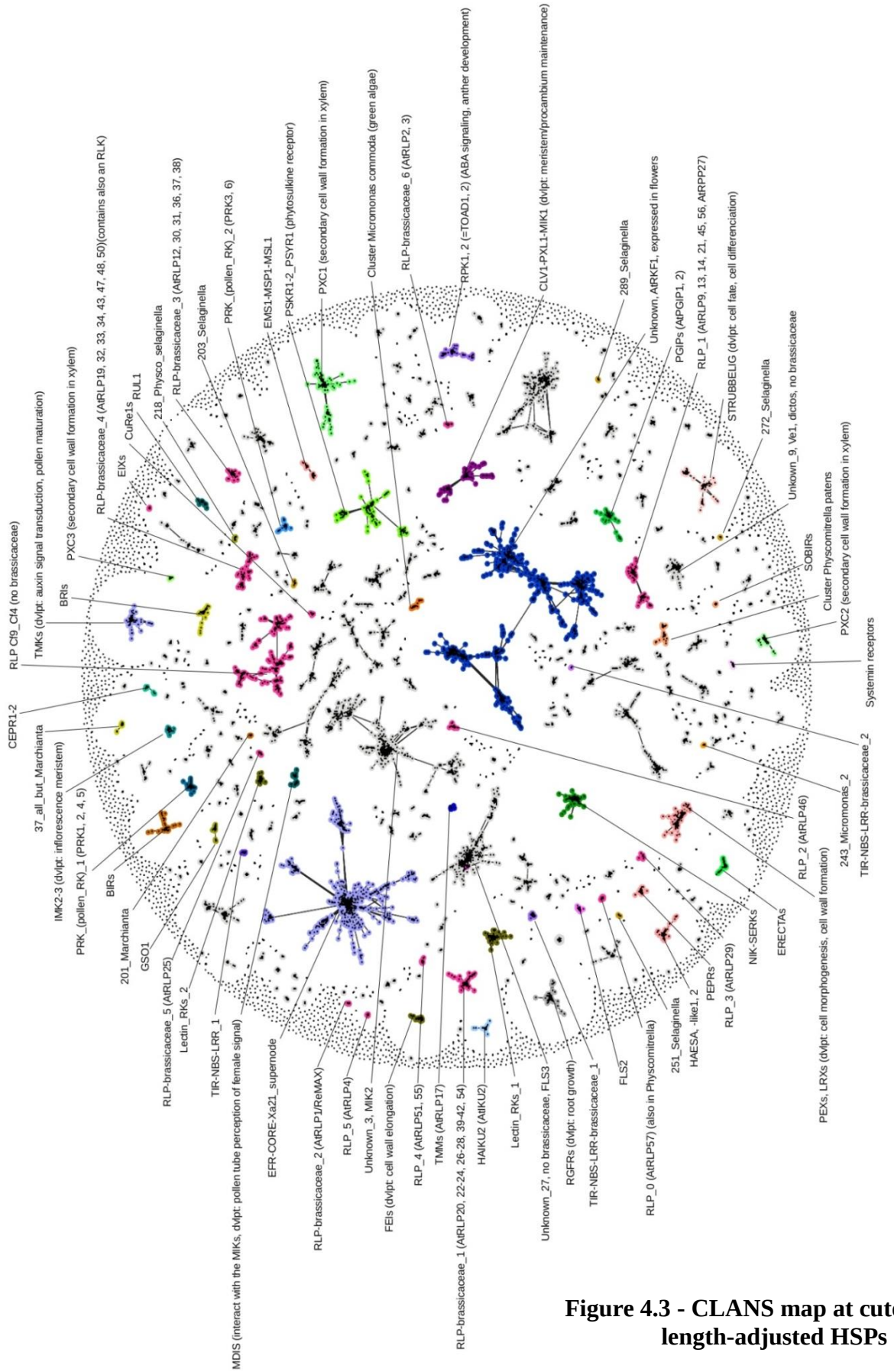

Figure 4.3 - CLANS map at cutoff 2.4 of length-adjusted HSPs

Based on 24 234 sequences from 51 plant UniProt Reference Proteomes. Map shows cluster formation after > 160 000 iterations.

Performing pairwise comparisons with the complete set of 24'234 LRR-sequences would give >5*10^8 combinations. In order to reduce the computing time, we established a cut-off at length-adjusted HSPs > 1 to generate the CLANS map, where still more than 5 million nodes were calculated. The CLANS map resulting from pairwise comparisons was run for about 160'000 iterations and clusters were named after known proteins within each cluster (Fig. 4.3).

Table 4.1 - Summary of the CLANS map analysis

Presence (+) or absence (-) of plant-specific LRR consensus, LRR-RLK- and LRR-RLP-architectures, as well as of protein families of interest could be accounted for in major plant groups by analysing the CLANS map. Of particular interest are CLV2 and SOBIR1, which are absent in monocots. For the full table, see Digital Table 2, as well as Digital Annex for the phylogenetic trees and FASTA files of each cluster of more than five sequences.

	green algae	*Marchantia polymorpha*	*Physcomitrella patens*	*Selaginella moellendorffii*	*Amborella trichopoda*	monocots	dicots
plant-specific LRR	+	+	+	+	+	+	+
LRR-RLK	(+)	+	+	+	+	+	+
LRR-RLP	(+)	+	+	+	+	+	+
NIK-SERK	-	+	+	+	+	+	+
CLV1	-	+	+	+	+	+	+
BIR	-	-	+	+	+	+	+
ERECTA	-	-	+	+	+	+	+
RLP_1	-	-	+	+	+	+	+
TMM	-	-	+	+	+	+	+
BRI1	-	-	-	-	+	+	+
SOBIR	-	-	-	-	+	-	+
CLV2	-	-	-	-	+	-	+
EFR-CORE-Xa21	-	-	-	-	+	+	+
FLS2	-	-	-	-	+	+	+
PEPR1	-	-	-	-	+	+	+

The first question we addressed was which taxa are present in which cluster. We generated phylogenetic trees for each selected cluster (see Digital Annex 1 for all figures of the phylogenetic trees for each cluster). We could not identify a cluster containing all species, yet some contain all multicellular plants, such as the NIK-SERKs, PXC1 and PXC2, or CLV1-PXL1-MIK1.

Many interesting information can be retrieved. For instance, the apparition of the NIK-SERK proteins seems to have preceded the evolution of their BIR negative regulators, for the former can be found in all branches more recently evolved than unicellular green algae (Table 4.1), while the latter are not present in *Merchantia polymorpha* (Table 4.1). BRI and BRI-likes emerged with Angiosperms (Table 4.1); indeed, no trace of a BRI1 or BRI1-like can be found in a BLASTp against the non-redundant database restricted to Acrogymnospermae (data not shown).

The presence of SOBIR can be detected in angiosperms but not in grasses (Table 4.1), where the protein lost part of the LRR domain and therefore does not show up in our dataset (Annex Fig. 2).

The cluster containing AtCLV2, implicated in shoot meristem maintenance, contains orthologs in all higher plants, with the exception of grasses, which again form a separate cluster, where it indeed misses 6 LRRs (Annex Fig. 3).

M. commoda and *C. subellipsoidea*, the two green algae present in the data set, do not seem to have proteins in common to multicellular plant species and thus, from this dataset, it is still not possible to know what evolved first: the structure or the function. Secondly, we can easily notice that LRR-RLPs evolved repeatedly in several species, with certain clusters being highly specific, such as the ones containing CuRe1 or ReMAX. Other LRR-RLPs clusters, such as RLP_0, contain up to 26 taxa spanning from *P. patens* up to higher plants, suggesting that these proteins did not evolve convergently in each taxum. This trivial result is nevertheless remarkable, for the current paradigm in plant

science is that LRR-RLPs are byproducts of older, more established LRR-RLKs. The function of this particular cluster remains to be characterized but the fact that there is only a low number of copies (38 proteins in total, see Digital Table 2) suggests that the function must be highly conserved and strongly selected for. In *A. thaliana*, AtRLP44 and AtRLP57 are the representative for this cluster. While AtRLP44 has been proposed to be involved in the BR signaling pathway (Wolf *et al.*, 2014), there is no double mutant line available for relevant phenotyping. Both genes have been also suggested as relatives of the OsPDOs, a family of rice developmental genes (Fritz-Laylin *et al.*, 2005).

Other clusters, such as unknown_27 or FLS2, are especially remarkable because they highlight two sides of a same coin when working with large amount of data. The cluster Unknown_27 contains the newly identified SlFLS3 receptor, which recognizes flgII-28, a second epitope from bacterial flagellin (Hind *et al.*, 2016). This cluster containes further 475 members from 29 taxa. At present, a physiological function or a ligand could not be associated to any of these other members. We can notice that Brassicaceae species are not present in this cluster, which corroborates the experimental evidence showing no PTI output in *A. thaliana* upon treatment with flgII-28 (Cai *et al.*, 2011). On the other hand, the FLS2 cluster, containing 52 members from 39 taxa, does not contain certain species among the spectrum of proteomes available, for which there is experimental evidence of defense responses to flg22, highlighting the problem in quality of the UniProt database. For instance, *Vitis vinifera* is known to have at least two copies of FLS2 (U. Fürst, personal communication) yet it fails to show up in this cluster. Indeed, when back checking on UniProt Reference Proteome database for AtFLS2 orthologs, there is no hits in *V. vinifera* and thus the problem lies in the database and not in our dataset.

The systemin perception in tomato was thought to be exclusive to Solanaceous species and to be a possible additional signaling system to the more widespread

PEPs. The identification of a cluster containing both SlSYSRE1 and SlSYSRE2 allowed us to discover the presence of similar proteins in other Solanaceous as well as in several grass species, raising the possibility that the systemin perception might be present in non-solanaceous species.

4.2 Molecular differences between LRR-RLKs and LRR-RLPs: converting a RLK into a RLP

4.2.1 Truncated EFR still undergoes complex formation with BAK1 but is not functional and does not recruit SOBIR1

Our first approach to understand the molecular difference between RLPs and RLKs was to truncate the kinase domain of EFR to make it look like a RLP (EFRΔkin, Fig. 4.4). Truncation of its kinase domain did not lead to a functional

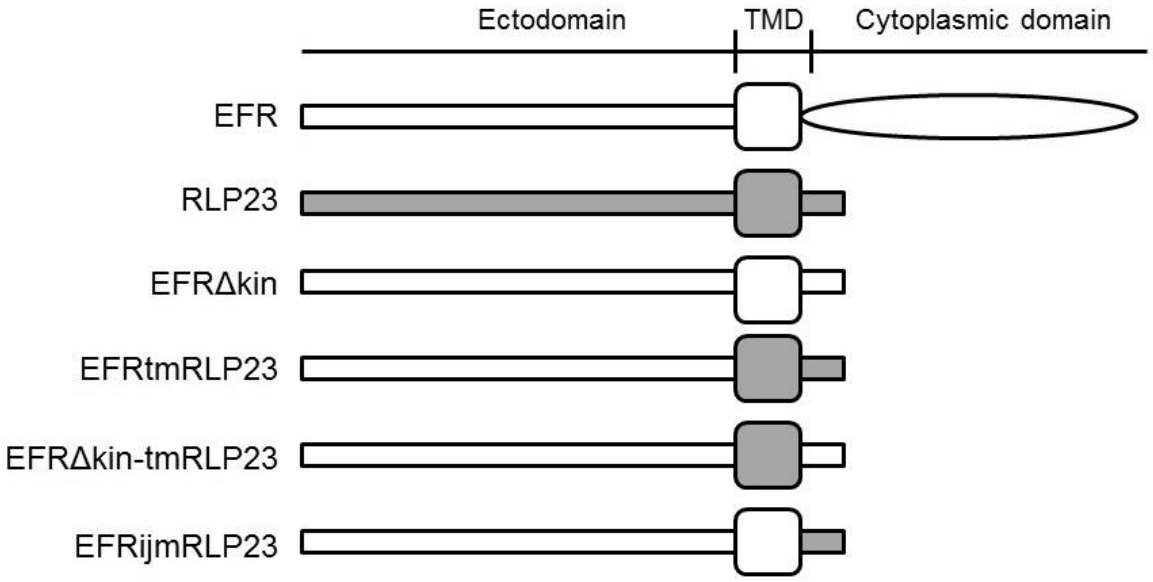

Figure 4.4 – Constructs used for turning a LRR-RLK into a LRR-RLP

To turn EFR into a RLP-like, we first truncated the kinase of EFR, resulting EFRΔkin. After that, we incorporated the TMD and C-tail of the functional RLP23 into EFRΔkin, to get EFRtmRLP23. We made two further constructs based on EFRΔkin containing the TMD of RLP23, EFRΔkin-tmRLP23, or the innerjuxtamembrane of RLP23, EFRijmRLP23. We built similar constructs using CLV2 or EIX2 parts, and other templates such as BRI1, CORE, SYSRE and PEPR1

EFR-receptor when tested for oxidative burst (Fig. 4.5) and ethylene production (Fig. 4.6) in transformed *N. benthamiana*. EFRΔkin could also not recruit SOBIR1, as shown in a co-immunoprecipitation from transformed *N. benthamiana* material (Fig. 4.7). Interestingly, EFRΔkin could still recruit BAK1 in a ligand-dependent manner thus strongly suggesting that the signal transduction and initiation of the signaling cascade works like a "zipper". Additional kinase truncation of various receptors, such as PEPR1, BRI1 or CORE were tested with similar output (Fig. 4.8).

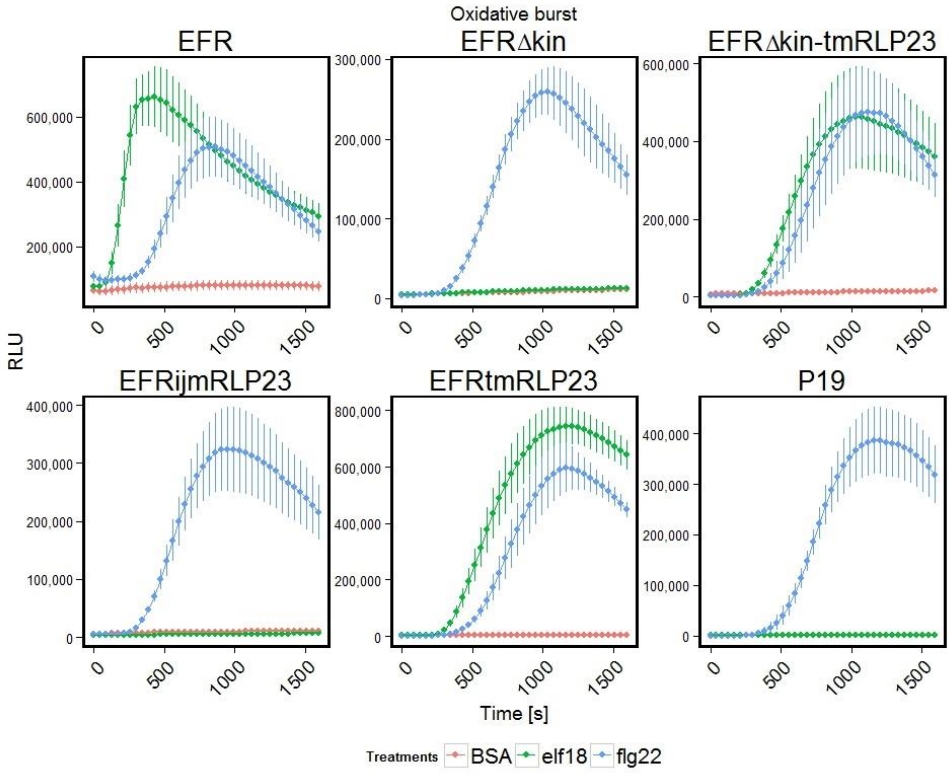

Figure 4.5 – Oxidative burst in transformed *N. benthamiana*

The immunity suppressor P19 was co-infiltrated in all transformations. Treatments were flg22 100 nM (blue, positive control), BSA (red, negative control) or elf18 100 nM. Data show mean ± SD in luminol-dependent light emission (RLU, relative light units) of at least 4 replicates.

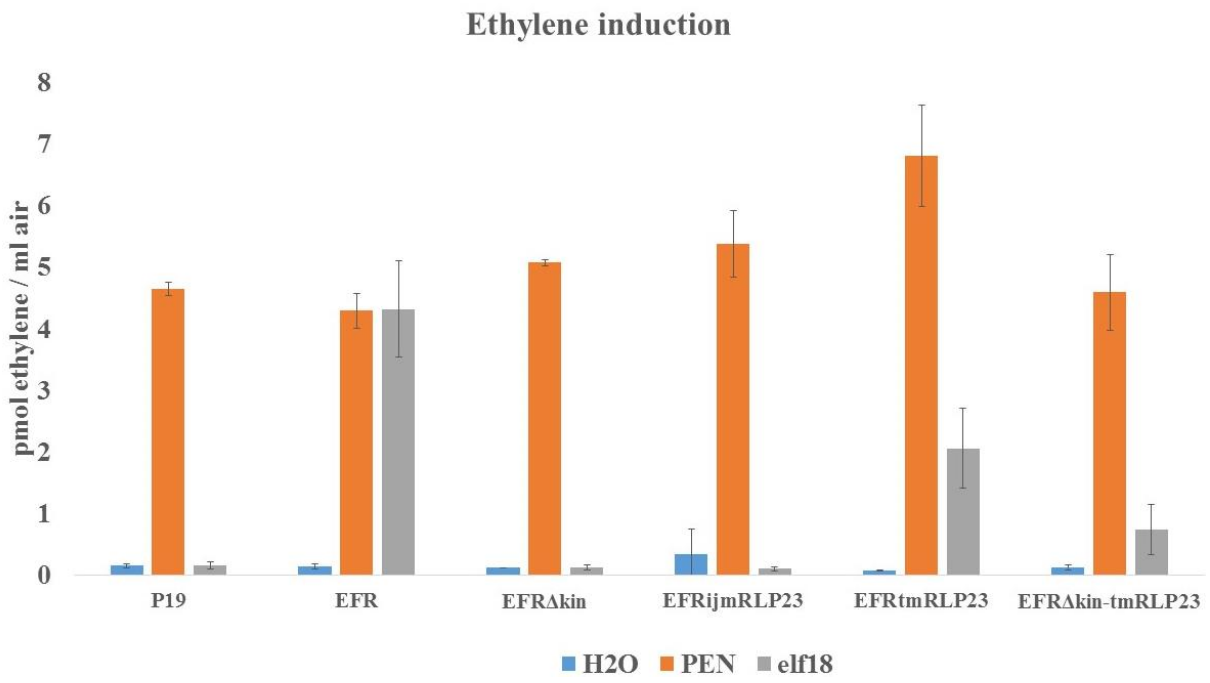

Figure 4.6 – Ethylene induction in transformed *N. benthamiana*

Ethylene induction in transformed leaf pieces treated for 3 h in the presence of 100 nM elf18 (grey), 4.5 µg Penicillium extract (orange, positive control) or water (blue, negative control). Values show mean ± SD in pmol ethylene per ml of air of 3 replicates.

4.2.2 EFRΔkin containing TMD and C-tail from RLP23 is functional and recruits SOBIR1

To investigate which domains are important for functionality as a RLP-like, we inserted in EFRΔkin the TMD and C-tail from AtRLP23, resulting in EFRtmRLP23 (see Fig. 4.4). EFRtmRLP23 proved to be functional in oxidative burst (Fig. 4.5) and ethylene production (Fig. 4.6). Consequently, EFRtmRLP23 could also recruit SOBIR1 as shown in a coIP experiment (Fig. 4.7). Additionally, we built and tested EFRtmEIX2, a similar construct based on SlEIX2 as RLP template, and obtained similar results (Fig. 4.9-4.11).

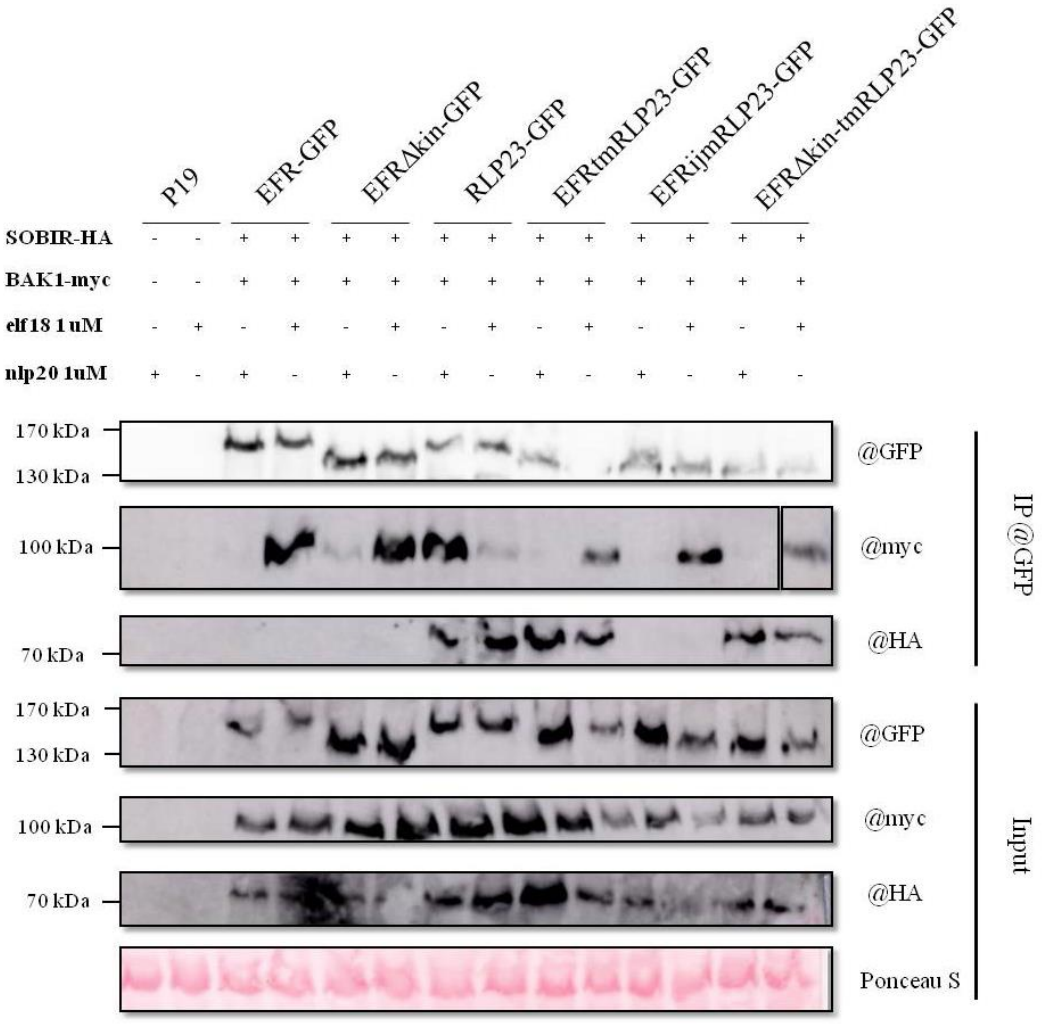

Figure 4.7 Co-immunprecipitation assay reveals interaction with SOBIR1 for constructs containing the TMD of RLP23

GFP-tagged receptors, SOBIR1-HA and BAK1-myc were expressed in *N. benthamiana* leaves for 72 h, were purified and tested for complex formation upon ligand-perception. Peptide were infiltrated at 1 µM for 3 min prior to harvest.

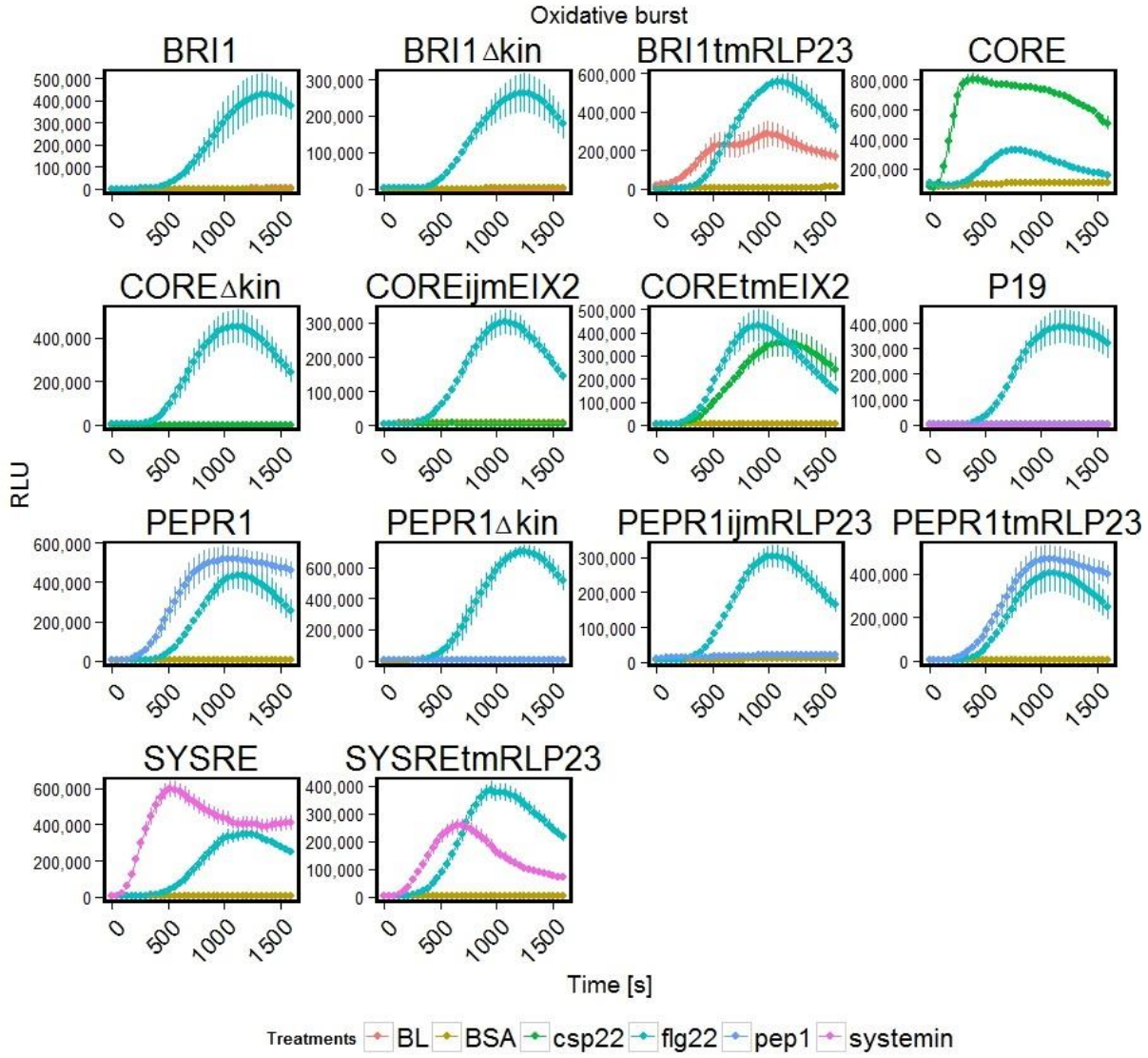

Figure 4.8 Oxidative burst in transformed *N. benthamiana*

The immunity suppressor P19 was co-infiltrated in all transformations. Treatments were flg22 100 nM (blue, positive control), BSA (yellow, negative control), pep1 100 nM (light blue), BL 1 uM (red), csp22 (green) or systemin 100 nM (pink). Data show mean ± SD in luminol-dependent light emission (RLU, relative light units) of at least 4 replicates.

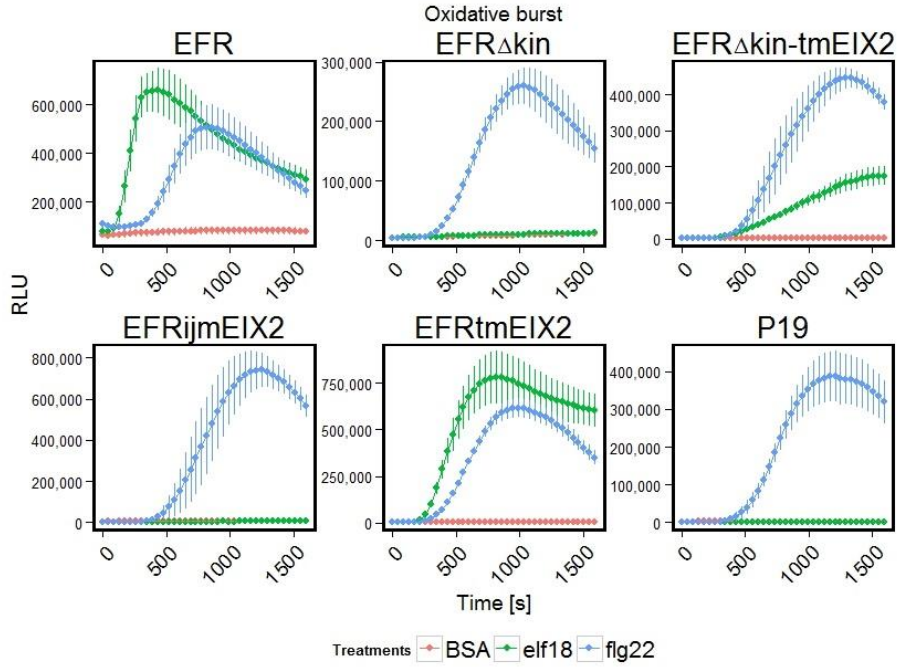

Figure 4.9 Oxidative burst in transformed *N. benthamiana*

The immunity suppressor P19 was co-infiltrated in all transformations. Treatments were flg22 100 nM (blue, positive control), BSA (red, negative control) or elf18 100 nM. Data show mean ± SD in luminol-dependent light emission (RLU, relative light units) of at least 4 replicates. Data for EFR, EFRΔkin and P19 are reused from Fig. 4.5.

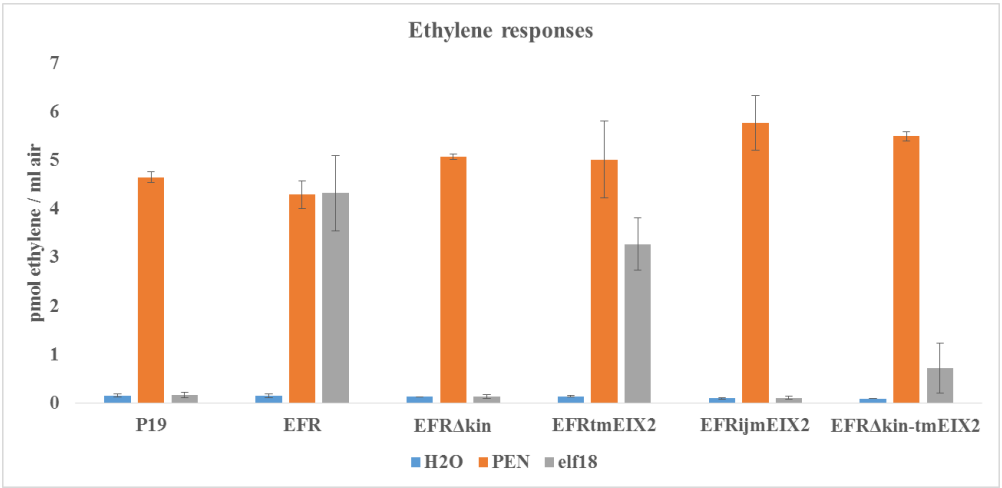

Figure 4.10 Ethylene induction in transformed *N. benthamiana*

Ethylene induction in transformed leaf pieces treated for 3 h in the presence of 100 nM elf18 (grey), 4.5 µg Penicillium extract (orange, positive control) or water (blue, negative control). Values show mean ± SD in pmol ethylene per ml of air of 3 replicates. Data for EFR, EFRΔkin and P19 are reused from Fig. 4.6.

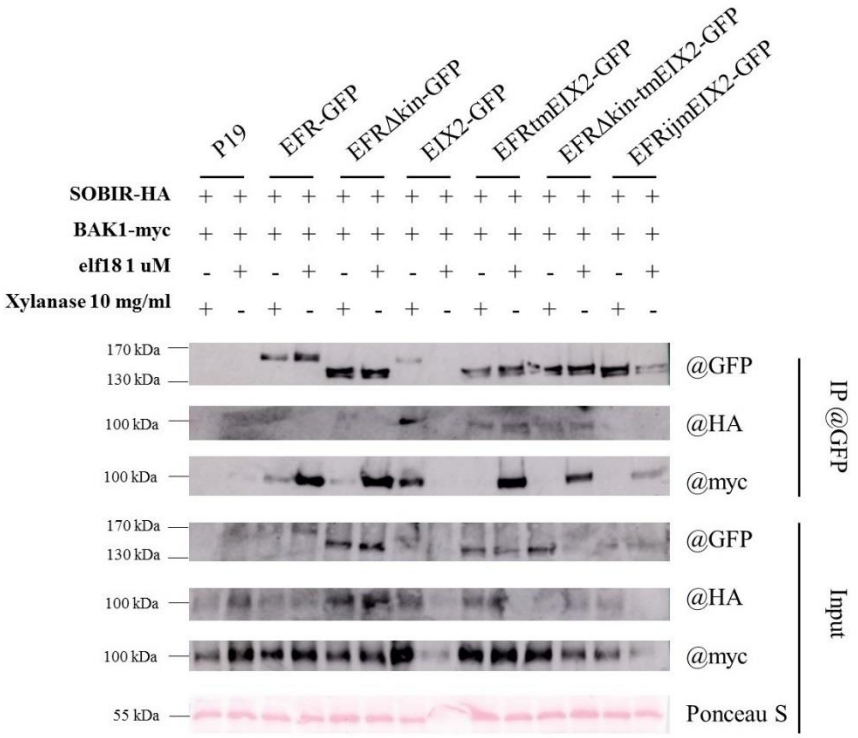

Figure 4.11 Co-immunprecipitation assay reveals interaction with SOBIR1 for constructs containing the TMD of EIX2

GFP-tagged receptors, SOBIR1-HA and BAK1-myc were expressed in *N. benthamiana* leaves for 72 h, were purified and tested for complex formation upon ligand-perception. Xylanase and elf18 were infiltrated at 10mg/ml and 1 µM, respectively, for 3 min prior to harvest.

4.2.3 EFRΔkin containing the TMD alone from RLP23 can recruit SOBIR1 and is functional

Further chimeric constructs were generated from EFRΔkin, replacing exclusively the TMD (EFRΔkin-tmRLP23) or the C-tail (EFRijmRLP23) of AtRLP23 (see Fig. 4.4). EFRijmRLP23 did not signal the perception of elf18 (Fig. 4.5, 4.6), similar to EFRΔkin. Accordingly, this construct could not recruit SOBIR1 (Fig. 4.7) but was able to recruit BAK1 after ligand perception. This suggests that SOBIR1 and BAK1 ectodomains do not directly interact. Conversely, EFRΔkin-tmRLP23, containing the TMD of RLP23 but a C-tail from truncated EFR kinase, proved to be functional in signaling elf18 perception and in recruiting SOBIR1 (Fig. 4.5-4.7). However, the amplitude and the kinetics of the responses seemed to be somewhat lower, suggesting that although

the TMD is decisive, additional information important for signal propagation is encoded in the C-tail of RLPs. Additionally, we built and tested, EFRΔkin-tmEIX2 and EFRijmEIX2, two similar constructs based on SlEIX2 and obtained similar results (Fig. 4.9-11).

4.2.4 What can we learn from the CLV3 pathway?

AtRLP10/CLV2 is involved in the shoot apical meristem (SAM) maintenance and interact constitutively with the pseudo-kinase CORYN (CRN) through a TMD-TMD interaction; they get together in the ER prior to being exported as a complex to the plasma membrane (Bleckmann *et al.*, 2010).
In a similar fashion as others RLPs, AtCLV2 contains an interaction surface with a (small)xxx(small) motif with a compensation on the other side of its TMD by large hydrophobic residues.

CLV3 is the ligand being recognized by CLV1 (and potentially by CLV2) and does not trigger PTI. Additional chimeric receptors, containing the ectodomain of AtEFR and the TMD and C-tail of AtCLV2 (EFRtmCLV2) or only the TMD of AtCLV2 and the iJM of a truncated EFR kinase (EFRΔkin-tmCLV2) were built and assessed for functionality. EFRtmCLV2 showed a significant oxidative burst in *N. benthamiana* after treatment with elf18 (Fig. 4.12a, b). Accordingly, ethylene production in plants expressing this construct was higher than the P19 negative control (Fig. 4.12c), yet did not reach comparable levels with other EFR RLP-like constructs (see above). Additional isolation of CLV2 TMD in the EFRΔkin-tmCLV2 construct resulted in detectable amount of ROS production but no detectable ethylene production (Fig. 4.12b and 4.12c).

Because CLV2 is a LRR-RLP whose interaction with both CRN and SOBIR1 was claimed, it is not clear how these two co-receptors are involved with CLV2 (Bleckmann *et al.*, 2010; Liebrand *et al.*, 2013; Bi *et al.*, 2015). To re-examine this, EFRtmCLV2 and EFRΔkin-tmCLV2 were immunoprecipitated and tested

for presence of CRN and / or SOBIR1 (Fig. 4.13). In our hands, these constructs could be detected with CRN but not with SOBIR1.

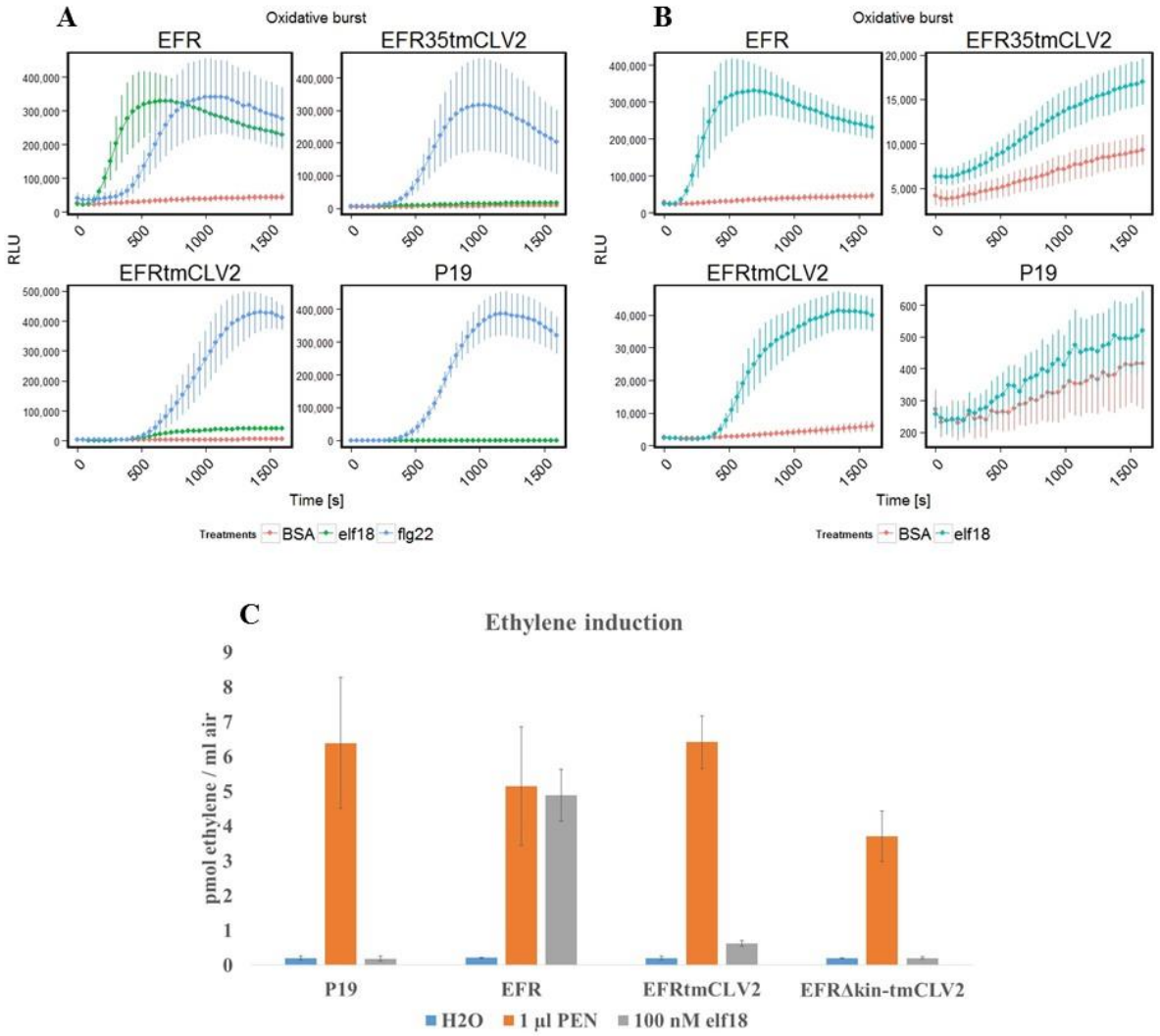

Figure 4.12 – TMD of CLV2 is also functional in EFRΔkin backbone

(A) Oxidative burst in *N. benthamiana*. Treatments were flg22 100 nM (blue, positive control), BSA (red, negative control), elf18 100 nM (green). Data show mean ± SD in luminol-dependent light emission (RLU, relative light units) of at least 4 replicates. (B) Same data as in A, but flg22 data were removed to better see what is happening at lower scale. BSA (red, negative control) and elf18 100 nM (blue). (C) Ethylene induction in transformed leaf pieces treated for 3 h in the presence of 100 nM elf18 (grey), 4.5 µg Penicillium extract (orange, positive control) or water (blue, negative control). Values show mean ± SD in pmol ethylene per ml of air of 3 replicates. Data for EFR and P19 are reused from Fig. 4.5 and Fig. 4.6.

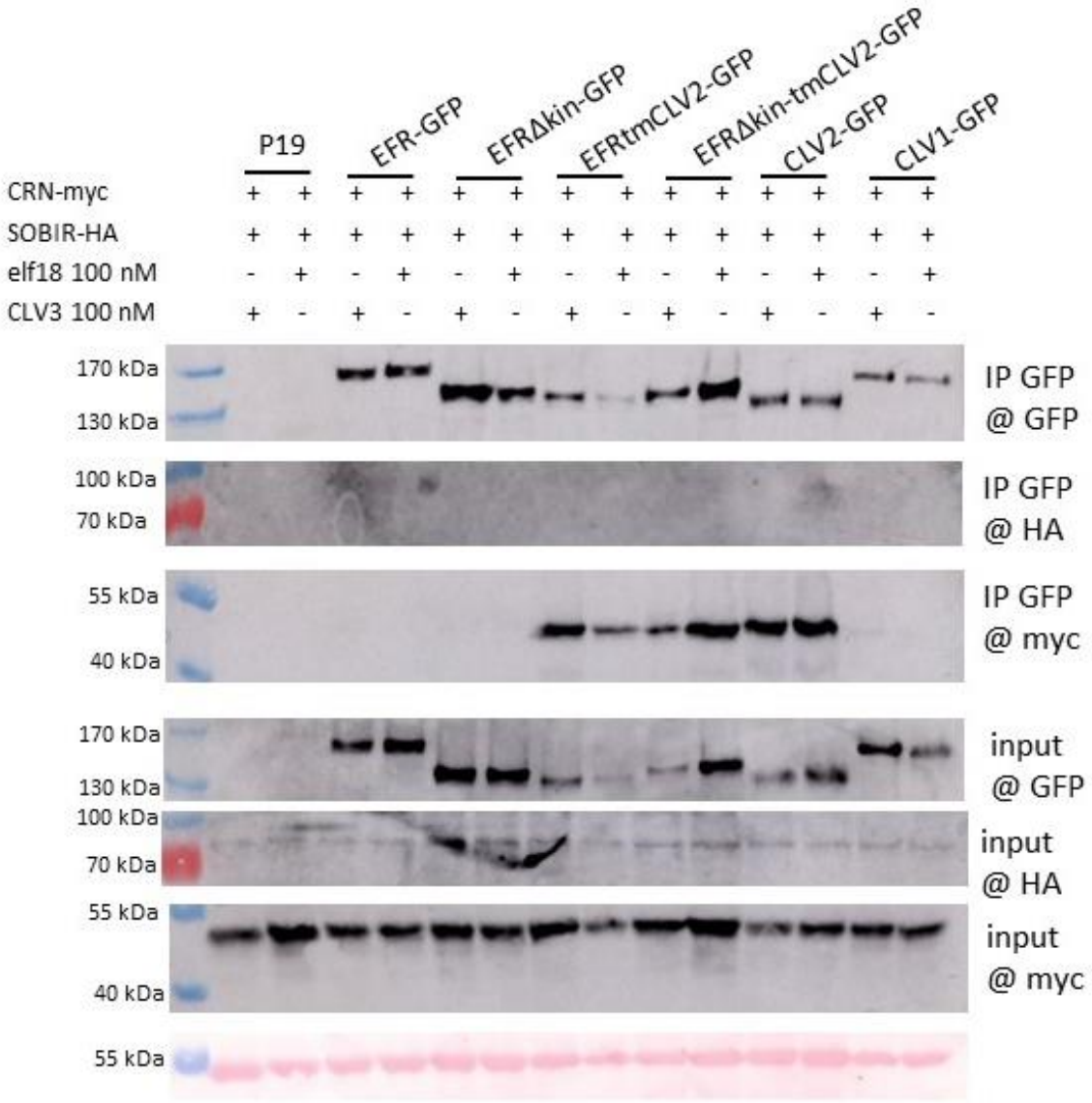

Figure 4.13 – Constructs containing the TMD of CLV2 co-immunprecipitate with CRN and not with SOBIR1

GFP-tagged receptors, SOBIR1-HA and CRN-myc were expressed in N. benthamiana leaves for 72 h, were purified and tested for complex formation upon ligand-perception. Peptide were infiltrated at 100 nM for 3 min prior to harvest.

Furthermore, CLV1 has been shown to directly bind the CLV3 peptide (Ogawa *et al.*, 2008; Ohyama *et al.*, 2009). Yet, RPK2 and CLV2 have been suggested as additional receptors for CLV3 recognition (Kayes and Clark, 1998; Bleckmann *et al.*, 2010; Kinoshita *et al.*, 2010; Zhu *et al.*, 2010; Pan *et al.*, 2016). These studies were however always based on loss-of-function in mutant plants. We

performed CLV3 binding assay with CLV1 and CLV2 with CRN, using CLV3 acridinium-labeled peptides with a 1000-folds excess of unlabeled competitors. Unfortunately, no binding could be detected for CLV2 in crude extracts (Fig. 4.14a). To test whether there was something wrong with the acri-CLV3 peptides, we performed a control experiment with CLV1, as well as with SlFLS2 and acri-flg22 as positive control. After immunoenrichment of AtCLV1-GFP and SlFLS2-GFP, we could detect binding of flg22 but not of CLV3 (Fig. 4.14b), thus pointing towards a failure in the placement of the acridinium side chain into the CLV3 peptides. This observation was subsequently confirmed via root-growth assay (P. Schulz & R. Simon, personal communication; see Annex Fig. 4).

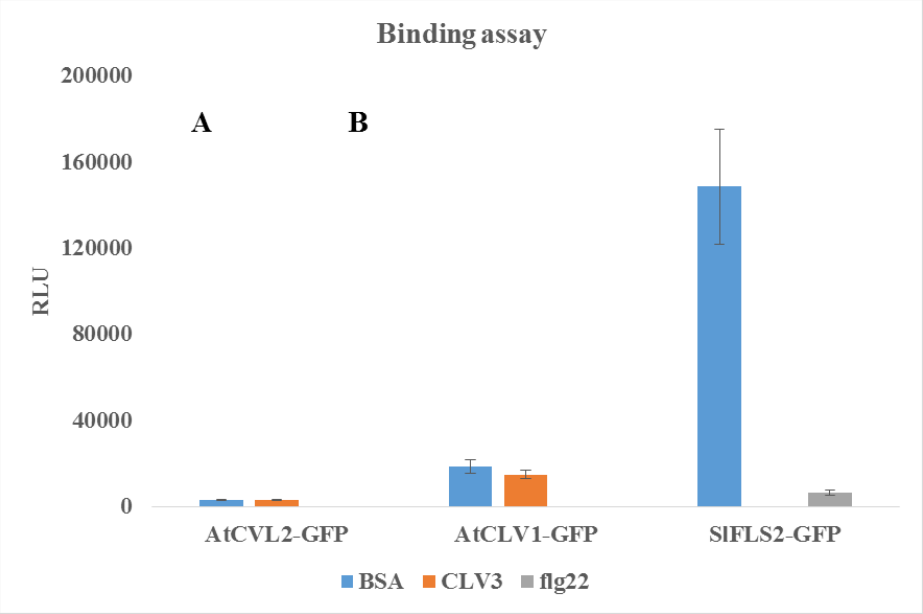

Figure 4.14 – CLV1 and CLV2 do not bind to acri-CLV3

No acri-CLV3 binding can be detected in crude extracts containing CLV2 (A), but also in immunopurified CLV1 (B). As control, SlFLS2 shows a nice binding to acri-flg22 in the absence of unlabelled competitors.

Finally, the CLV3-CLV1 is a remarkable study case, for it is one of the very few known LRR-RLKs whose co-receptor has not yet been identified with high certainty. CLV1 homodimer as well as heterodimeric complex formation with CLV2 have been suggested (Bleckmann *et al.*, 2010), but there is no supported

evidence as to the real composition of the CLV1 receptorsome. Here, we tested the naive hypothesis that CLV1, as a LRR-RLK, could be interacting with SERK3. We additionally wanted to test again whether the LRR-RLP CLV2 interact with SOBIR1 and/or SERK3. *N. benthamiana* transformation with GFP labeled CLV1, CLV2, EFR and RLP23 (as controls), as well as SOBIR1-HA and SERK3-myc, should give us a direct clue as to their potential interaction which could be peptide-dependent. As depicted on Figure 4.15, the positive controls EFR and RLP23 displayed the previously reported interaction with SERK3 on a ligand-dependent manner. Additionally, RLP23 was forming a constitutive interaction with SOBIR1. Neither SERK3 nor SOBIR1 could be coimmunoprecipitated with CLV1 or CLV2, independent from the presence of the (putative) ligand CLV3 (Fig. 4.15). The absence of SOBIR1-CLV2 interaction observed in Fig. 4.13 is here confirmed. The lack of complex formation of SERK3 in this experiment could be a good hint that this protein is not a co-receptor for CLV1/CLV2, yet the possibility remains that a third player, necessary for correct complex activation or complex exportation to the plasma membrane, might not be present in *N. benthamiana* leaves. Further experiments using other SERKs and the NIKs should be conducted to fully discard them from the list of potential candidates.

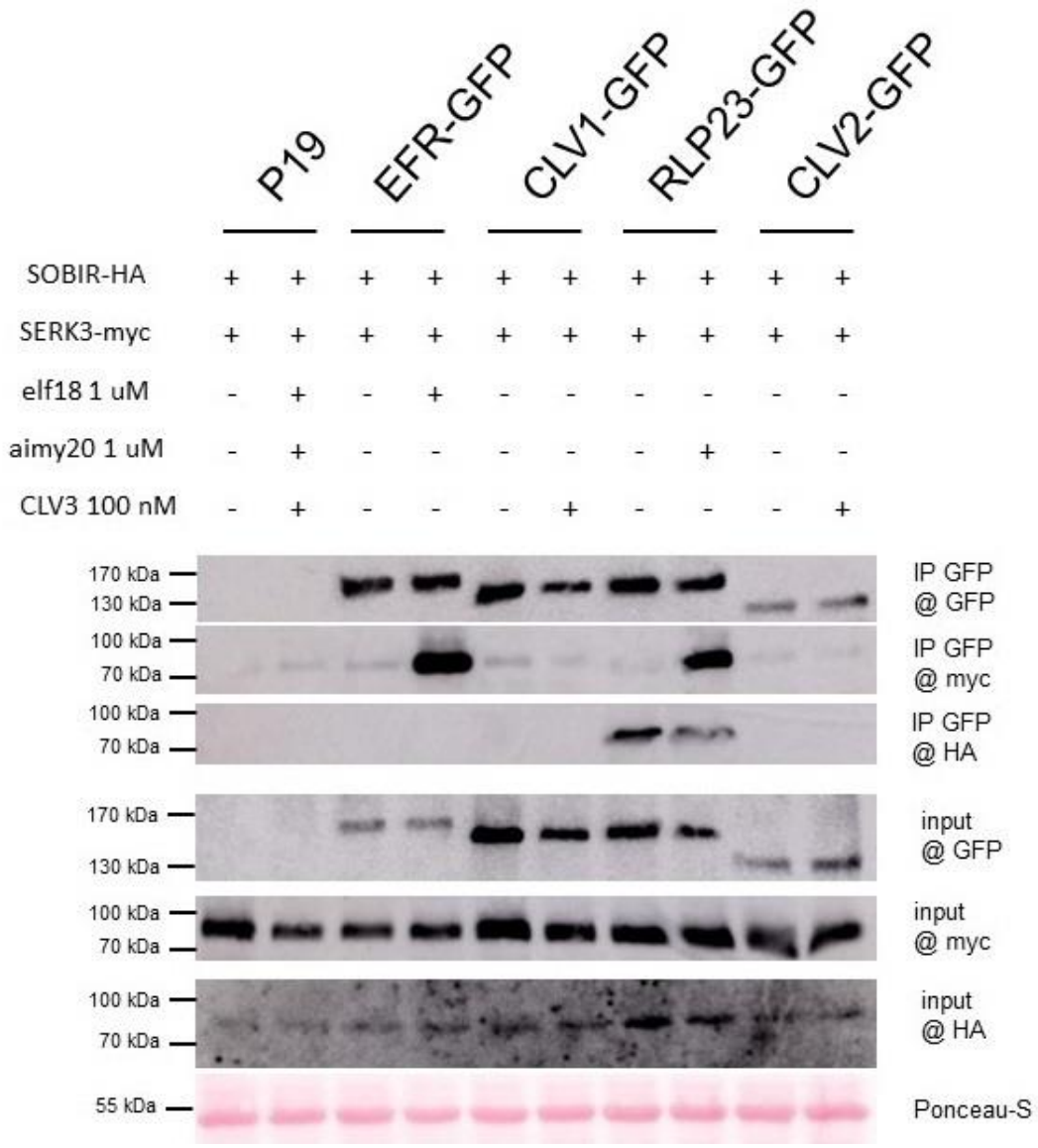

Figure 4.15 – Neither CLV1 nor CLV2 interact with BAK1 or SOBIR1

GFP-tagged receptors, SOBIR1-HA and BAK1-myc were expressed in *N. benthamiana* leaves for 72 h, were purified and tested for complex formation upon ligand-perception. Peptide were infiltrated at 1 µM for 3 min prior to harvest.

4.3 Molecular differences between LRR-RLKs and LRR-RLPs: converting a RLP into a RLK

To identify the molecular characteristics of RLKs and based on the previous results, we generated chimeric receptors containing the ectodomain of RLP23 and either the TMD and kinase of SOBIR1 (RLP23tmkSOBIR1) or the TMD of SOBIR1 and the cytoplasmic C-tail of RLP23 (RLP23tmSOBIR1, Fig. 4.16) to assess what molecular features are important for RLK-like functionality. As

control, we built similar construct based on EIX2 and EFRΔkin. We transiently expressed these constructs in *N. benthamiana*, a RLP23-, EIX2- and EFR-free background, and could observe for all constructs a gain of perception to nlp20, xylanase and elf18, respectively (Fig. 4.17-19). The constitutive interaction with SOBIR1 and the ligand-dependent interaction with BAK1 for RLP23tmkSOBIR1 and EFRtmkSOBIR1 was subsequently shown in a co-immunoprecipitation assay from transformed *N. benthamiana* material (Fig. 4.20), thus suggesting a tripartite kinase complex. Finally, to determine whether these constructs truly behave like RLKs, we measured the induction of FRK1 in protoplasts of *A. thaliana* sobir1-12 mutants transiently expressing either RLP23tmkSOBIR1 or RLP23tmSOBIR1. As depicted in Figure 4.21, RLP23tmkSOBIR1, but not RLP23tmSOBIR1, could induce FRK1 expression, thus showing that the former does behave like a RLK.

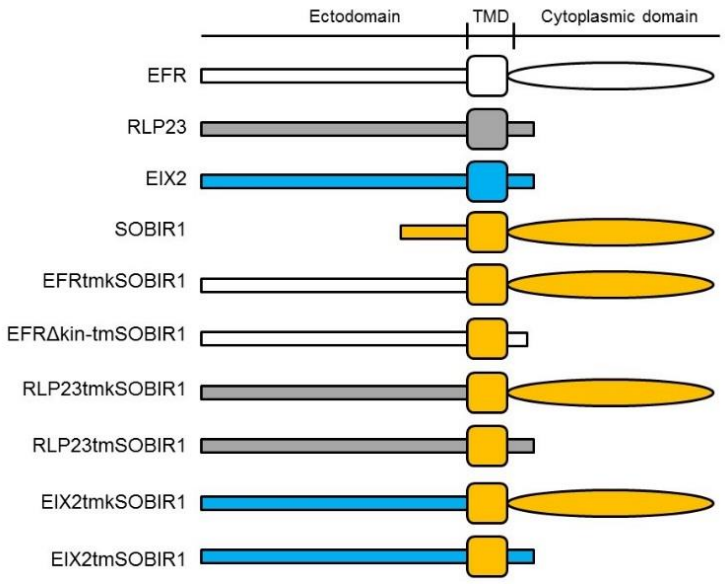

Figure 4.16 Constructs used for turning a LRR-RLP into a LRR-RLK

To turn RLP23 or EIX2 into a RLK-like, we added the TMD and the kinase of SOBIR1. To ensure that the resulting RLP23tmkSOBIR1 and EIX2tmkSOBIR1 behaves like a RLK, we built RLP23tmSOBIR1 and EIX2tmSOBIR1 as control. We also built EFRtmkSOBIR and EFRΔkin-tmSOBIR1 as controls.

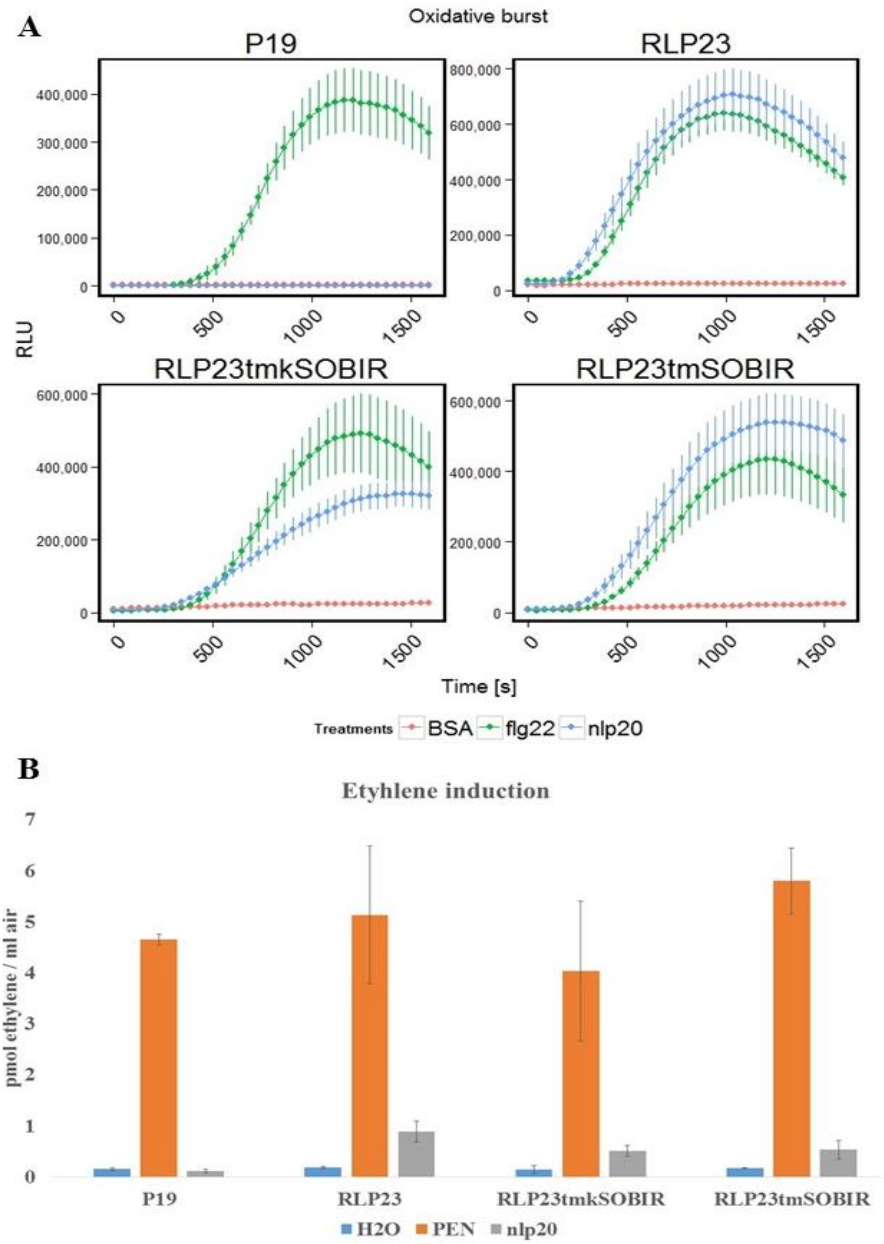

Figure 4.17 - RLP23 constructs containing the TMD of SOBIR1 can propagate nlp20 signaling

(A) Oxidative burst, treatments were flg22 100 nM (green, positive control), BSA (red, negative control) or nlp20 100 nM (blue). Data show mean ± SD in luminol-dependent light emission (RLU, relative light units) of at least 4 replicates. (B) Ethylene induction in transformed leaf pieces treated for 3 h in the presence of 100 nM nlp20 (grey), 4.5 µg Penicillium extract (orange, positive control) or water (blue, negative control). Values show mean ± SD in pmol ethylene per ml of air of 3 replicates. Data for P19 are reused from Fig. 4.5 and 4.6.

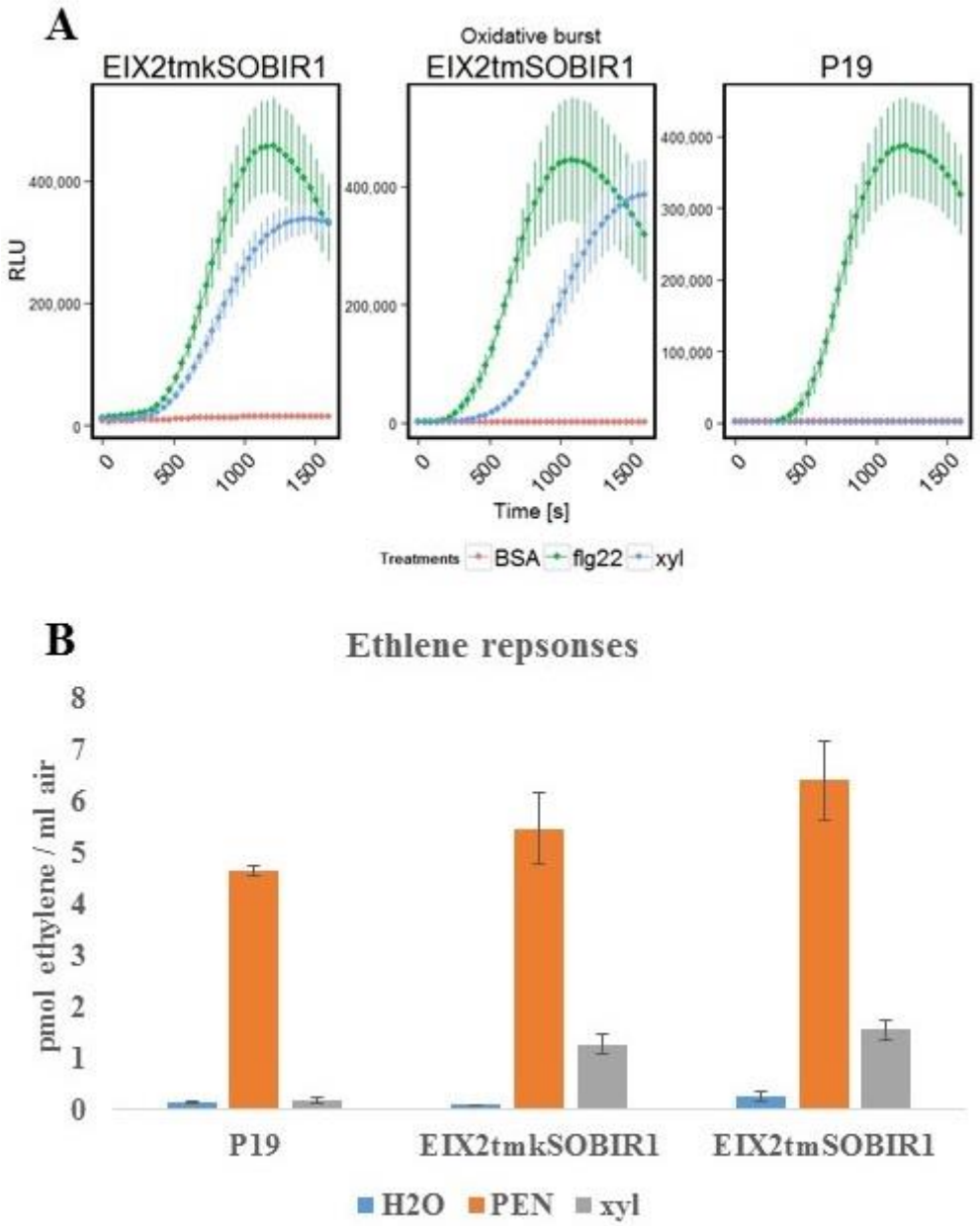

Figure 4.18 EIX2 constructs containing the TMD of SOBIR1 can propagate xylanase signaling

(A) Oxidative burst, treatments were flg22 100 nM (green, positive control), BSA (red, negative control) or xylanase 1 mg/ml (blue). Data show mean ± SD in luminol-dependent light emission (RLU, relative light units) of at least 4 replicates. (B) Ethylene induction in transformed leaf pieces treated for 3 h in the presence of 1 mg xylanase (grey), 4.5 µg Penicillium extract (orange, positive control) or water (blue, negative control). Values show mean ± SD in pmol ethylene per ml of air of 3 replicates. Data for P19 are reused from Fig. 4.5 and 4.6.

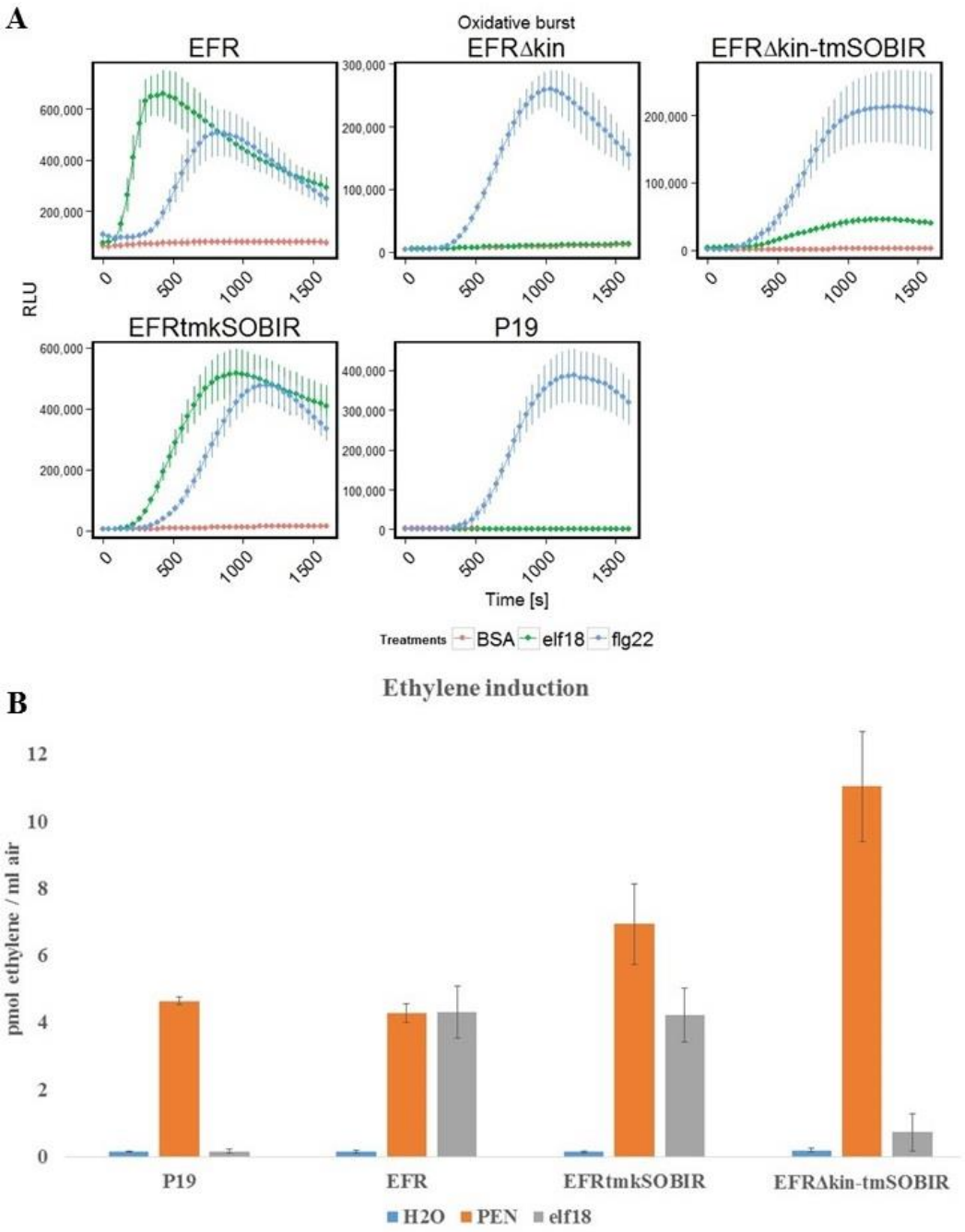

Figure 4.19 EFR constructs containing the TMD of SOBIR1 can propagate elf18 signaling

(A) Oxidative burst, treatments were flg22 100 nM (blue, positive control), BSA (red, negative control) or elf18 100 nM (green). Data show mean ± SD in luminol-dependent light emission (RLU, relative light units) of at least 4 replicates. (B) Ethylene induction in transformed leaf pieces treated for 3 h in the presence of 100 nM elf18 (grey), 4.5 µg Penicillium extract (orange, positive control) or water (blue, negative control). Values show mean ± SD in pmol ethylene per ml of air of 3 replicates. Data for EFR, EFRΔkin and P19 are reused from Fig. 4.5 and 4.6.

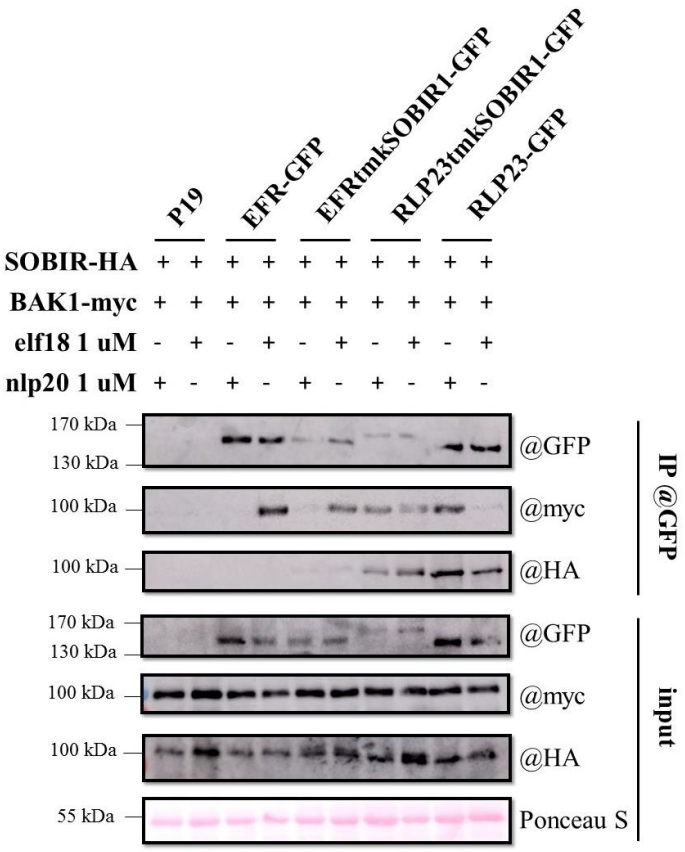

Figure 4.20 - Coimmunoprecipitation of RLP23tmkSOBIR1 with SOBIR1 and BAK1

GFP-tagged receptors, SOBIR1-HA and BAK1-myc were expressed in *N. benthamiana* leaves for 72 h, were purified and tested for complex formation upon ligand-perception. Peptide were infiltrated at 1 µM for 3 min prior to harvest.

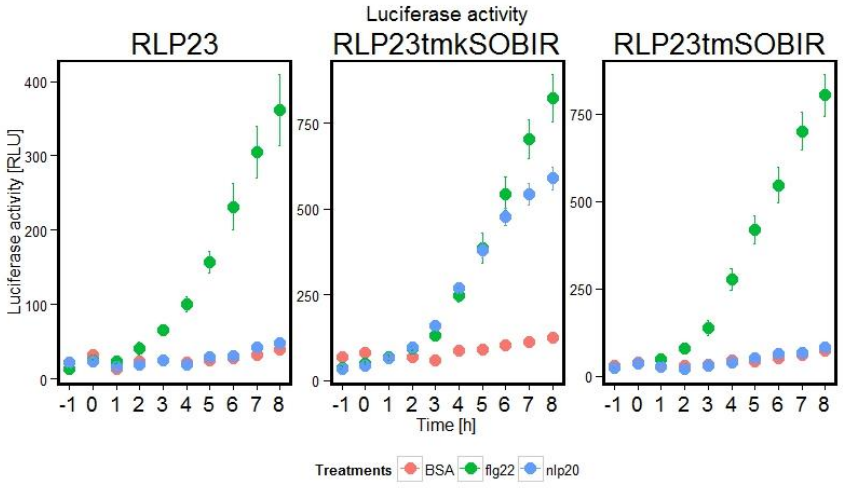

Figure 4.21 – RLP23tmkSOBIR can induce FRK1 in A. thaliana sobir1-12 mutant

Induction of the reporter gene pFRK1::luc in protoplasts of *A. thaliana* sobir1-12 mutant complemented with RLP23, RLP23tmkSOBIR or RLP23tmSOBIR and treated with BSA (red), flg22 (green) or with nlp20 (blue).

4.4 Analysis of TMD sequences using Shannon's entropy

Based on the above results, we extracted from our CLANS map (see section Results 4.1) the sequences of SOBIR1, EFR, RLP23, FLS2 and EIX2 and their respective homologs from other plant species and aligned their TMD sequences. We then analyzed the variation of the canonical TMD sequences and calculated the entropy for each position, using Shannon's equation (Shannon, 1948). After that, we plotted the resulting consensus sequences, with uppercase symbols representing the amino acids that are highly conserved and lowercase letters representing positions where there is some variation among the canonical sequences. We fitted the entropy of each position to a hypothetical α-helix momentum. The angle in a straight α-helix is of 3.63 residues per turn, but natural variations can present angles of 3.5 (7 residues over 2 complete turns, depicted as 7/2), 3.6 (18/5), 3.66 (11/3) or 3.75 (15/4) (Lupas and Bassler, 2017). We fitted the entropies of our TMD canonical sequences on the best helical momentum, as based on the conservation of each position of the TMD. As depicted on Fig. 4.22, the TMD sequences of EIXs, RLP23s and SOBIR1s contain a highly conserved GxxxG motif, whereas the TMD of EFRs or FLS2s do not present such a motif. Moreover, the TMD of LRR-RLPs and SOBIR1 are richer in aromatic residues which are located opposite, before or after to the GxxxG motif. Such residues are in contrast not present in such proportions in the TMDs of LRR-RLKs.

Furthermore, the GxxxG motif in the TMD of SOBIR1 locates in the first half of the sequence, whereas this motif appears in the middle and final sections of the TMD from LRR-RLPs, thus suggesting that other residues are playing a role and might act as key-hole actors to ensure the specificity of interaction.

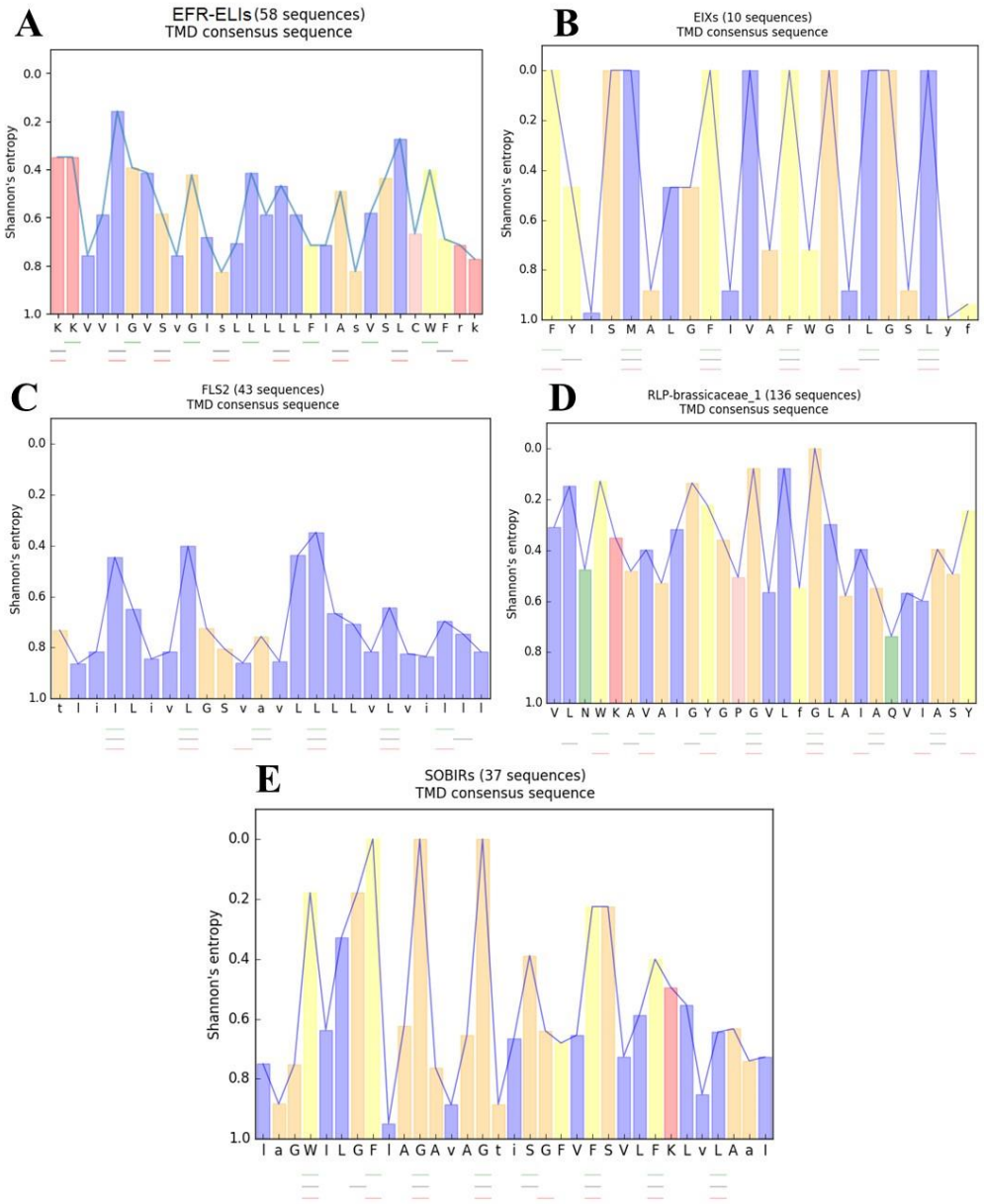

Figure 4.22 – Entropy analysis of TMD consensus sequences

The entropy of each position in canonical TMD sequences reveals the conservation momentum of the α-helix for LRR-RLKs and LRR-RLPs. (A) EFR and EFR-likes (ELIs, 58 sequences), (B) EIX2 (10 sequences), (C) FLS2 (43 sequences), (D) RLP23 and homologs from Brassicaceae (136 sequences), (E) SOBIR1 (37 sequences). Entropy of 0.0 means high conservation (no variation), entropy of 1.0 means low conservation (high variation). Red for charged residues (R, K), green for polar residues (N, Q), salmon for proline (P), orange for small side chain residues (G, S, T, A), blue for hydrophobic residues (I, L, V) and yellow for hydrophobic residues with an aromatic ring (F, Y, W). The best three models for α-helix momentum are indicated below the consensus sequence and show entropy fits.

5. Discussion

Signal transduction across the plasma membrane is a highly-studied field of research, yet the encoding of specificity is not fully understood. The LRR structure is particularly well suited for protein-protein interaction and is present in all kingdoms of life (Kobe and Kajava, 2001), even though plant and animal LRR receptors evolved convergently (Ausubel, 2005; Fliegmann and Felix, 2016). There exists several subfamilies of LRR architectures which vary in the length of the repeated motifs as well as in the secondary structure in the segment binding two LRRs (Kobe and Kajava, 2001). For instance, the LRRs present in the LRR subfamily of the Ribonuclease-Inhibitors, initially identified in pigs is typically 28-29 residues long and contains a α-helix in the variable region of the LRR (Kobe & Kajava, 2001). In plants, the typical LRR sequence for extracellular receptors is 24 residues long, with a IPxxLxxLxxLxxLxLxxNxL(T/S)Gx consensus, where x can be any residue (Kobe and Kajava, 2001; Mueller *et al.*, 2012*a*). The terminal NxxxG motif is thought to be a plant-specific LRR hallmark and can highly facilitate the recognition of plant LRR-proteins (G. Felix, personal communication). LRR-RLKs and -RLPs are part of the wide array of cell surface-located receptors that mediates the perception of certain pathogens (among other signals) and that require specific co-receptors to initiate the cytoplasmic signaling cascade. The evolution of this receptor clade in plants has been reported to various degrees of depth, going from single species, to whole vascular plants (Fritz-Laylin *et al.*, 2005; Mondragon-Palomino and Gaut, 2005; Yue *et al.*, 2012; Liu *et al.*, 2017). Certain genetic components have been recently identified in *P. patens* and *S. moellendorfii*, revealing the presence of LRR-RLK in early land plants (Liu *et al.*, 2017). Yet, computer-based reports failed so far to grasp the dynamics of domain swaps that acts on the evolution the LRR-containing proteins. For instance, there is no published systematical study on both LRR-RLPs and –

RLKs. In the present work, we identified 24’324 proteins in 51 UniProt reference proteomes. We could identify at least two clusters of LRR-containing proteins in the unicellular green algae *Micromonas commoda*. They do not contain signal peptides, TMD nor kinase domain. Their LRR consensus sequence is xPAEIG(Q/R)LxxLxxLxLxxNxLTS, highly similar to the pattern identified in land plants, yet the green algae LRRs seem to be one amino acid shorter than the LRRs of higher plants and the typical NxxxG motif is not present in LRRs from green algae. Back-checking for presence of LRR-RLK-type proteins in the non-redundant database of NCBI for green algae, we could identify many similar kinase proteins and LRR-containing proteins, but only few combining both (data not shown). This suggests that the LRR-RLK archetype was already present at the separation of Chlorophyta and Streptophyta, yet most likely without a predominant functionality as RLKs. Furthermore, we could find, by back-checking the NCBI databases, the presence of 24 amino acid long LRRs with the NxxxG motif in brown algae, thus suggesting that only green algae present the anomalies discussed above.

EMS1, CLV1, FEIs, PXC1 and PXC2, as well as the NIKs and SERKs are LRR proteins already present in moss, liverwort and Lycophytes. Apparently, the LRR-proteins then further got multiplied and adopted different architectures. The very “successful” EFR-type receptors (further referred to as ECX21 family) started appearing at the emergence of Spermatophyte. The ECX21 family consists of 21 LRRs, a single TMD and a kinase, and is the most represented receptor type in higher plants. Yet only three of them, EFR, CORE and Xa21, are functionally characterized so far. There are only 5 members of ECX21 in *A. thaliana*, 9 in *S. lycopersicum*, 71 in *O. sativa* subsp. *indica* but 178 in *Eucalyptus grandis*, thus showing the flexibility in further developing the repertoire of ECX21. Although EFR, CORE and Xa21 are all involved in immunity, the ultimate function of the ECX21 family remains largely unknown.

Multiplication of genes involved in PTI is thought to contribute to the fitness of plants and to compensate for their sessile lifestyle (Ausubel, 2005). By duplicating PTI-involved ECX21 members and with modifications in the surface-exposed residues forming the LRR binding pocket, plants might increase their chances of detecting mutated or novel PAMPs, e.g. the flagellin from *A. tumefaciens* (Felix *et al.*, 1999), and thus could be a survival strategy in an arms-race perspective. Further characterization of ECX21 members would be of particular interest in future studies to assess whether this hypothesis holds true.

A very broadly represented type of receptor clusters in the RKF1 cluster. The former are present in all flowering species, indeed, we found no evidence of RKFs-likes in either *S. moellendorfii, P. patens*, *M. polymorpha* or green algae. RKF1, RKF2 and RKF3 were shown to be active in pollen grain in *A. thaliana* (Takahashi *et al.*, 1998). Our results present at least 13 other cluster members in *A. thaliana*, while the sister species *Brassica napus, B. rapa* and *B. olearacea* all have over 40 members of this otherwise uncharacterized protein cluster. *Amborella trichopoda* has 3 proteins which belongs to this cluster.

The NIK-SERKs are co-receptor in immunity and development and have been well characterized in several species. In *A. thaliana*, the NIKs have been shown to be involved in viral immunity, while the SERKs play a central role in developmental and immune processes. Yet there are other family members whose functions still remain elusive. Of particular interest are AT5G65240 and AT5G10290 because they locate evolutionarily between the 5 AtSERKs and the 3 AtNIKS and are most likely also involved in immunity-related signaling pathway.

From our analysis, we can see that LRR-RLKs likely evolved prior to LRR-RLPs, or at least that the LRR-RLKs are more conserved than LRR-RLPs. Even though we found traces of both receptor-types in green algae, these archaic proteins do not relate to any LRR-protein found in higher plants and contain a

similar yet slightly off-consensus LRR sequence. These differences are not present in brown algae, meaning that the typical plant-specific LRR-RLKs and LRR-RLPs already evolved prior to the emergence of green algae. Yet green algae somehow evolved a variation of this LRR-subfamily and further studies should focus on that variation to understand its selective driving pressure.

While LRR-RLKs need a SERK-type co-receptor to propagate PAMP perception across the membrane, LRR-RLPs additionally need an adaptor kinase such as SOBIR1 or CRN to make up their lack of kinase. SOBIR1 was first identified as a negative regulator of BIR1, itself a negative regulator of PRRs (Gao *et al.*, 2009), but it quickly turned out that SOBIR1 was also involved in signaling in a more direct way, since it is forming constitutive interaction with many immune-related RLPs (Liebrand *et al.*, 2013). The LRR-RLP CLV2, involved in meristem maintenance in the apical cells of the roots (Kayes and Clark, 1998; Jeong *et al.*, 1999), needs the CRN adaptor to work correctly (Muller *et al.*, 2008; Bleckmann *et al.*, 2010; Zhu *et al.*, 2010). The molecular features from SOBIR1 that are important for interaction with LRR-RLPs have been previously discussed (Gust and Felix, 2014; Bi *et al.*, 2015). The positively charged amino acids of the SOBIR1 outerjuxtamembrane domain are thought to facilitate the interaction with negatively charged residues in the outerjuxtamembrane domain of RLPs (Gust and Felix, 2014). This is of particular interest since the outerjuxtamembrane domain residues of FLS2 or EFR are positively charged, similar to SOBIR1, and thus could prevent dimerization of non-specific receptor pairs. Moreover, the GxxxG motif identified in SOBIR1 TMD was shown to be crucial for successful interaction with the tomato RLPs Cf-4, Ve1 and EIX2 (Bi *et al.*, 2015). Interestingly, CLV2 and CRN also interact through their TMDs (Bleckmann *et al.*, 2010), and also in this couple GxxxG-like motifs can be found on both partners.

The requirements for RLPs to dimerize with SOBIR1, on the other hand, remain unclear. In the present study, we demonstrated that the TMD context is sufficient for turning a LRR-RLK in a SOBIR1-dependent LRR-RLP-like. We showed that LRR-RLPs are more than simple truncations of LRR-RLKs and further narrowed down the region important for recruiting SOBIR1 to the TMD only, as opposed to the C-tail only of LRR-RLPs. We also propose that enrichment in aromatic residues might have an additional effect in stabilizing the constitutive interaction between LRR-RLPs and SOBIR1 because their higher hydrophobicity makes up for the slightly unstable flat GxxxG surface located on the opposite side of the TMD α-helix. We could also show that the TMD of CLV2 is sufficient to recruit CRN to form a complex with chimeric receptors at the plasma membrane. In this case, however, CRN worked as an immune-related adaptor kinase since the EFRtmCLV2-CRN constellation was functional in propagating downstream signaling into the defense pathway, thus further supporting our hypothesis. Finally, we performed a reverse experiment and turned a LRR-RLP into a functional SOBIR1-independent LRR-RLK by fusing SOBIR1 kinase to RLP23, EIX2 and EFRΔkin.

Our first approach in understanding the molecular differences between LRR-RLKs and LRR-RLPs consisted in truncating the kinase of LRR-RLKs. We used CORE, PEPR1, EFR and BRI1 to see whether ligand perception in the apoplast could still induce signaling via oxidative burst and ethylene production in transformed *N. benthamiana*. Although correctly expressed, neither of COREΔkin, PEPR1Δkin, EFRΔkin or BRI1Δkin did induce an oxidative burst when treated with their respective ligands. Truncation of the EFR kinase still allows the ligand-dependent formation of a complex with SERK3 (Fig. 4.7 and 4.10). This observation fits the idea that the activation of PRRs complexes at the plasma membrane works like a zipper, with the ectodomains of the receptor and co-receptor establishing contact after ligand perception, then their TMDs are

brought in close proximity and finally kinases are close to another and phosphoactivation can take place to initiate cytoplasmic signaling events.

After elf18 perception by EFR but also by EFRΔkin, SERK3 is attracted to the complex through its ectodomain and by a stabilized TMD dimer formation. How exactly SERK3 is able to sense the activation of the PRRs is not yet fully understood, but we can emit two main hypotheses: (i) a structural modification of the PRR after ligand perception allows SERK3 to approach the complex and/or (ii) the presence of the ligand create a repulsive force for potential complex inhibitors. The crystal structure of FLS2 has been solved in 2013 by Sun and colleagues and shows nicely the interaction sites between SERK3 (co-crystalized), FLS2 and flg22 (Sun *et al.*, 2013*b*). It also shows that SERK3 directly interacts with the ligand through a loose loop on the N-terminal part of the LRR domain. However, it does not show significant conformation changes in the presence or absence of the ligand. Similar observations were made for the crystal AtPEPR1-AtPep1 (Tang *et al.*, 2015). There is up to date no available crystal structure for EFR, but it is thought to behave like FLS2 and PEPR1, and thus no structural changes are expected to take place during ligand binding. On the other hand, the crystal of the phytosulfokine (PSK) receptor 1 (PSKR1), another LRR-RLK, showed that the ligand binds to the island domain of PSKR1, thus bringing conformational changes which allow the co-receptors SERK1 or SERK2 to approach PSKR1 (Wang *et al.*, 2015). Crystallography has the drawback of not showing dynamic reactions and shows only steady states. Rapid structural modification of an activated FLS2 or EFR cannot be ruled out and could be not caught in crystallographic expriments. On the other hand, the presence of certain complex inhibitors like the BIRs prevent the activation of the complex without a ligand by interacting directly with unactivated PRRs, such as FLS2, via their ectodomains (Huang *et al.*, 2017; Imkampe *et al.*, 2017; Ma *et al.*, 2017). The exact mechanism of PRR release from their interaction with the

BIRs after ligand perception has not yet been fully explained, but the crystal structure of SERK3 and BIR1 ectodomains revealed that the C-terminal part FLS2 that interacts with SERK3 overlaps with BIR1 (Ma *et al.*, 2017), thus suggesting indeed a slight structural modification of FLS2 after flg22-binding that should enable FLS2 to outcompete BIR1 in the interaction with SERK3. In the presence of a native EFR and after elf18 perception, SERK3 and EFR kinases are transphosphorylating and this initiates cytoplasmic signaling cascades leading to immune responses (Lu *et al.*, 2010; Roux *et al.*, 2011; Macho *et al.*, 2014). In the case of EFRΔkin and to a broader extent of the other tested PRRΔkin, however, the phosphoactivation and thus immune responses cannot take place. The absence of a kinase in EFRΔkin does not prevent complex formation with SERK3 after elf18 perception and thus suggests that the interaction with negative regulators also takes place in the apoplasme, which was subsequently confirmed in Y2H assay (S. Schulz, personal communication) and through crystal structures (Ma *et al.*, 2017). Accordingly, SOBIR1 could not be detected in immunoprecipitated EFRΔkin.

Our main approach to better understand the molecular requirements of a functional LRR-RLP, was to introduce parts of a functional RLP into the non-signaling truncated kinase PRR templates. We worked in parallel with EIX2 and RLP23, since RLP23 contains a GxxxG motif in its transmembrane, whereas EIX2 does not, yet both of these RLPs were shown to be SOBIR1-dependent (Albert *et al.*, 2015; Bi *et al.*, 2015). We first fused the ectodomain of EFR with the TMD and the cytoplasmic C-tail of RLP23 or EIX2. Both EFRtmRLP23 and EFRtmEIX2 were functional as receptors for their respective ligands in oxidative burst and ethylene responses. The same was observed for BRI1tmRLP23, SYSREtmRLP23, PEPR1tmRLP23 and COREtmEIX2. Immunoprecipitation of EFRtmRLP23 and EFRtmEIX2 revealed that both constructs were constitutively co-precipitating SOBIR1 and, in a ligand-

dependent manner, SERK3. Thus, incorporating the TMD and the C-tail of a functional RLP was sufficient to convert these RLKs into SOBIR1-interacting RLP-type of receptors. The case of BRI1tmRLP23 is of particular interest since it represents a text book example of reprogramming based on a chimeric approach. Treatment with BL does not trigger any immune responses in plants expressing BRI1 or BRIΔkin, but fusing an immune-related cytoplasmic part to its ectodomain makes BL treatment induce immune responses. This resembles the approach by He et al. (2000) with swapping Xa21 and BRI1 kinases that led to immune responses on the BRI1kXa21 construct after BL treatment. This procedure turned a developmental RLK into an immunity RLK, while we turned a developmental RLK to an immunity RLP.

To further narrow-down the critical domain for RLP functionality, we fused the ectodomain of EFR, the TMD of RLP23 or EIX2 and a truncated EFR kinase. EFRΔkin-tmRLP23 and EFRΔkin-tmEIX2 were both functional in oxidative burst and induction of ethylene responses. Consequently they interacted constitutively with SOBIR1 and in a ligand-dependent manner with SERK3, similar to EFRtmRLP23, EFRtmEIX2, native RLP23 and EIX2. On the other hand, the fusion of EFR ectodomain and TMD to the cytoplasmic C-tail of either RLP23 or EIX2 did not result in functionally competent receptors. Indeed, EFRijmRLP23 and EFRijmEIX2 were correctly expressed but no oxidative burst, induction of ethylene responses or interaction with SOBIR1 could be observed. Similar observation were made with COREijmEIX2 and PEPR1ijmRLP23. This suggests that the C-tail of RLPs is not responsible for the interaction with SOBIR1. In EFRΔkin-tmRLP23 and EFRΔkin-tmEIX2, the amplitude and speed of responses were somewhat reduced as compared to EFRtmRLP23 and EFRtmEIX2, in which the C-tails of RLPs are present. There must therefore be further information encoded in the cytoplasmic tail of the RLPs, which are typically no longer than ~30 residues. The exact function of

these are currently poorly understood, but Fradin et al. (2014) reported on the interaction of both Ve1 and Ve2 C-tails with SOBIR1. On the other hand, deletion of the C-tail of RLP23 was shown not to impact its interaction with SOBIR1 nor the functionality of the system (I. Albert, personal communication). Our results suggest that the C-tail of RLPs is not necessary for functionality, yet they allow a better signaling. The exact role of these tails remains yet to be studied.

SOBIR1 seems to require the complete GxxxGxxxG motif in the TMD, the inner as well as the outer juxtamembrane (iJM and oJM respectively) and a signal peptide as minimal construct to be able to dimerize with LRR-RLPs (Bi *et al.*, 2015). The negatively charged residues present in the oJM of RLPs are thought to help mediating the interaction with SOBIR1, through an interaction with its positively charged oJM residues (Gust and Felix, 2014). In the present thesis, however, the functional chimeric RLPs generated from intact EFR ectodomains (including oJM), having similar oJM charges as SOBIR1, tend to reject that hypothesis. On the other hand, we observed only a weak interaction of EFRtmkSOBIR1 with SOBIR1 in coimmunoprecipitation assay (Fig. 4.20). This suggests that similar charges in the oJM are indeed suboptimal and tend to prevent unwanted interaction between LRR-RLKs and SOBIR1, but that TMD-mediated interaction can override this security mechanism.

By studying separately the TMD and C-tail from RLP23, we were able to discriminate which of these subdomains is able to provide a platform for dimerization with SOBIR1. The TMD from EFR was not able to mediate SOBIR1 recruitment, while this recruitment was achieved when replaced by the TMD of either RLP23 or EIX2. Furthermore, it seems that there is additional information encoded in the C-tail of native RLPs which are able to give high and long-lasting responses. In the constructs we generated the responses were comparable with full length native RLKs when both the TMD and the C-tail

were present in the chimeras, but were somewhat lower when only the TMD was inserted. Previous trials trying to turn AtBRI1 in a PTI-involved PRR were successfully achieved when its kinase was swapped with the kinase domain of either AtEFR (M. Albert, personal communication) or OsXa21 (He *et al.*, 2000). Yet the BRI1-EFR chimera was shown to have a quite high background when expressed transiently in *N. benthamiana* (M. Albert, personal communication), most likely due to the presence of naturally produced BL.

The interactions between TMDs is thought not to follow a sequence-to-motif paradigm (Cymer *et al.*, 2012; Fink *et al.*, 2012; Li *et al.*, 2012). The GxxxG motif has been shown to be important in some TMD heterodimer complexes but has also been identified in the non-interacting surface of the TM helix. In the case of the SOBIR1-RLPs interactions, it seems that the GxxxGxxxG motif is important for SOBIR1 (Bi *et al.*, 2015) whereas this motif knows some variations in RLPs, e.g. in SlEIX2, SlCure or AtReMAX. When comparing the transmembrane residues of RLPs and RLKs beyond the presence of the glycine motif, it becomes clear that hydrophobic residues containing an aromatic rings (Trp, Tyr and Phe) are more frequently present in RLPs than in RLKs (Fig. 4.22). The strongly hydrophobic aromatic side chains are known to be important for stabilizing the TMDs and this might be crucial when one side of the TMD helix is flat or less hydrophobic (A. Lupas, personal communication). Unterreitmeier et al. (2007) could show, for instance, that the presence of a Phe residue before a GxxxG motif could help stabilizing the helix and increase the self-interaction of TMD proteins in bacteria. In our TMD analysis, we observe that the hydrophobic residues with aromatic ring tend to locate on the opposite of the GxxxG motif and we propose that they counterbalance the disturbance in hydrophobicity due to the presence of several small residues on the one side. We also observed that the GxxxG motif in SOBIR1 is located slightly upstream of the GxxxG motif in LRR-RLPs, thus suggesting that other residues might well

play a role in the interaction specificity by acting as knob-into-holes actors (Lupas and Bassler, 2017).

Interestingly, chimeric constructs consisting of the ectodomain of EFR and the TMD of CLV2 were functional in oxidative burst and induction of ethylene responses and provided enough information to recruit CRN, the co-receptor of native CLV2. Previous studies presented evidence that SOBIR1 might be interacting with CLV2 (Liebrand *et al.*, 2013; Bi *et al.*, 2015), yet the exact role of such an interaction remained elusive. In the present study, we could find CRN but not SOBIR1 when immunoprecipitating CLV2. The presence of CRN in complex with EFRtmCLV2 and EFRΔkin-tmCLV2 strengthens our hypothesis that TMD sequence alone can dictate the preference in choice of co-receptor. It appears that constitutive interactions are mediated through highly specific TMD-TMD interactions and that these are only achieved when not only the GxxxG motif is located at the correct position in the lipid bilayer, but also that adjacent, more voluminous residues must be able to fit together to allow both TMDs to be brought in close proximity. Moreover, the complementary constructs based on CLV2 ectodomain coupled to the TMD and C-tail of RLP23 or EIX2 were not conclusive in initiating immune responses (data not shown). This could be due to the fact that CLV3 might not be the correct ligand for CLV2, as demonstrated in binding assays. The acri-labeled CLV3 peptide was added to crude extract of plant material expressing CLV2-GFP and CRN, but we could not detect a reduced light emission in the presence of 1000-fold excess unlabeled CLV3 competitors. As control, we immunoenriched CLV1-GFP and performed the same experiment but could not detect acri-CLV3 binding in the absence of competitors, thus suggesting that the acridinium moiety somehow reduce the affinity of CLV3 for the receptor. This was further demonstrated in root-growth assay in *A. thaliana* seedlings (Annex Fig. 4). Further assays should definitely focus on solving the CLV2-CLV3 issue, as well as alternative approaches such

as the use of chimeric receptors to better understand the CLE-perception system in plants.

We tested the simple hypothesis of co-receptor choice as dictated by TMD context by endorsing the idea that the bi-molecular RLKs formed by the RLP-SOBIR1 pair might be fused to form a functional RLK. We fused the TMD and kinase of SOBIR1 to RLP23, EIX2 and EFR to see whether the addition of a kinase domain to a RLP could convert the latter in a LRR-RLK. RLP23tmkSOBIR1, EIX2tmkSOBIR1, and EFRtmkSOBIR1 proved to be functional in oxidative burst and induction of ethylene responses, but we could not determine whether these constructs were indeed working as RLK-like or still as RLPs. We generated further constructs on RLP23, EIX2 and EFRΔkin templates, where we incorporated only the TMD of SOBIR1. RLP23tmSOBIR1, EIX2tmSOBIR1 and EFRΔkin-tmSOBIR1 were also all functional in oxidative burst and induction of ethylene responses. This suggest that the TMD of SOBIR1 can replace the TMD of RLPs and still allow signaling to take place. These combined results do not directly allow us to discriminate for SOBIR1-independent functionality, but allow us to observe that SOBIR1 TMD can dimerize, since RLP23tmkSOBIR1 and EFRtmkSOBIR1 are functional and interact constitutively with SOBIR1 as shown through co-immunoprecipitation (Fig. 4.20). The formation of such a tripartite kinase complex, composed from RLP23/EFRtmkSOBIR1, SOBIR1 and BAK1 kinases after ligand-perception, was never documented in plant immunity and originates certainly from the chimeric approach. Yet, the fact that SOBIR1 is present in the complex suggests that it does not occupy the same side for interaction as BAK1 since it does not obstruct signal transduction and should thus be located behind the receptor. Follow-up experiments should focus on this very interesting observation to understand the role of the SOBIR1 ectodomain: is it interacting with the ligand? Is it really doing something important in PAMP-signaling?

Further assays in protoplasts of *A. thaliana* sobir1-12 mutant transformed with either RLP23tmkSOBIR1 or RLP23tmSOBIR1 showed that RLP23tmkSOBIR1 behaves like a LRR-RLK since a clear induction of the pFRK1::luc reporter was observed after nlp20 treatment. This demonstrates that LRR-RLPs and SOBIR1 indeed are a bi-molecular equivalent to LRR-RLKs. Despite the fact that RLP23tmkSOBIR can also interact with SOBIR1, it seems that the presence of three kinase domains in the signaling complex did not affect signaling. Finally, we could also show that SOBIR1 kinase can replace the kinase of EFR in immunity signaling, as demonstrated with EFRtmkSOBIR1.

The core results of our findings can be summarized as depicted in Fig. 5.1. We propose (i) that the TMD dictates which co-receptor can be recruited, (ii) that RLPs are more complex than kinase truncated RLKs, but (iii) that RLKs can be formed from addition of a kinase on a RLP (Fig. 5.1). Finally, we hypothesize that the ligand-dependent interaction of the PRRs with SERK-type co-receptors are independent of the constitutively interacting SOBIR1 involved with LRR-RLPs. This suggests that SOBIR1 might be located on the other side of the PRRs and do not interact directly with the ligand (Fig. 5.1). The typical difference in speed of responses observed between RLKs and RLPs most likely lay in the limiting amount of SERKs at the cell surface. FLS2 and BRI1 were shown to be present at the plasma membrane in separated nanoclusters and that different pools of SERK3 were present in these nanoclusters (Bücherl *et al.*, 2017; Hutten *et al.*, 2017). Since RLPs involved in immunity evolved in several taxa repeatedly, it seems only logical that they are specific to a certain class of pathogens which create selective pressure on a given species, whereas “general” immune RLKs such as FLS2 are of higher interest since they can detect a broader spectrum of pathogens. This functional distinction reminds the separation of innate and acquired immunities of animals and may well be a new way of looking at plant immunity.

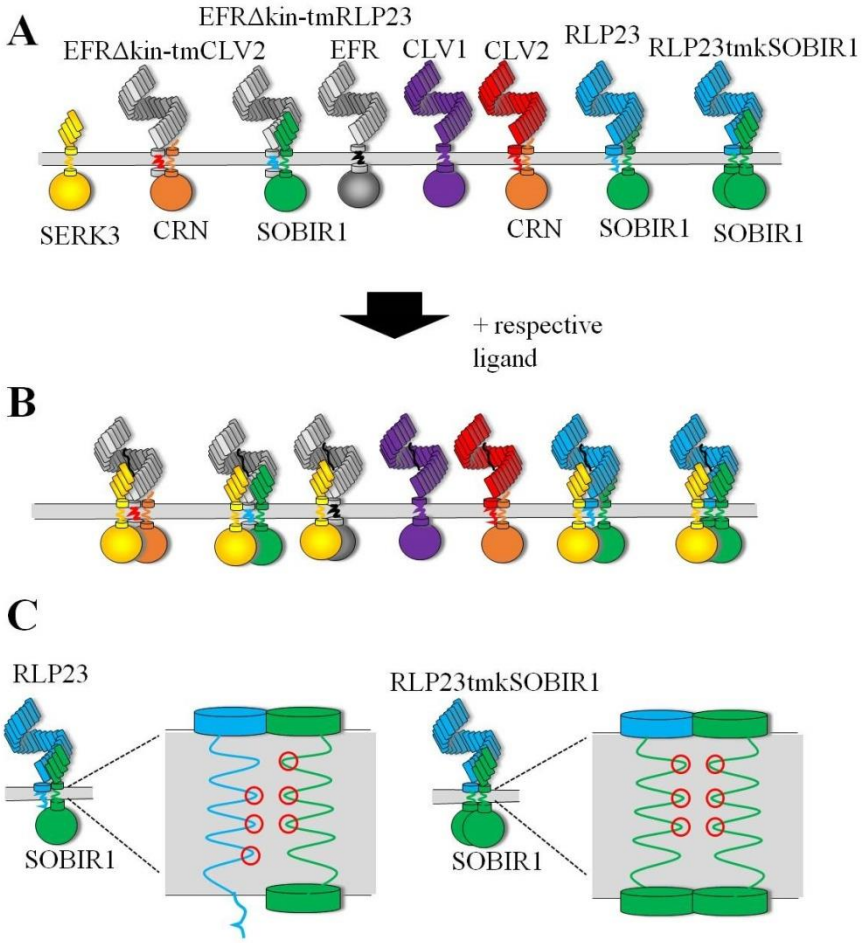

Figure 5.1 – Model for the interaction of LRR-RLPs with SOBIR1

(A) There is a constitutive interaction with the kinase adaptor SOBIR1 for PRR that contain the TMD of an LRR-RLP involved in immunity or of SOBIR1. The adaptor kinase CRN interacts with PRR that have the TMD of CLV2. (B) After ligand perception, SERK3 joins the activated PRRs from immunity but not CLV1 nor CLV2. (C) Because RLP23tmkSOBIR1 interacts with SOBIR1 constitutively but because it does not require it to signal in *A. thaliana* sobir1-12 mutant plants, we propose that the glycine residues (red circles) present in the GxxxG motifs of LRR-RLPs are facing the rear face of where the binding take place, so as to not disturb the ligand-dependent interaction with SERK3.

6. Conclusion

In the present work, we dissected the molecular basis for difference between LRR-RLKs and LRR-RLPs. Besides the obvious presence/absence of a kinase, the sequence context of the TMD allows specific constitutively-interacting co-receptor to approach LRR-RLPs to form functional signaling platforms. The presence of a GxxxG motif as hydrophobically weaker, more open interaction surface has to be counter-balanced by large hydrophobic residues that should anchor and stabilize the receptor in the membrane. Further studies should focus on the regulatory mechanisms that prevent SOBIR1 from homodimerizing, given that its TMD presents a flat surface large enough to interact with a broad spectrum of RLPs and constructs containing another SOBIR1 TMD.

In conclusion, we propose that the LRR-RLK archetype was already present in a rustic form in unicellular green algae and that LRR-RLPs evolved later in several species. The partial loss of SOBIR1 LRRs in grasses lead this family to evolve other work-arounds, such as the accelerated development of ECX21 receptors. LRR-RLPs are species-specific whereas LRR-RLKs are older and more broadly distributed. LRR-RLPs must have been selected to respond to specific pathogens, explaining in the same time their slower responses as compared to LRR-RLKs. They act as a supplementary level of defenses and might reflect the adaptive immunity of animals on an evolutionary scale.

Acknowledgments

I am very thankful to...

- Prof. Georg Felix for giving me the chance to pursue my doctoral degrees, for his skilful guidance, for the motivating discussions and the good wines and cheese every now and then after work.

- Dr. Markus Albert for his guidance, for keeping an eye on what I did and for cheering me up during countless hours of cloning. And of course for loosing on purpose during the tisch-kicker breaks.

- Prof. Thorsten Nürnberger for being my second thesis reviewer.

- Patrick Schulz and Prof. Rüdiger Simon for the CLV material and extra data.

- Prof. Andrei Lupas for giving me the opportunity to join the Max-Planck Institute. Also big thanks to Jens Baßler and Laura Weidmann for guiding me through the strange world of programmers, for feeding me with pastries for almost a year and for our shared loved of popping balloons.

- Ursula Fürst, Lei Wang, and Vahid Fallahzadeh-Mamaghani for bringing such a good mood in the lab and for making a big difference on bad days. Also to Ilonka Bock and Petra Neumann for helping getting a running lab.

- All the students who helped getting results along the way, with a special emphasis to Melissa Weldle for her dedicated work.

- Liane Schön for her help in understanding the German administration and for her support in resolving any kind of problems.

- All actual and ex-members of the plant biochemistry department for the support, for the daily lab-life and for putting bacteria in the shakers for me on Sundays!

- Family and friends for moral support and for helping me having fun outside of work.

- My beloved wife for her daily support, for teaching me German, for helping me holding through the rough times and for her spreading smile. And also for our daughter and all the happiness she brings in the world.

References

Aan Den Toorn M, Albrecht C, De Vries S. 2015. On the origin of SERKs: Bioinformatics analysis of the somatic embryogenesis receptor kinases. Molecular Plant **8**, 762–782.

Abramovitch RB, Anderson JC, Martin GB. 2006. Bacterial elicitation and evasion of plant innate immunity. Nature Reviews Molecular Cell Biology **7**, 601–611.

Albert M. 2013. Peptides as triggers of plant defence. Journal of experimental botany **64**, 5269–79.

Albert I, Böhm H, Albert M, *et al.* 2015. An RLP23–SOBIR1–BAK1 complex mediates NLP-triggered immunity. Nature Plants **1**, 15140.

Albert M, Jehle AK, Lipschis M, Mueller K, Zeng Y, Felix G. 2010*a*. Regulation of cell behaviour by plant receptor kinases: Pattern recognition receptors as prototypical models. European journal of cell biology **89**, 200–7.

Albert M, Jehle AK, Mueller K, Eisele C, Lipschis M, Felix G. 2010*b*. Arabidopsis thaliana pattern recognition receptors for bacterial elongation factor Tu and flagellin can be combined to form functional chimeric receptors. The Journal of biological chemistry **285**, 19035–42.

Albert M, Jehle AK, Mueller K, Eisele C, Lipschis M, Felix G. 2010*c*. Arabidopsis thaliana pattern recognition receptors for bacterial elongation factor Tu and flagellin can be combined to form functional chimeric receptors. The Journal of biological chemistry **285**, 19035–42.

Albrecht C, Boutrot F, Segonzac C, Schwessinger B, Gimenez-Ibanez S, Chinchilla D, Rathjen JP, de Vries SC, Zipfel C. 2012. Brassinosteroids inhibit pathogen-associated molecular pattern-triggered immune signaling independent of the receptor kinase BAK1. Proceedings of the National Academy of Sciences **109**, 303–308.

Alonso JM, Hirayama T, Roman G, Nourizadeh S, Ecker JR. 1999. EIN2, a Bifunctional Transducer of Ethylene and Stress Responses in Arabidopsis. Science **284**, 2148–2152.

Alvarez ME, Pennell RI, Meijer PJ, Ishikawa A, Dixon RA, Lamb C. 1998. Reactive oxygen intermediates mediate a systemic signal network in the establishment of plant immunity. Cell **92**, 773–784.

Apel K, Hirt H. 2004. REACTIVE OXYGEN SPECIES: Metabolism, Oxidative Stress, and Signal Transduction. Annual Review of Plant Biology **55**, 373–399.

Asai S, Ichikawa T, Nomura H, Kobayashi M, Kamiyoshihara Y, Mori H, Kadota Y, Zipfel C, Jones JDG, Yoshioka H. 2013. The variable domain of a plant calcium-dependent protein kinase (CDPK) confers subcellular localization and substrate recognition for NADPH oxidase. Journal of Biological Chemistry **288**, 14332–14340.

Asai T, Tena G, Plotnikova J, Willmann MR, Chiu W-L, Gomez-Gomez L, Boller T, Ausubel FM, Sheen J. 2002. MAP kinase signalling cascade in Arabidopsis innate immunity. Nature **415**, 977–83.

Ausubel FM. 2005. Are innate immune signaling pathways in plants and animals conserved? Nature Immunology **6**, 973–979.

Bartels S, Lori M, Mbengue M, Verk M Van, Klauser D, Hander T, Böni R, Robatzek S, Boller T. 2013. The family of peps and their precursors in arabidopsis: Differential expression and localization but similar induction of pattern-Triggered immune responses. Journal of Experimental Botany **64**, 5309–5321.

Belkhadir Y, Jaillais Y, Epple P, Balsemao-Pires E, Dangl JL, Chory J. 2012. Brassinosteroids modulate the efficiency of plant immune responses to microbe-associated molecular patterns. Proceedings of the National Academy of Sciences **109**, 297–302.

Bella J, Hindle KL, McEwan P a, Lovell SC. 2008. The leucine-rich repeat structure. Cellular and molecular life sciences : CMLS **65**, 2307–33.

Bentham A, Burdett H, Anderson PA, Williams SJ, Kobe B. 2016. Animal NLRs provide structural insights into plant NLR function. Annals of Botany, mcw171.

Bi G, Liebrand TWH, Bye RR, Postma J, van der Burgh AM, Robatzek S, Xu X, Joosten MH a. J. 2015. SOBIR1 requires the GxxxG dimerization motif in its transmembrane domain to form constitutive complexes with receptor-like proteins. Molecular Plant Pathology, n/a-n/a.

Bleckmann A, Weidtkamp-Peters S, Seidel CAM, Simon R. 2010. Stem Cell Signaling in Arabidopsis Requires CRN to Localize CLV2 to the Plasma Membrane. Plant Physiology **152**, 166–176.

Blume B, Nürnberger T, Nass N, Scheel D. 2000. Receptor-Mediated Increase in Cytoplasmic Free Calcium Required for Activation of Pathogen Defense in Parsley. the Plant Cell **12**, 1425–1440.

Böhm H, Albert I, Fan L, Reinhard A, Nürnberger T. 2014*a*. Immune receptor complexes at the plant cell surface. Current Opinion in Plant Biology **20**, 47–54.

Böhm H, Albert I, Oome S, Raaymakers TM, Van den Ackerveken G, Nürnberger T. 2014*b*. A Conserved Peptide Pattern from a Widespread Microbial Virulence Factor Triggers Pattern-Induced Immunity in Arabidopsis. PLoS Pathogens **10**.

Bojar D, Martinez J, Santiago J, Rybin V, Bayliss R, Hothorn M. 2014. Crystal structures of the phosphorylated BRI1 kinase domain and implications for brassinosteroid signal initiation. The Plant journal **78**, 31–43.

Boller T, Felix G. 2009. A renaissance of elicitors: perception of microbe-associated molecular patterns and danger signals by pattern-recognition receptors. Annual review of plant biology **60**, 379–406.

Boutrot F, Segonzac C, Chang KN, Qiao H, Ecker JR, Zipfel C, Rathjen JP. 2010. Direct transcriptional control of the Arabidopsis immune receptor FLS2 by the ethylene-dependent transcription factors EIN3 and EIL1. Proceedings of the National Academy of Sciences **107**, 14502–14507.

Bradley DJ, Kjellbom P, Lamb CJ. 1992. Elicitor- and wound-induced oxidative cross-linking of a proline-rich plant cell wall protein: A novel, rapid defense response. Cell **70**, 21–30.

Brand U, Fletcher JC, Hobe M, Meyerowitz EM, Simon R. 2000. Dependence of Stem Cell Fate in Arabidopsis on a Feedback Loop Regulated by CLV3 Activity. Science **289**, 617–619.

Brutus A, Sicilia F, Macone A, Cervone F, De Lorenzo G. 2010. A domain swap approach reveals a role of the plant wall-associated kinase 1 (WAK1) as a receptor of oligogalacturonides. Proceedings of the National Academy of Sciences **107**, 9452–9457.

Bücherl CA, Jarsch IK, Schudoma C, Segonzac C, Mbengue M, Robatze S, MacLean D, Ott T, Zipfe C. 2017. Plant immune and growth receptors share common signalling components but localise to distinct plasma membrane nanodomains. eLife **6**.

Butenko MA, Patterson SE, Grini PE, Stenvik G-E, Amundsen SS, Mandal A, Aalen RB. 2003. INFLORESCENCE DEFICIENT IN ABSCISSION Controls Floral Organ Abscission in Arabidopsis and Identifies a Novel Family of Putative Ligands in Plants. The Plant Cell **15**, 2296–2307.

Cai R, Lewis J, Yan S, *et al.* 2011. The plant pathogen Pseudomonas syringae pv. tomato is genetically monomorphic and under strong selection to evade tomato immunity. PLoS pathogens **7**, e1002130.

Caplan J, Padmanabhan M, Dinesh-Kumar SP. 2008. Plant NB-LRR Immune Receptors: From Recognition to Transcriptional Reprogramming. Cell Host and Microbe **3**, 126–135.

Champion A, Picaud A, Henry Y. 2004. Reassessing the MAP3K and MAP4K relationships. Trends in Plant Science **9**, 123–129.

Chen L-Q, Hou B-H, Lalonde S, *et al.* 2010. Sugar transporters for intercellular exchange and nutrition of pathogens. Nature **468**, 527–532.
Chinchilla D, Bauer Z, Regenass M, Boller T, Felix G. 2006. The Arabidopsis Receptor Kinase FLS2 Binds flg22 and Determines the Specificity of Flagellin Perception. the Plant Cell **18**, 465–476.
Chinchilla D, Zipfel C, Robatzek S, Kemmerling B, Nürnberger T, Jones JDG, Felix G, Boller T. 2007. A flagellin-induced complex of the receptor FLS2 and BAK1 initiates plant defence. Nature **448**, 497–500.
Choi HW, Manohar M, Manosalva P, Tian M, Moreau M, Klessig DF. 2016. Activation of Plant Innate Immunity by Extracellular High Mobility Group Box 3 and Its Inhibition by Salicylic Acid. PLoS Pathogens **12**, 1–21.
Chu Z, Yuan M, Yao J, *et al.* 2006. Promoter mutations of an essential gene for pollen development result in disease resistance in rice. , 1250–1255.
Clapham DE. 1995. Calcium signaling. Cell **80**, 259–268.
Clark SE, Running MP, Meyerowitz EM. 1993. CLAVATA1, a regulator of meristem and flower development in Arabidopsis. Development **119**, 397–418.
Clark S, Running M, Meyerowitz E. 1995. *CLAVATA3* is a specific regulator of shoot and floral meristem development affecting the same processes as *CLAVATA1*. Development **121**, 2057–2067.
Clark SE, Williams RW, Meyerowitz EM. 1997. The CLAVATA1 Gene Encodes a Putative Receptor Kinase That Controls Shoot and Floral Meristem Size in Arabidopsis. Cell **89**, 575–585.
Clarke CR, Chinchilla D, Hind SR, Taguchi F, Miki R, Ichinose Y, Martin GB, Leman S, Felix G, Vinatzer BA. 2013. Allelic variation in two distinct Pseudomonas syringae flagellin epitopes modulates the strength of plant immune responses but not bacterial motility. The New phytologist **200**, 847–60.
Colcombet J, Boisson-Dernier A, Ros-Palau R, Vera CE, Schroeder JI. 2005. Arabidopsis SOMATIC EMBRYOGENESIS RECEPTOR KINASES1 and 2 are essential for tapetum development and microspore maturation. The Plant Cell … **17**, 3350–3361.
Couto D, Niebergall R, Liang X, *et al.* 2016. The Arabidopsis Protein Phosphatase PP2C38 Negatively Regulates the Central Immune Kinase BIK1. PLoS Pathogens **12**, 1–24.
Cui J, Bahrami AK, Pringle EG, Hernandez-Guzman G, Bender CL, Pierce NE, Ausubel FM. 2005. Pseudomonas syringae manipulates systemic plant defenses against pathogens and herbivores. Proceedings of the National Academy of Sciences **102**, 1791–1796.
Curran AR, Engelman DM. 2003. Sequence motifs, polar interactions and conformational changes in helical membrane proteins. Current Opinion in Structural Biology **13**, 412–417.
Cymer F, Veerappan A, Schneider D. 2012. Transmembrane helix-helix interactions are modulated by the sequence context and by lipid bilayer properties. Biochimica et Biophysica Acta - Biomembranes **1818**, 963–973.
Desikan R, Hancock JT, Bright J, Harrison J, Weir I, Hooley R, Neill SJ. 2005. A Role for ETR1 in Hydrogen Peroxide Signaling in Stomatal Guard Cells. Plant Physiology **137**, 831–834.
Dóczi R, Brader G, Pettkó-Szandtner A, Rajh I, Djamei A, Pitzschke A, Teige M, Hirt H. 2007. The *Arabidopsis* Mitogen-Activated Protein Kinase Kinase MKK3 Is Upstream of Group C Mitogen-Activated Protein Kinases and Participates in Pathogen Signaling. The Plant Cell **19**, 3266–3279.
Dodd AN, Kudla J, Sanders D. 2010. The Language of Calcium Signaling. Annual Review of Plant Biology **61**, 593–620.
Dodds PN, Rathjen JP. 2010. Plant immunity: towards an integrated view of plant-pathogen interactions. Nature reviews. Genetics **11**, 539–48.

Doke N. 1985. NADPH-dependent O2\n- generation in membrane fractions isolated from wounded potato tubers inoculated with Phytophthora infestans. Physiological Plant Pathology **27**, 311–322.

Doura AK, Kobus FJ, Dubrovsky L, Hibbard E, Fleming KG. 2004. Sequence context modulates the stability of a GxxxG-mediated transmembrane helix-helix dimer. Journal of Molecular Biology **341**, 991–998.

Dubiella U, Seybold H, Durian G, Komander E, Lassig R, Witte C-P, Schulze WX, Romeis T. 2013. Calcium-dependent protein kinase/NADPH oxidase activation circuit is required for rapid defense signal propagation. Proceedings of the National Academy of Sciences **110**, 8744–8749.

Dunin-Horkawicz S, Kopec KO, Lupas AN. 2014. Prokaryotic ancestry of eukaryotic protein networks mediating innate immunity and apoptosis. Journal of Molecular Biology **426**, 1568–1582.

Dunning FM, Sun W, Jansen KL, Helft L, Bent AF. 2007. Identification and mutational analysis of Arabidopsis FLS2 leucine-rich repeat domain residues that contribute to flagellin perception. The Plant cell **19**, 3297–313.

Duxbury Z, Ma Y, Furzer OJ, Huh SU, Cevik V, Jones JDG, Sarris PF. 2016. Pathogen perception by NLRs in plants and animals: Parallel worlds. BioEssays **38**, 769–781.

Enkhbayar P, Kamiya M, Osaki M, Matsumoto T, Matsushima N. 2003. Structural Principles of Leucine-Rich Repeat (LRR) Proteins. Proteins: Structure, Function, and Bioinformatics **54**, 394–403.

Evdokimov a G, Anderson DE, Routzahn KM, Waugh DS. 2001. Unusual molecular architecture of the Yersinia pestis cytotoxin YopM: a leucine-rich repeat protein with the shortest repeating unit. Journal of molecular biology **312**, 807–21.

Felix G, Duran JD, Volko S, Boller T. 1999. Plants have a sensitive perception system for the most conserved domain of bacterial flagellin. Plant Journal **18**, 265–276.

Felix G, Regenass M, Spanu P, Boller T. 1994. The protein phosphatase inhibitor calyculin A mimics elicitor action in plant cells and induces rapid hyperphosphorylation of specific proteins as revealed by pulse labelling with [33 P]phosphate. Proceedings of the National Academy of Sciences of the United States of America **91**, 952–956.

Fink A, Sal-Man N, Gerber D, Shai Y. 2012. Transmembrane domains interactions within the membrane milieu: Principles, advances and challenges. Biochimica et Biophysica Acta (BBA) - Biomembranes **1818**, 974–983.

Fliegmann J, Felix G. 2016. Immunity: Flagellin seen from all sides. Nature Plants **2**, 16136.

Fradin EF, Zhang Z, Rovenich H, Song Y, Liebrand TWH, Masini L, Van Den Berg GCM, Joosten MHAJ, Thomma BPHJ. 2014. Functional analysis of the tomato immune receptor Ve1 through domain swaps with its non-functional homolog Ve2. PLoS ONE **9**.

Frei dit Frey N, Mbengue M, Kwaaitaal M, *et al.* 2012. Plasma Membrane Calcium ATPases Are Important Components of Receptor-Mediated Signaling in Plant Immune Responses and Development. Plant Physiology **159**, 798–809.

Fritz-Laylin LK, Krishnamurthy N, Tör M, Sjölander K V., Jones JD. 2005. Phylogenomic Analysis of the Receptor-Like Proteins of Rice and Arabidopsis. Plant Physiology **138**, 611–623.

Gao M, Wang X, Wang D, *et al.* 2009. Regulation of cell death and innate immunity by two receptor-like kinases in Arabidopsis. Cell host & microbe **6**, 34–44.

Garrett KA, Dendy SP, Frank EE, Rouse MN, Travers SE. 2006. Climate Change Effects on Plant Disease: Genomes to Ecosystems. Annual Review of Phytopathology **44**, 489–509.

Glazebrook J. 2005. Contrasting Mechanisms of Defense Against Biotrophic and Necrotrophic Pathogens. Annual Review of Phytopathology **43**, 205–227.

Godiard L, Sauviac L, Torii KU, Grenon O, Mangin B, Grimsley NH, Marco Y. 2003.

ERECTA, an LRR receptor-like kinase protein controlling development pleiotropically affects resistance to bacterial wilt. Plant Journal **36**, 353–365.
Gómez-Gómez L, Bauer Z, Boller T. 2001. Both the extracellular leucine-rich repeat domain and the kinase activity of FLS2 are required for flagellin binding and signaling in Arabidopsis. The Plant Cell **13**, 1155–1163.
Gómez-Gómez L, Boller T. 2000. FLS2: An LRR receptor–like kinase involved in the perception of the bacterial elicitor flagellin in Arabidopsis. Molecular cell **5**, 1003–1011.
Gou X, Yin H, He K, Du J, Yi J, Xu S, Lin H, Clouse SD, Li J. 2012. Genetic evidence for an indispensable role of somatic embryogenesis receptor kinases in brassinosteroid signaling. PLoS genetics **8**, e1002452.
Grant M, Brown I, Adams S, Knight M, Ainslie A, Mansfield J. 2000. The RPM1 plant disease resistance gene facilitates a rapid and sustained increase in cytosolic calcium that is necessary for the oxidative burst and hypersensitive cell death. Plant Journal **23**, 441–450.
Guex N, Peitsch MC. 1997. SWISS-MODEL and the Swiss-PdbViewer: An environment for comparative protein modeling. Electrophoresis **18**, 2714–2723.
Gust A a, Felix G. 2014. Receptor like proteins associate with SOBIR1-type of adaptors to form bimolecular receptor kinases. Current Opinion in Plant Biology **21**, 104–111.
Halter T, Imkampe J, Mazzotta S, *et al.* 2014. The leucine-rich repeat receptor kinase BIR2 is a negative regulator of BAK1 in plant immunity. Current biology : CB **24**, 134–43.
Haruta M, Sabat G, Stecker K, Minkoff BB, Sussman MR. 2014. A Peptide Hormone and Its Receptor Protein Kinase Regulate Plant Cell Expansion. Science **343**, 408–411.
He K, Gou X, Yuan T, Lin H, Asami T, Yoshida S, Russell SD, Li J. 2007. BAK1 and BKK1 Regulate Brassinosteroid-Dependent Growth and Brassinosteroid-Independent Cell-Death Pathways. Current Biology **17**, 1109–1115.
He Z, Wang Z-Y, Li J, Zhu Q, Lamb C, Ronald P, Chory J. 2000. Perception of Brassinosteroids by the Extracellular Domain of the Receptor Kinase BRI1. Science **288**, 2360–2363.
Heese A, Hann DR, Gimenez-Ibanez S, Jones AME, He K, Li J, Schroeder JI, Peck SC, Rathjen JP. 2007. The receptor-like kinase SERK3/BAK1 is a central regulator of innate immunity in plants. Proceedings of the National Academy of Sciences of the United States of America **104**, 12217–22.
Hegenauer V, Furst U, Kaiser B, Smoker M, Zipfel C, Felix G, Stahl M, Albert M. 2016. Detection of the plant parasite Cuscuta reflexa by a tomato cell surface receptor. Science **353**, 478–481.
Hind SR, Strickler SR, Boyle PC, *et al.* 2016. Tomato receptor FLAGELLIN-SENSING 3 binds flgII-28 and activates the plant immune system. Nature Plants **2**, 16128.
Holton N, Nekrasov V, Ronald PC, Zipfel C. 2015. The phylogenetically-related pattern recognition receptors EFR and XA21 recruit similar immune signaling components in monocots and dicots. PLoS pathogens **11**, e1004602.
Hothorn M, Belkhadir Y, Dreux M, Dabi T, Noel JP, Wilson I a, Chory J. 2011. Structural basis of steroid hormone perception by the receptor kinase BRI1. Nature **474**, 467–71.
Huang S, Nie S, Wang S, Liu J, Zhang Y, Wang X. 2017. SlBIR3 Negatively Regulates PAMP Responses and Cell Death in Tomato. International Journal of Molecular Sciences **18**, 1966.
Huffaker A, Pearce G, Ryan CA. 2006. An endogenous peptide signal in Arabidopsis activates components of the innate immune response. Proceedings of the National Academy of Sciences **103**, 10098–10103.
Huffaker A, Ryan CA. 2007. Endogenous peptide defense signals in Arabidopsis differentially amplify signaling for the innate immune response. Proceedings of the National

Academy of Sciences **104**, 10732–10736.
Hutten SJ, Hamers DS, Den Toorn MA, Van Esse W, Nolles A, B??cherl CA, De Vries SC, Hohlbein J, Borst JW. 2017. Visualization of BRI1 and SERK3/BAK1 nanoclusters in Arabidopsis roots. PLoS ONE **12**, 1–19.
Ichimura K, Shinozaki K, Tena G, *et al.* 2002. Mitogen-activated protein kinase cascades in plants: A new nomenclature. Trends in Plant Science **7**, 301–308.
Imkampe J, Halter T, Huang S, *et al.* 2017. The Arabidopsis Leucine-rich Repeat Receptor Kinase BIR3 Negatively Regulates BAK1 Receptor Complex Formation and Stabilizes BAK1. The Plant Cell, tpc.00376.2017.
Jabs T, Tschope M, Colling C, Hahlbrock K, Scheel D. 1997. Elicitor-stimulated ion fluxes and O2- from the oxidative burst are essential components in triggering defense gene activation and phytoalexin synthesis in parsley. Proceedings of the National Academy of Sciences of the United States of America **94**, 4800–4805.
Jehle AK, Fürst U, Lipschis M, Albert M, Felix G. 2013*a*. Perception of the novel MAMP eMax from different *Xanthomonas* species requires the *Arabidopsis* receptor-like protein ReMAX and the receptor kinase SOBIR. Plant Signaling & Behavior **8**, e27408.
Jehle AK, Lipschis M, Albert M, Fallahzadeh-Mamaghani V, Fürst U, Mueller K, Felix G. 2013*b*. The receptor-like protein ReMAX of Arabidopsis detects the microbe-associated molecular pattern eMax from Xanthomonas. The Plant cell **25**, 2330–40.
Jeong S, Trotochaud AE, Clark SE. 1999. The Arabidopsis CLAVATA2 Gene Encodes a Receptor-like Protein Required for the Stability of the CLAVATA1 Receptor-like Kinase. The Plant Cell **11**, 1925–1934.
Jiménez-Góngora T, Kim S-K, Lozano-Durán R, Zipfel C. 2015. Flg22-Triggered Immunity Negatively Regulates Key BR Biosynthetic Genes. Frontiers in Plant Science **6**, 1–7.
Jones JDG, Dangl JL. 2006. The plant immune system. Nature **444**, 323–9.
Jones D, Thomas C, Hammond-Kosack K, Balint-Kurti P, Jones J. 1994. Isolation of the tomato Cf-9 gene for resistance to Cladosporium fulvum by transposon tagging. Science **266**, 789–793.
Jordá L, Sopeña-Torres S, Escudero V, Nuñez-Corcuera B, Delgado-Cerezo M, Torii KU, Molina A. 2016. ERECTA and BAK1 Receptor Like Kinases Interact to Regulate Immune Responses in Arabidopsis. Frontiers in Plant Science **7**, 1–15.
Kadota Y, Shirasu K, Zipfel C. 2015. Regulation of the NADPH oxidase RBOHD during plant immunity. Plant and Cell Physiology.
Kadota Y, Sklenar J, Derbyshire P, *et al.* 2014. Direct Regulation of the NADPH Oxidase RBOHD by the PRR-Associated Kinase BIK1 during Plant Immunity. Molecular Cell **54**, 43–55.
Kajava A V. 1998. Structural diversity of leucine-rich repeat proteins. J Mol Biol **277**, 519–527.
Kajava A V., Anisimova M, Peeters N. 2008. Origin and evolution of GALA-LRR, a new member of the CC-LRR subfamily: From plants to bacteria? PLoS ONE **3**.
Kaku H, Nishizawa Y, Ishii-Minami N, Akimoto-Tomiyama C, Dohmae N, Takio K, Minami E, Shibuya N. 2006. Plant cells recognize chitin fragments for defense signaling through a plasma membrane receptor. Proceedings of the National Academy of Sciences **103**, 11086–11091.
Karlova R, Boeren S, Russinova E, Aker J, Vervoort J, de Vries S. 2006. The Arabidopsis somatic embryogenesis receptor-like kinase1 protein complex includes brassinosteroid-insensitive1. The Plant Cell **18**, 626–638.
Kayes JM, Clark SE. 1998. *CLAVATA2*, a regulator of meristem and organ development in *Arabidopsis*. Development (Cambridge, England) **125**, 3843–3851.

Keller T, Damude HG, Werner D, Doerner P, Dixon RA, Lamb C. 1998. A Plant Homolog of the Neutrophil NADPH Oxidase gp91 phox Subunit Gene Encodes a Plasma Membrane Protein with Ca 2+ Binding Motifs. The Plant Cell **10**, 255.
Keppler LD. 1989. Active Oxygen Production During a Bacteria-Induced Hypersensitive Reaction in Tobacco Suspension Cells. Phytopathology **79**, 974.
Khan M, Subramaniam R, Desveaux D. 2016. Of guards, decoys, baits and traps: Pathogen perception in plants by type III effector sensors. Current Opinion in Microbiology **29**, 49–55.
Kinoshita A, Betsuyaku S, Osakabe Y, Mizuno S, Nagawa S, Stahl Y, Simon R, Yamaguchi-Shinozaki K, Fukuda H, Sawa S. 2010. RPK2 is an essential receptor-like kinase that transmits the CLV3 signal in Arabidopsis. Development **137**, 4327–4327.
Kiyohara S, Sawa S. 2012. CLE signaling systems during plant development and nematode infection. Plant and Cell Physiology **53**, 1989–1999.
Kobe B, Deisenhofer J. 1993. Crystal structure of porcine ribonuclease inhibitor, a protein with leucine-rich repeats. Nature **366**, 751–756.
Kobe B, Kajava AV. 2001. The leucine-rich repeat as a protein recognition motif. Current opinion in structural biology **11**, 725–32.
Koller T, Bent AF. 2014. FLS2-BAK1 extracellular domain interaction sites required for defense signaling activation. PloS one **9**, e111185.
Krol E, Mentzel T, Chinchilla D, *et al.* 2010. Perception of the Arabidopsis danger signal peptide 1 involves the pattern recognition receptor AtPEPR1 and its close homologue AtPEPR2. Journal of Biological Chemistry **285**, 13471–13479.
Kumpf RP, Shi C-L, Larrieu A, Sto IM, Butenko MA, Peret B, Riiser ES, Bennett MJ, Aalen RB. 2013. Floral organ abscission peptide IDA and its HAE/HSL2 receptors control cell separation during lateral root emergence. Proceedings of the National Academy of Sciences **110**, 5235–5240.
Lacombe S, Rougon-Cardoso A, Sherwood E, *et al.* 2010. Interfamily transfer of a plant pattern-recognition receptor confers broad-spectrum bacterial resistance. Nature Biotechnology **28**, 365–369.
Laluk K, Luo H, Chai M, Dhawan R, Lai Z, Mengiste T. 2011. Biochemical and Genetic Requirements for Function of the Immune Response Regulator BOTRYTIS-INDUCED KINASE1 in Plant Growth, Ethylene Signaling, and PAMP-Triggered Immunity in *Arabidopsis*. The Plant Cell **23**, 2831–2849.
Leon-Reyes A, Van der Does D, De Lange ES, Delker C, Wasternack C, Van Wees SCM, Ritsema T, Pieterse CMJ. 2010. Salicylate-mediated suppression of jasmonate-responsive gene expression in arabidopsis is targeted downstream of the jasmonate biosynthesis pathway. Planta **232**, 1423–1432.
Li J. 2010. Multi-tasking of somatic embryogenesis receptor-like protein kinases. Current opinion in plant biology **13**, 509–14.
Li J, Chory J. 1997. A putative leucine-rich repeat receptor kinase involved in brassinosteroid signal transduction. Cell **90**, 929–938.
Li L, Li M, Yu L, *et al.* 2014. The FLS2-associated kinase BIK1 directly phosphorylates the NADPH oxidase RbohD to control plant immunity. Cell Host and Microbe **15**, 329–338.
Li J, Wen J, Lease KA, Doke JT, Tax FE, Walker JC. 2002. BAK1, an Arabidopsis LRR receptor-like protein kinase, interacts with BRI1 and modulates brassinosteroid signaling. Cell **110**, 213–222.
Li E, Wimley WC, Hristova K. 2012. Transmembrane helix dimerization: Beyond the search for sequence motifs. Biochimica et Biophysica Acta - Biomembranes **1818**, 183–193.
Li J, Zhao-Hui C, Batoux M, Nekrasov V, Roux M, Chinchilla D, Zipfel C, Jones JD. 2009. Specific ER quality control components required for biogenesis of the plant innate immune receptor EFR. Proceedings of the … **106**, 15973–15978.

Liebrand TWH, van den Berg GCM, Zhang Z, *et al.* 2013. Receptor-like kinase SOBIR1/EVR interacts with receptor-like proteins in plant immunity against fungal infection. Proceedings of the National Academy of Sciences of the United States of America **110**, 10010–5.

Liebrand TWH, van den Burg H a, Joosten MH a J. 2014. Two for all: receptor-associated kinases SOBIR1 and BAK1. Trends in plant science **19**, 123–32.

Lin W, Lu D, Gao X, Jiang S. 2013. Inverse modulation of plant immune and brassinosteroid signaling pathways by the receptor-like cytoplasmic kinase BIK1. Proceedings of the National Academy of Sciences of the United States of America **110**, 12114–12119.

Liu P-L, Du L, Huang Y, Gao S-M, Yu M. 2017. Origin and diversification of leucine-rich repeat receptor-like protein kinase (LRR-RLK) genes in plants. BMC Evolutionary Biology **17**, 47.

Liu Z, Wu Y, Yang F, Zhang Y, Chen S, Xie Q, Tian X, Zhou J-M. 2013. BIK1 interacts with PEPRs to mediate ethylene-induced immunity. Proceedings of the National Academy of Sciences **110**, 6205–6210.

Lori M, Van Verk MC, Hander T, Schatowitz H, Klauser D, Flury P, Gehring CA, Boller T, Bartels S. 2015. Evolutionary divergence of the plant elicitor peptides (Peps) and their receptors: Interfamily incompatibility of perception but compatibility of downstream signalling. Journal of Experimental Botany **66**, 5315–5325.

Lozano-Durán R, Macho AP, Boutrot F, Segonzac C, Somssich IE, Zipfel C. 2013. The transcriptional regulator BZR1 mediates trade-off between plant innate immunity and growth. eLife **2**, e00983.

Lu S-W, Chen S, Wang J, Yu H, Chronis D, Mitchum MG, Wang X. 2009. Structural and Functional Diversity of CLAVATA3/ESR (CLE)-Like Genes from the Potato Cyst Nematode Globodera rostochiensis. Molecular Plant-Microbe Interactions MPMI **221094**, 1128–1142.

Lu D, Lin W, Gao X, Wu S, Cheng C, Avila J, Heese A, Devarenne TP, He P, Shan L. 2011. Direct Ubiquitination of Pattern Recognition Receptor FLS2 Attenuates Plant Innate Immunity. Science **332**, 1439–1442.

Lu D, Wu S, Gao X, Zhang Y, Shan L, He P. 2010. A receptor-like cytoplasmic kinase, BIK1, associates with a flagellin receptor complex to initiate plant innate immunity. Proceedings of the National Academy of Sciences of the United States of America **107**, 496–501.

Lupas AN, Bassler J. 2017. Coiled Coils – A Model System for the 21st Century. Trends in Biochemical Sciences **42**, 130–140.

Ma C, Liu Y, Bai B, Han Z, Tang J, Zhang H, Yaghmaiean H, Zhang Y, Chai J. 2017. Structural basis for BIR1-mediated negative regulation of plant immunity. Cell Res, 1–4.

Ma Y, Walker RK, Zhao Y, Berkowitz GA. 2012. Linking ligand perception by PEPR pattern recognition receptors to cytosolic Ca2+ elevation and downstream immune signaling in plants. Proceedings of the National Academy of Sciences **109**, 19852–19857.

Ma X, Xu G, He P, Shan L. 2016. SERKing Coreceptors for Receptors. Trends in Plant Science **21**, 1017–1033.

Macho AP, Lozano-Durán R, Zipfel C. 2015. Importance of tyrosine phosphorylation in receptor kinase complexes. Trends in plant science **20**, 269–272.

Macho AP, Schwessinger B, Ntoukakis V, *et al.* 2014. A Bacterial Tyrosine Phosphatase Inhibits Plant Pattern Recognition Receptor Activation. Science **343**, 1509–1512.

Masachis S, Segorbe D, Turrà D, *et al.* 2016. A fungal pathogen secretes plant alkalinizing peptides to increase infection. Nature Microbiology **1**, 16043.

Masle J, Gilmore SR, Farquhar GD. 2005. The ERECTA gene regulates plant transpiration efficiency in Arabidopsis. Nature **436**, 866–870.

Di Matteo A, Federici L, Mattei B, Salvi G, Johnson KA, Savino C, De Lorenzo G, Tsernoglou D, Cervone F. 2003. The crystal structure of polygalacturonase-inhibiting protein (PGIP), a leucine-rich repeat protein involved in plant defense. Proceedings of the National Academy of Sciences of the United States of America **100**, 10124–8.

McAndrew R, Pruitt RN, Kamita SG, Pereira JH, Majumdar D, Hammock BD, Adams PD, Ronald PC. 2014. Structure of the OsSERK2 leucine-rich repeat extracellular domain. Acta Crystallographica Section D Biological Crystallography **70**, 3080–3086.

McCann HC, Nahal H, Thakur S, Guttman DS. 2012. Identification of innate immunity elicitors using molecular signatures of natural selection. Proceedings of the National Academy of Sciences **109**, 4215–4220.

Melnyk RA, Kim S, Curran AR, Engelman DM, Bowie JU, Deber CM. 2004. The Affinity of GXXXG Motifs in Transmembrane Helix-Helix Interactions Is Modulated by Long-range Communication. Journal of Biological Chemistry **279**, 16591–16597.

Meng X, Chen X, Mang H, Liu C, Yu X, Gao X, Torii KU, He P, Shan L. 2015. Differential Function of Arabidopsis SERK Family Receptor-like Kinases in Stomatal Patterning. Current Biology **25**, 2361–2372.

Meng X, Zhang S. 2013. MAPK Cascades in Plant Disease Resistance Signaling. Annual Review of Phytopathology **51**, 245–266.

Meng X, Zhou J, Tang J, Li B, de Oliveira MV V, Chai J, He P, Shan L. 2016. Ligand-Induced Receptor-like Kinase Complex Regulates Floral Organ Abscission in Arabidopsis. Cell Reports **14**, 1330–1338.

Mersmann S, Bourdais G, Rietz S, Robatzek S. 2010. Ethylene Signaling Regulates Accumulation of the FLS2 Receptor and Is Required for the Oxidative Burst Contributing to Plant Immunity. Plant Physiology **154**, 391–400.

Mithoe SC, Ludwig C, Pel MJ, *et al.* 2016. Attenuation of pattern recognition receptor signaling is mediated by a MAP kinase kinase kinase. EMBO reports **17**, 441–454.

Mithöfer A, Ebel J, Felle HH. 2005. Cation fluxes cause plasma membrane depolarization involved in beta-glucan elicitor-signaling in soybean roots. Molecular plant-microbe interactions : MPMI **18**, 983–990.

Miya A, Albert P, Shinya T, Desaki Y, Ichimura K, Shirasu K, Narusaka Y, Kawakami N, Kaku H, Shibuya N. 2007. CERK1, a LysM receptor kinase, is essential for chitin elicitor signaling in Arabidopsis. Proceedings of the National Academy of Sciences **104**, 19613–19618.

Monaghan J, Matschi S, Romeis T, Zipfel C. 2015. The calcium-dependent protein kinase CPK28 negatively regulates the BIK1-mediated PAMP-induced calcium burst. Plant Signaling & Behavior **10**, e1018497.

Monaghan J, Matschi S, Shorinola O, *et al.* 2014. The calcium-dependent protein kinase CPK28 buffers plant immunity and regulates BIK1 turnover. Cell Host and Microbe **16**, 605–615.

Mondragon-Palomino M, Gaut BS. 2005. Gene conversion and the evolution of three leucine-rich repeat gene families in arabidopsis thaliana. Molecular Biology and Evolution **22**, 2444–2456.

Morales J, Kadota Y, Zipfel C, Molina A, Torres MA. 2016. The Arabidopsis NADPH oxidases RbohD and RbohF display differential expression patterns and contributions during plant immunity. Journal of Experimental Botany **67**, 1663–1676.

Mueller K, Bittel P, Chinchilla D, Jehle AK, Albert M, Boller T, Felix G. 2012*a*. Chimeric FLS2 receptors reveal the basis for differential flagellin perception in Arabidopsis and tomato. The Plant cell **24**, 2213–24.

Mueller K, Chinchilla D, Albert M, Jehle AK, Kalbacher H, Boller T, Felix G. 2012*b*. Contamination risks in work with synthetic peptides: flg22 as an example of a pirate in

commercial peptide preparations. The Plant cell **24**, 3193–7.
Muller R, Bleckmann A, Simon R. 2008. The Receptor Kinase CORYNE of Arabidopsis Transmits the Stem Cell-Limiting Signal CLAVATA3 Independently of CLAVATA1. the Plant Cell Online **20**, 934–946.
Nadeau J a, Sack FD. 2002. Control of stomatal distribution on the *Arabidopsis* leaf surface. Science **296**, 1697–1700.
Naito K, Taguchi F, Suzuki T, Inagaki Y, Toyoda K, Shiraishi T, Ichinose Y. 2008. Amino acid sequence of bacterial microbe-associated molecular pattern flg22 is required for virulence. Molecular plant-microbe interactions : MPMI **21**, 1165–74.
Nam KH, Li J. 2002. BRI1/BAK1, a receptor kinase pair mediating brassinosteroid signaling. Cell **110**, 203–212.
Nekrasov V, Li J, Batoux M, *et al.* 2009. Control of the pattern-recognition receptor EFR by an ER protein complex in plant immunity. The EMBO Journal **28**, 3428–3438.
Nimchuk ZL, Tarr PT, Meyerowitz EM. 2011. An Evolutionarily Conserved Pseudokinase Mediates Stem Cell Production in Plants. The Plant Cell **23**, 851–854.
Nühse TS, Peck SC, Hirt H, Boller T. 2000. Microbial elicitors induce activation and dual phosphorylation of the Arabidopsis thaliana MAPK 6. Journal of Biological Chemistry **275**, 7521–7526.
Nürnberger T, Brunner F, Kemmerling B, Piater L, Nurnberger T, Brunner F, Kemmerling B, Piater L. 2004. Innate immunity in plants and animals: strinking similarities and obvious differences. Immunological Reviews **198**, 249–266.
Ogawa M, Shinohara H, Sakagami Y, Matsubayashi Y. 2008. Arabidopsis CLV3 Peptide Directly Binds CLV1 Ectodomain. Science **319**, 294–294.
Oh M-H, Wang X, Wu X, Zhao Y, Clouse SD, Huber SC. 2010. Autophosphorylation of Tyr-610 in the receptor kinase BAK1 plays a role in brassinosteroid signaling and basal defense gene expression. Proceedings of the National Academy of Sciences **107**, 17827–17832.
Ohyama K, Shinohara H, Ogawa-Ohnishi M, Matsubayashi Y. 2009. A glycopeptide regulating stem cell fate in Arabidopsis thaliana. Nature Chemical Biology **5**, 578–580.
Oome S, Raaymakers TM, Cabral A, Samwel S, Böhm H, Albert I, Nürnberger T, Van den Ackerveken G. 2014. Nep1-like proteins from three kingdoms of life act as a microbe-associated molecular pattern in *Arabidopsis*. Proceedings of the National Academy of Sciences **111**, 16955–16960.
Pan L, Lv S, Yang N, Lv Y, Liu Z, Wu J, Wang G. 2016. The Multifunction of CLAVATA2 in Plant Development and Immunity. Frontiers in Plant Science **7**, 1573.
Petutschnig EK, Jones AME, Serazetdinova L, Lipka U, Lipka V. 2010. The Lysin Motif Receptor-like Kinase (LysM-RLK) CERK1 is a major chitin-binding protein in Arabidopsis thaliana and subject to chitin-induced phosphorylation. Journal of Biological Chemistry **285**, 28902–28911.
Pitzschke A, Schikora A, Hirt H. 2009. MAPK cascade signalling networks in plant defence. Current Opinion in Plant Biology **12**, 421–426.
Postma J, Liebrand TWH, Bi G, Evrard A, Bye RR, Mbengue M, Joosten MHAJ, Robatzek S. 2015. The Cf-4 receptor-like protein associates with the BAK1 receptor-like kinase to initiate receptor endocytosis and plant immunity. bioRxiv, 627–642.
Rahikainen M, Pascual J, Alegre S, Durian G, Kangasjärvi S. 2016. PP2A Phosphatase as a Regulator of ROS Signaling in Plants. Antioxidants **5**, 8.
Ranf S. 2016. Immune Sensing of Lipopolysaccharide in Plants and Animals: Same but Different. PLoS Pathogens **12**, 1–7.
Ranf S, Gisch N, Schäffer M, *et al.* 2015. A lectin S-domain receptor kinase mediates lipopolysaccharide sensing in Arabidopsis thaliana. Nature Immunology **16**, 426–433.

Replogle A, Wang J, Bleckmann A, Hussey RS, Baum TJ, Sawa S, Davis EL, Wang X, Simon R, Mitchum MG. 2011. Nematode CLE signaling in Arabidopsis requires CLAVATA2 and CORYNE. Plant Journal **65**, 430–440.

Replogle AJ, Wang J, Paolillo V, Smeda J, Kinoshita A, Durbak A, Tax FE, Wang X, Sawa S, Mitchum MG. 2012. Synergistic Interaction of CLAVATA1, CLAVATA2, and RECEPTOR-LIKE PROTEIN KINASE 2 in Cyst Nematode Parasitism of Arabidopsis. Molecular Plant-Microbe Interactions **26**, 120726074929003.

Ron M, Avni A. 2004. The Receptor for the Fungal Elicitor Ethylene-Inducing Xylanase Is a Member of a Resistance- Like Gene Family in Tomato. The Plant Cell **16**, 1604–1615.

Ross A, Yamada K, Hiruma K, Yamashita-Yamada M, Lu X, Takano Y, Tsuda K, Saijo Y. 2014. The Arabidopsis PEPR pathway couples local and systemic plant immunity. EMBO Journal **33**, 62–75.

Roux M, Schwessinger B, Albrecht C, Chinchilla D, Jones A, Holton N, Malinovsky FG, Tör M, de Vries S, Zipfel C. 2011. The Arabidopsis leucine-rich repeat receptor-like kinases BAK1/SERK3 and BKK1/SERK4 are required for innate immunity to hemibiotrophic and biotrophic pathogens. The Plant cell **23**, 2440–55.

Rushton PJ, Somssich IE, Ringler P, Shen QJ. 2010. WRKY transcription factors. Trends in Plant Science **15**, 247–258.

Russ WP, Engelman DM. 2000. The GxxxG motif: A framework for transmembrane helix-helix association. Journal of Molecular Biology **296**, 911–919.

Russinova E, Borst J-W, Kwaaitaal M, Caño-Delgado AI, Yin Y, Chory J, de Vries S. 2004. Heterodimerization and endocytosis of Arabidopsis brassinosteroid receptors BRI1 and AtSERK3 (BAK1). The Plant Cell **16**, 3216–3229.

Santiago J, Brandt B, Wildhagen M, Hohmann U, Hothorn LA, Butenko MA, Hothorn M. 2016. Mechanistic insight into a peptide hormone signaling complex mediating floral organ abscission. eLife **5**, 1–19.

Santiago J, Henzler C, Hothorn M. 2013. Molecular mechanism for plant steroid receptor activation by somatic embryogenesis co-receptor kinases. Science (New York, N.Y.) **341**, 889–92.

Schneider D, Engelman DM. 2004. Motifs of two small residues can assist but are not sufficient to mediate transmembrane helix interactions. Journal of Molecular Biology **343**, 799–804.

Schoonbeek H jan, Wang HH, Stefanato FL, Craze M, Bowden S, Wallington E, Zipfel C, Ridout CJ. 2015. Arabidopsis EF-Tu receptor enhances bacterial disease resistance in transgenic wheat. New Phytologist **206**, 606–613.

Schulze B, Mentzel T, Jehle AK, Mueller K, Beeler S, Boller T, Felix G, Chinchilla D. 2010. Rapid heteromerization and phosphorylation of ligand-activated plant transmembrane receptors and their associated kinase BAK1. The Journal of biological chemistry **285**, 9444–51.

Schwessinger B, Rathjen JP. 2015. Changing SERKs and priorities during plant life. Trends in Plant Science **20**, 531–533.

Schwessinger B, Roux M, Kadota Y, Ntoukakis V, Sklenar J, Jones A, Zipfel C. 2011. Phosphorylation-dependent differential regulation of plant growth, cell death, and innate immunity by the regulatory receptor-like kinase BAK1. PLoS genetics **7**, e1002046.

Segonzac C, Macho AP, Sanmartín M, Ntoukakis V, Sánchez-serrano JJ, Zipfel C. 2014. Negative control of BAK 1 by protein phosphatase 2 A during plant innate immunity. , 1–11.

Segonzac C, Nimchuk ZL, Beck M, Tarr PT, Robatzek S, Meyerowitz EM, Zipfel C. 2012. The Shoot Apical Meristem Regulatory Peptide CLV3 Does Not Activate Innate Immunity. The Plant Cell **24**, 3186–3192.

Senes A, Gerstein M, Engelman DM. 2000. Statistical analysis of amino acid patterns in

transmembrane helices: the GxxxG motif occurs frequently and in association with β-branched residues at neighboring positions. Journal of Molecular Biology **296**, 921–936.
Shan L, He P, Li J, Heese A, Peck SC, Nürnberger T, Martin GB, Sheen J. 2008. Bacterial effectors target the common signaling partner BAK1 to disrupt multiple MAMP receptor-signaling complexes and impede plant immunity. Cell host & microbe **4**, 17–27.
Shannon CE. 1948. A mathematical theory of communication. The Bell System Technical Journal **27**, 379–423, 623–656.
Shimizu T, Nakano T, Takamizawa D, *et al.* 2010. Two LysM receptor molecules, CEBiP and OsCERK1, cooperatively regulate chitin elicitor signaling in rice. Plant Journal **64**, 204–214.
Shiu S, Bleecker AB. 2003. Expansion of the Receptor-Like Kinase / Pelle Gene Family and Receptor-Like Proteins in Arabidopsis. Plant physiology **132**, 530–543.
Shpak ED. 2013. Diverse roles of ERECTA family genes in plant development. Journal of Integrative Plant Biology **55**, 1238–1250.
Shpak ED, Berthiaume CT, Hill EJ, Torii KU. 2004. Synergistic interaction of three ERECTA-family receptor-like kinases controls Arabidopsis organ growth and flower development by promoting cell proliferation. Development **131**, 1491–1501.
Shpak ED, Mcabee JM, Pillitteri LJ, Torii KU. 2005. Stomatal Patterning and Differentiation by Synergistic Interactions of Receptor Kinases. Science **309**, 290–293.
Smith JM, Salamango DJ, Leslie ME, Collins CA, Heese A. 2014. Sensitivity to Flg22 Is Modulated by Ligand-Induced Degradation and de Novo Synthesis of the Endogenous Flagellin-Receptor FLAGELLIN-SENSING2. Plant Physiology **164**, 440–454.
Spanu P, Grosskopf DG, Felix G, Boller T. 1994. The Apparent Turnover of 1-Aminocyclopropane-1-Carboxylate Synthase in Tomato Cells Is Regulated by Protein Phosphorylation and Dephosphorylation. Plant physiology **106**, 529–535.
Sun Y, Han Z, Tang J, Hu Z, Chai C, Zhou B, Chai J. 2013*a*. Structure reveals that BAK1 as a co-receptor recognizes the BRI1-bound brassinolide. Cell Research **23**, 1326–1329.
Sun Y, Li L, Macho AP, Han Z, Hu Z, Zipfel C, Zhou J-M, Chai J. 2013*b*. Structural basis for flg22-induced activation of the Arabidopsis FLS2-BAK1 immune complex. Science (New York, N.Y.) **342**, 624–8.
Sun K, Wolters A-MA, Vossen JH, Rouwet ME, Loonen AEHM, Jacobsen E, Visser RGF, Bai Y. 2016. Silencing of six susceptibility genes results in potato late blight resistance. Transgenic Research **25**, 731–742.
Takahashi T, Mu J, Gasch A, Chua N. 1998. Identification by PCR of receptor-like protein kinases from Arabidopsis flowers. Plant Molecular Biology, 587–596.
Tanaka K, Choi J, Cao Y, Stacey G. 2014. Extracellular ATP acts as a damage-associated molecular pattern (DAMP) signal in plants. Frontiers in plant science **5**, 446.
Tang J, Han Z, Sun Y, Zhang H, Gong X, Chai J. 2015. Structural basis for recognition of an endogenous peptide by the plant receptor kinase PEPR1. Cell Research **25**, 110–120.
Thaler JS, Fidantsef a L, Duffey SS, Bostock RM. 1999. Trade-offs in plant defense against pathogens and herbivores: a field demonstration of chemical elicitors of induced resistance. Journal of Chemical Ecology **25**, 1597–1609.
Thaler JS, Humphrey PT, Whiteman NK. 2012. Evolution of jasmonate and salicylate signal crosstalk. Trends in Plant Science **17**, 260–270.
Thomma BPHJ, Eggermont K, Penninckx IAMA, Mauch-Mani B, Vogelsang R, Cammue BPA, Broekaert WF. 1998. Separate jasmonate-dependent and salicylate-dependent defense-response pathways in Arabidopsis are essential for resistance to distinct microbial pathogens. Proceedings of the National Academy of Sciences **95**, 15107–15111.
Thuerig B, Felix G, Binder A, Boller T, Tamm L. 2006. An extract of Penicillium chrysogenum elicits early defense-related responses and induces resistance in Arabidopsis

thaliana independently of known signalling pathways. Physiological and Molecular Plant Pathology **67**, 180–193.

Tintor N, Ross a., Kanehara K, Yamada K, Fan L, Kemmerling B, Nurnberger T, Tsuda K, Saijo Y. 2013. Layered pattern receptor signaling via ethylene and endogenous elicitor peptides during Arabidopsis immunity to bacterial infection. Proceedings of the National Academy of Sciences **110**, 6211–6216.

Tintor N, Saijo Y. 2014. ER-mediated control for abundance, quality, and signaling of transmembrane immune receptors in plants. Frontiers in Plant Science **5**, 2008–2013.

Torii KU, Mitsukawa N, Oosumi T, Matsuura Y, Yokoyama R, Whittier RF, Komeda Y. 1996. The Arabidopsis ERECTA Gene Encodes a Putative Receptor Protein Kinase with Extracellular Leucine-Rich Repeats. The Plant Cell **8**, 735–746.

De Torres M, Mansfield JW, Grabov N, Brown IR, Ammouneh H, Tsiamis G, Forsyth A, Robatzek S, Grant M, Boch J. 2006. Pseudomonas syringae effector AvrPtoB suppresses basal defence in Arabidopsis. Plant Journal **47**, 368–382.

Torres MA, Dangl JL. 2005. Functions of the respiratory burst oxidase in biotic interactions, abiotic stress and development. Current Opinion in Plant Biology **8**, 397–403.

Torres MA, Dangl JL, Jones JDG. 2002. Arabidopsis gp91phox homologues AtrbohD and AtrbohF are required for accumulation of reactive oxygen intermediates in the plant defense response. Proceedings of the National Academy of Sciences **99**, 517–522.

Trempel F, Kajiura H, Ranf S, Grimmer J, Westphal L, Zipfel C, Scheel D, Fujiyama K, Lee J. 2016. Altered glycosylation of exported proteins, including surface immune receptors, compromises calcium and downstream signaling responses to microbe-associated molecular patterns in Arabidopsis thaliana. BMC Plant Biology **16**, 31.

Unterreitmeier S, Fuchs A, Schäffler T, Heym RG, Frishman D, Langosch D. 2007. Phenylalanine Promotes Interaction of Transmembrane Domains via GxxxG Motifs. Journal of Molecular Biology **374**, 705–718.

Vert G, Chory J. 2006. Downstream nuclear events in brassinosteroid signalling. Nature **441**, 96–100.

Vetter MM, Kronholm I, He F, Häweker H, Reymond M, Bergelson J, Robatzek S, de Meaux J. 2012. Flagellin perception varies quantitatively in Arabidopsis thaliana and its relatives. Molecular biology and evolution **29**, 1655–67.

Villarroel CA, Jonckheere W, Alba JM, Glas JJ, Dermauw W, Haring MA, Van Leeuwen T, Schuurink RC, Kant MR. 2016. Salivary proteins of spider mites suppress defenses in Nicotiana benthamiana and promote mite reproduction. Plant Journal **86**, 119–131.

Voinnet O, Rivas S, Mestre P, Baulcombe D. 2003. An enhanced transient expression system in plants based on suppression of gene silencing by the p19 protein of tomato bushy stunt virus. The Plant Journal **33**, 949–956.

Wang L, Albert M, Einig E, Fürst U, Krust D, Felix G. 2016. The pattern-recognition receptor CORE of Solanaceae detects bacterial cold-shock protein. Nature Plants **2**, 16185.

Wang G, Ellendorff U, Kemp B, *et al.* 2008. A Genome-Wide Functional Investigation into the Roles of Receptor-Like Proteins in Arabidopsis. Plant Physiology **147**, 503–517.

Wang J, Li H, Han Z, Zhang H, Wang T, Lin G, Chang J, Yang W, Chai J. 2015. Allosteric receptor activation by the plant peptide hormone phytosulfokine. Nature **525**, 265–268.

Wang X, Mitchum MG, Gao B, Li C, Diab H, Baum TJ, Hussey RS, Davis EL. 2005. A parasitism gene from a plant-parasitic nematode with function similar to CLAVATA3/ESR (CLE) of Arabidopsis thaliana. Molecular Plant Pathology **6**, 187–191.

Wang ZY, Nakano T, Gendron J, *et al.* 2002. Nuclear-localized BZR1 mediates brassinosteroid-induced growth and feedback suppression of brassinosteroid biosynthesis.

Developmental Cell **2**, 505–513.
Wang J, Replogle A, Hussey R, Baum T, Wang X, Davis EL, Mitchum MG. 2011. Identification of potential host plant mimics of CLAVATA3/ESR (CLE)-like peptides from the plant-parasitic nematode Heterodera schachtii. Molecular Plant Pathology **12**, 177–186.
Wang W, Xie ZP, Staehelin C. 2014. Functional analysis of chimeric lysin motif domain receptors mediating Nod factor-induced defense signaling in Arabidopsis thaliana and chitin-induced nodulation signaling in Lotus japonicus. Plant Journal **78**, 56–69.
Wildhagen M, Butenko MA, Aalen RB, Felix G, Albert M. 2015. A Chemiluminescence Based Receptor-ligand Binding Assay Using Peptide Ligands with an Acridinium Ester Label. Bio-Protocol **5**, 2–7.
Willmann R, Lajunen HM, Erbs G, Newman M, Kolb D, Tsuda K. 2011. Mediate Bacterial Peptidoglycan Sensing and Immunity To Bacterial Infection. Proceedings of the National Academy of Sciences **108**, 19824–19829.
Wolf S, van der Does D, Ladwig F, *et al.* 2014. A receptor-like protein mediates the response to pectin modification by activating brassinosteroid signaling. Proceedings of the National Academy of Sciences **111**, 15261–15266.
Wu W, Wu Y, Gao Y, Li M, Yin H, Lv M, Zhao J, Li J, He K. 2015. Somatic embryogenesis receptor-like kinase 5 in the ecotype Landsberg erecta of Arabidopsis is a functional RD LRR-RLK in regulating brassinosteroid signaling and cell death control. Frontiers in Plant Science **6**, 1–16.
Wulff BBH. 2001. Domain Swapping and Gene Shuffling Identify Sequences Required for Induction of an Avr-Dependent Hypersensitive Response by the Tomato Cf-4 and Cf-9 Proteins. the Plant Cell Online **13**, 255–272.
Wulff BBH, Heese A, Tomlinson-Buhot L, Jones D a, de la Peña M, Jones JDG. 2009. The major specificity-determining amino acids of the tomato Cf-9 disease resistance protein are at hypervariable solvent-exposed positions in the central leucine-rich repeats. Molecular plant-microbe interactions : MPMI **22**, 1203–1213.
Wyrsch I, Dom A, Geldner N, Boller T. 2015. Tissue-specific FLAGELLIN-SENSING 2 (FLS2) expression in roots restores immune responses in Arabidopsis fls2 mutants. **2**.
Yamaguchi Y, Huffaker A. 2011. Endogenous peptide elicitors in higher plants. Current Opinion in Plant Biology **14**, 351–357.
Yamaguchi Y, Huffaker A, Bryan AC, Tax FE, Ryan CA. 2010. PEPR2 Is a Second Receptor for the Pep1 and Pep2 Peptides and Contributes to Defense Responses in Arabidopsis. The Plant Cell **22**, 508–522.
Yamaguchi Y, Pearce G, Ryan CA. 2006. The cell surface leucine-rich repeat receptor for AtPep1, an endogenous peptide elicitor in Arabidopsis, is functional in transgenic tobacco cells. Proceedings of the National Academy of Sciences **103**, 10104–10109.
Yang SF, Hoffman NE. 1984. ETHYLENE BIOSYNTHESIS AND ITS REGULATION IN HIGHER PLANTS. Annual Review of Plant Biology **35**, 155–89.
Yin Y, Wang ZY, Mora-Garcia S, Li J, Yoshida S, Asami T, Chory J. 2002. BES1 accumulates in the nucleus in response to brassinosteroids to regulate gene expression and promote stem elongation. Cell **109**, 181–191.
Yoo S-D, Cho Y-H, Sheen J. 2007. Arabidopsis mesophyll protoplasts: a versatile cell system for transient gene expression analysis. Nature protocols **2**, 1565–72.
Yue J, Meyers BC, Chen J, Tian D, Yang S. 2012. Tracing the origin and evolutionary history of plant nucleotide-binding site – leucine-rich repeat (NBS-LRR) genes. , 1049–1063.
Zhang W, Fraiture M, Kolb D, Loffelhardt B, Desaki Y, Boutrot FFG, Tor M, Zipfel C, Gust AA, Brunner F. 2013. Arabidopsis RECEPTOR-LIKE PROTEIN30 and Receptor-Like Kinase SUPPRESSOR OF BIR1-1/EVERSHED Mediate Innate Immunity to Necrotrophic

Fungi. The Plant Cell **25**, 4227–4241.
Zhang L, Kars I, Essenstam B, Liebrand TWH, Wagemakers L, Elberse J, Tagkalaki P, Tjoitang D, van den Ackerveken G, van Kan JAL. 2014. Fungal Endopolygalacturonases Are Recognized as Microbe-Associated Molecular Patterns by the Arabidopsis Receptor-Like Protein RESPONSIVENESS TO BOTRYTIS POLYGALACTURONASES1. Plant Physiology **164**, 352–364.
Zhang J, Li W, Xiang T, *et al.* 2010. Receptor-like cytoplasmic kinases integrate signaling from multiple plant immune receptors and are targeted by a Pseudomonas syringae effector. Cell Host and Microbe **7**, 290–301.
Zhang Z, Thomma BPHJ. 2013. Structure-function aspects of extracellular leucine-rich repeat-containing cell surface receptors in plants. Journal of Integrative Plant Biology **55**, 1212–1223.
Zhang J, Zhou JM. 2010. Plant immunity triggered by microbial molecular signatures. Molecular Plant **3**, 783–793.
Zheng Y, Zhu Z. 2016. Relaying the Ethylene Signal: New Roles for EIN2. Trends in Plant Science **21**, 2–4.
Zhou J, Peng Z, Long J, *et al.* 2015. Gene targeting by the TAL effector PthXo2 reveals cryptic resistance gene for bacterial blight of rice. Plant Journal **82**, 632–643.
Zhu S, Li Y, Vossen JH, Visser RGF, Jacobsen E. 2012. Functional stacking of three resistance genes against Phytophthora infestans in potato. Transgenic Research **21**, 89–99.
Zhu Y, Wang Y, Li R, Song X, Wang Q, Huang S, Jin JB, Liu CM, Lin J. 2010. Analysis of interactions among the CLAVATA3 receptors reveals a direct interaction between CLAVATA2 and CORYNE in Arabidopsis. Plant Journal **61**, 223–233.
Zipfel C, Kunze G, Chinchilla D, Caniard A, Jones JDG, Boller T, Felix G. 2006. Perception of the Bacterial PAMP EF-Tu by the Receptor EFR Restricts Agrobacterium-Mediated Transformation. Cell **125**, 749–760.

List of figures and tables

Figure 1.1 - Overview of PAMP-triggered immunity (PTI) in plants 2
Figure 1.2 - LRR-RLKs and LRR-RLPs with SOBIR1 look similar 5
Figure 1.3 - Crystal structure of FLS2-SERK3-flg22 complex (data from Sun et al., 2013) 7
Figure 1.4 - RLPs and SOBIR1s share a common motif in their transmembrane domain (Figure from Gust & Felix, 2014) 10
Figure 1.5 - Regulation of PRR at the plasma membrane 19
Figure 3.1 - Workflow for the analysis of LRR-protein evolution 33
Figure 4.1 - Taxonomic list of used plant reference proteomes from UniProt 36
Figure 4.2 - CLANS map for the *A. thaliana* proteome 37
Figure 4.3 - CLANS map at cutoff 2.4 of length-adjusted HSPs 38
Figure 4.4 – Constructs used for turning a LRR-RLK into a LRR-RLP 42
Figure 4.5 – Oxidative burst in transformed *N. benthamiana* *43*
Figure 4.6 – Ethylene induction in transformed *N. benthamiana* *44*
Figure 4.7 - Co-immunprecipitation assay reveals interaction with SOBIR1 for constructs containing the TMD of RLP23 45
Figure 4.8 - Oxidative burst in transformed *N. benthamiana* *46*
Figure 4.9 - Oxidative burst in transformed *N. benthamiana.* *47*
Figure 4.10 - Ethylene induction in transformed *N. benthamiana.* *47*
Figure 4.11 - Co-immunprecipitation assay reveals interaction with SOBIR1 for constructs containing the TMD of EIX2 48
Figure 4.12 – TMD of CLV2 is also functional in EFRΔkin backbone 50
Figure 4.13 – Constructs containing the TMD of CLV2 co-immunprecipitate with CRN and not with SOBIR1 51
Figure 4.14 – CLV1 and CLV2 do not bind to acri-CLV3 52
Figure 4.15 – Neither CLV1 nor CLV2 interact with BAK1 or SOBIR1 54
Figure 4.16 - Constructs used for turning a LRR-RLP into a LRR-RLK 55
Figure 4.17 - RLP23 constructs containing the TMD of SOBIR1 can propagate nlp20 signaling 56
Figure 4.18 - EIX2 constructs containing the TMD of SOBIR1 can propagate xylanase signaling 57
Figure 4.19 - EFR constructs containing the TMD of SOBIR1 can propagate elf18 signaling 58
Figure 4.20 - Coimmunoprecipitation of RLP23tmkSOBIR1 with SOBIR1 and BAK1 59
Figure 4.21 – RLP23tmkSOBIR can induce FRK1 in *A. thaliana* sobir1-12 mutant 59
Figure 4.22 – Entropy analysis of TMD consensus sequences 61
Figure 5.1 – Model for the interaction of LRR-RLPs with SOBIR1 75

Table 3.1 - List of bioinformatic tools and their corresponding websites 34
Table 4.1 - Summary of the CLANS map analysis 39

List of abbreviations

%	percent
Δ	truncated
°C	degree Celsius
35S	promoter of cauliflower mosaic virus
A	alanine
aa	amino acid
acri	acridinium
At	*Arabidopsis thaliana*
ATP	adenosine triphosphate
AvrPto	avirulence protein of Pseudomonas syringae pv. tomato
BAK1	BRI1-interacting kinase 1, see SERK
BES1	BRI1 EMS suppressor 1
BIR	BAK1-interacting kinase
BKK1	BAK1-like 1
BL	brassinolide
BLAST	basic local alignment search tool
bp	base-pair
BR	brassinosteroid
BRI1	Brassinosteroid insensitive 1
BSA	Bovine serum albumin
Ca2+	Calcium ion
cDNA	complementary DNA
Cf	*Cladosporium fulvum*
Cl-	chlore ion
CLANS	cluster analysis of sequences
CLV1	CLAVATA 1 (RLK)
CLV2	CLAVATA 2 (RLP)
CLV3	CLAVATA 3, peptide that belongs of the CLE family with the amino acid sequence RTVPSGPDPLHHH
coIP	co-immunoprecipitation
Col-0	Columbia-0, an *A. thaliana* accession
CORE	Cold-shock protein receptor
CPK	Ca2+-dependent protein kinase
CRN	CORYNE
csp22	peptide of the bacterial cold shock protein with the amino acid sequence AVGTVKWFNAEKGFGFITPDDG
C-tail	cytoplasmic tail
ctrl	control
CuRe1	Cuscuta receptor 1
D	aspartic acid
DAMP	damage-associated molecular pattern

DMSO	dimethylsulfoxide
dNTPs	Deoxyribonucleotide triphosphate
DTT	dithiothreitol
e.g.	example given
EFR	EF-Tu receptor
EF-Tu	Elongation factor Tu
EIX2	Ethylene-induced xylanase receptor 2
elf18	peptide of EF-Tu with the amino acid sequence ac-SKEKFERTKPHVNVGTIG
eppi	1.5 ml eppendorf tube
ER	endoplasmic reticulum
ETI	effector-triggered immunity
F	phenylalanine
flg22	peptide of bacterial flagellin with the amino acid sequence QRLSTGSRINSAKDDAAGLQIA
flgII-28	peptide of bacterial flagellin with the amino acid sequence ESTNILQRMRELAVQSRNDSNSATDREA
FLS2	Flagellin-sensitive 2
FLS3	Flagellin-sensitive 3
FRK1	FLG22-induced receptor-like kinase 1
fw	forward
G	gylcine
g	gram
g	gravitational acceleration
GFP	green fluorescent protein
h	hour
H+	hydrogen ion
HR	hypersensitive response
I	isoleucine
ijm	innerjuxtamembrane
IP	immunoprecipitation
JA	jasmonic acid
K+	potassium ion
kDa	kilodalton
l	liter
L	leucine
LB	lysogeny broth
L*er*-0	Landsberg-0, an *A. thaliana* accession
LRR	leucine-rich repeat
Luc	luciferase
LysM	lysine motif
m	milli

M	molar
MAPK	mitogen-activated protein kinase
min	minute
mRNA	RNA messenger
n	nano
N	asparagine
Na2+	sodium ion
NADPH	nicotinamide adenine dinucleotide phosphate
Nb	*Nicotiana benthamiana*
NB-LRR	nucleotide binding-leucine rich repeat
NCBI	National Center for Biotechnology Information
NIK	NSP-interacting receptor kinase
nlp20	peptide of the necrosis and ethylene-inducing peptide 1-like proteins, with sequence AIMYSWYFPLDSPVTGLGHR
nt	nucleotide
ojm	outerjuxtamembrane
Os	*Oryza sativa*
ox. burst	oxidative burst
P	proline
PAMP	pathogen-associated molecular pattern
PCR	polymerase chain reaction
PDB	protein data base
Pen	Extract of *Penicillium chrysogenum*
PEPR1	Pep1 receptor 1
PM	plasma membrane
PRR	pattern recognition receptor
PTI	PAMP-triggered immunity
R	arginine
rev	reverse
R-gene	resistance gene
RLCK	receptor-like cytoplasmic kinase
RLK	receptor-like kinase
RLP	receptor-like protein
RLU	relative light units
RNA	ribonucleic acid
ROS	reactive oxygen species
rpm	rotation per minute
s	second
S	serine
SA	salicylic acid
SAM	shoot apical meristem
SAR	systemic acquired resistance
SERK1	Somatic embryogenesis receptor kinase 1

SERK2	Somatic embryogenesis receptor kinase 2
SERK3	Somatic embryogenesis receptor kinase 3, also known as BAK1
SERK4	Somatic embryogenesis receptor kinase 4, also known as BKK1
SERK5	Somatic embryogenesis receptor kinase 5
S-gene	susceptibility gene
Sl	*Solanum lycopersicum*
SOBIR1	Suppressor of bir1
ssRNA	single-stranded RNA
SYSRE	systemin receptor
T	threonine
TF	transcription factor
TIR	toll-Interleukin 1
TLR	Toll-like receptor
Tm	melting temperature
tm	transmembrane domain
TMD	transmembrane domain
tmk	transmembrane and kinase domains
µ, u	micro
UniProt	Universal Protein resource
V	valine
Ve1	Verticillium1
Ve2	Verticillium2
W	tryptophane
w/v	weight per volume
WT	wild type
x	any residue
Y	tyrosine
Y2H	yeast-two-hybrid

Annex

Annex Table 1 - List of primers

Name	Sequence (3' -> 5')
EFR_topo_REV	CATAGTATGCATGTCCGTATTTAACATC
EFR_topo_FW	CACCATGAAGCTGTCCTTTTCACTTGTTTTC
M13_FW	GTAAAACGACGGCCAG
M13_REV	CAGGAAACAGCTATGAC
EIX2 topo FW	CACCATGGGCAAAAGAACTAATCCAAG
EIX2 REV	GTTCCTTAGCTTTCCCTTCAGTC
EFR-ijmEIX2 FW	TTGTGGCTTCTCTGTGTTGGTTCCGTTCGTGGAGGAATGCCTACTTCAC
EFR-ijmEIX2 REV	GTGAAGTAGGCATTCCTCCACGAACGGAACCAACACAGAGAAGCCACAA
EFR-tmEIX2 FW	AGCCTCTGTCAGTTAGAAAGAAATTTTATGTATCAATGGTGCTAGG
EFR-tmEIX2 REV	CCTAGCACCATTGATACATAAAATTTCTTTCTAACTGACAGAGGCT
EFRΔkin rev	TGCACTATGAAGCTCTTCATAACTTACCTT
EFRijmRLP23_fw	GTGGCTTCTCTGTGTTGGTTCAAACCGGAGTGGCTTGTCAAG
EFRijmRLP23_rev	CTTGACAAGCCACTCCGGTTTGAACCAACACAGAGAAGCCAC
EFRtmRLP23_fw	GCCTCTGTCAGTTAGAAAGAAAGTGTTGAACGGGAGAGCAGTGGC
EFRtmRLP23_rev	GCCACTGCTCTCCCGTTCAACACTTTCTTTCTAACTGACAGAGGC
PEPR1 topo fw	CACCATGAAGAATCTTGGGGGGTTGTTC
RLP23 rev	ACGCTTTCTGCGTTTATTCAGACC
PEPR1tmEIX2 fw	GAGTGGCCTTAGCACCTGGCAATTTTATGTATCAATGGTGCTAGG
PEPR1tmEIX2 rev	CCTAGCACCATTGATACATAAAATTGCCAGGTGCTAAGGCCACTC
PEPR1ijmEIX2 fw	GCTCTTGTTTTCATTTGCCTACGTTCGTGGAGGAATGCCTACTTCAC
PEPR1ijmEIX2 rev	GTGAAGTAGGCATTCCTCCACGAACGTAGGCAAATGAAAACAAGAGC
PEPR1tmRLP23 fw	GAGTGGCCTTAGCACCTGGCAAGTGTTGAACGGGAGAGCAGTGGC
PEPR1tmRLP23 rev	GCCACTGCTCTCCCGTTCAACACTTGCCAGGTGCTAAGGCCACTC
PEPR1ijmRLP23 fw	GCTCTTGTTTTCATTTGCCTAAAACCGGAGTGGCTTGTCAAG
PEPR1ijmRLP23 rev	CTTGACAAGCCACTCCGGTTTTAGGCAAATGAAAACAAGAGC
CORE1tmRLP23 fw	GGAAATCAGGTTTTCCCTTGAAAAAAGTGTTGAACGGGAGAGCAGTGGC
CORE1tmRLP23 rev	GCCACTGCTCTCCCGTTCAACACTTTTTTCAAGGGAAAACCTGATTTCC
CORE1tmEIX2 fw	GGAAATCAGGTTTTCCCTTGAAAAAATTTTATGTATCAATGGTGCTAGG
CORE1tmEIX2 rev	CCTAGCACCATTGATACATAAAATTTTTTCAAGGGAAAACCTGATTTCC
CORE1ijmRLP23 fw	GATAGTTTGTTTTCTTGGCATAAAACCGGAGTGGCTTGTCAAG
CORE1ijmRLP23 rev	CTTGACAAGCCACTCCGGTTTTATGCCAAGAAAACAAACTATC
CORE1ijmEIX2 fw	GATAGTTTGTTTTCTTGGCATACGTTCGTGGAGGAATGCCTACTTCAC
CORE1ijmEIX2 rev	GTGAAGTAGGCATTCCTCCACGAACGTATGCCAAGAAAACAAACTATC
SYSRE1tmEIX2 fw	CACAAGTAAAATGGAAGTTTTATGTATCAATGGTGCTAGG
SYSRE1tmEIX2 rev	CCTAGCACCATTGATACATAAAACTTCCATTTTACTTGTG
SYSRE1tmRLP23 fw	CACAAGTAAAATGGAAGGTGTTGAACGGGAGAGCAGTGGC
SYSRE1tmRLP23 rev	GCCACTGCTCTCCCGTTCAACACCTTCCATTTTACTTGTG
SYSRE1ijmEIX2 fw	GCAATGTACTTACTAGTGACTCGTTCGTGGAGGAATGCCTACTTCAC
SYSRE1ijmEIX2 rev	GTGAAGTAGGCATTCCTCCACGAACGAGTCACTAGTAAGTACATTGC
SYSRE1ijmRLP23 fw	GCAATGTACTTACTAGTGACTAAACCGGAGTGGCTTGTCAAG
SYSRE1ijmRLP23 rev	CTTGACAAGCCACTCCGGTTTAGTCACTAGTAAGTACATTGC

EFRΔkin-tmRLP23 fw	CAATAGCACAAGTTATTGCTTCATACATGAAGAGGAAAAAGAAAAAC
EFRΔkin-tmRLP23 rev	GTTTTTCTTTTTCCTCTTCATGTATGAAGCAATAACTTGTGCTATTG
BRI1ijmEIX2 fw	TTTGGGCTGATCCTTGTTGGTCGTTCGTGGAGGAATGCCTACTTCAC
BRI1ijmEIX2 rev	GTGAAGTAGGCATTCCTCCACGAACGACCAACAAGGATCAGCCCAAA
BRI1ijmRLP23 fw	TTTGGGCTGATCCTTGTTGGTAAACCGGAGTGGCTTGTCAAG
BRI1ijmRLP23 rev	CTTGACAAGCCACTCCGGTTTACCAACAAGGATCAGCCCAAA
BRI1Δkin rev	CTTCCAATTGGTGTTGTTAGC
BRI1tmEIX2 fw	GAGATCTCATGGAAGGAGACCATTTTATGTATCAATGGTGCTAGG
BRI1tmEIX2 rev	CCTAGCACCATTGATACATAAAATGGTCTCCTTCCATGAGATCTC
BRI1tmRLP23 fw	GAGATCTCATGGAAGGAGACCAGTGTTGAACGGGAGAGCAGTGGC
BRI1tmRLP23 rev	GCCACTGCTCTCCCGTTCAACACTGGTCTCCTTCCATGAGATCTC
CLV1Δkin rev	TTCTTTAAGACACTCGAGAAC
CLV1 fw topo	CACCATGGCGATGAGACTTTTGAAGAC
CLV1ijmEIX2 fw	GATCCTAATCAGTGTAGCGATTCGTTCGTGGAGGAATGCCTACTTCAC
CLV1ijmEIX2 rev	GTGAAGTAGGCATTCCTCCACGAACGAATCGCTACACTGATTAGGATC
CLV1ijmRLP23 fw	GATCCTAATCAGTGTAGCGATTAAACCGGAGTGGCTTGTCAAG
CLV1ijmRLP23 rev	CTTGACAAGCCACTCCGGTTTAATCGCTACACTGATTAGGATC
CLV1tmEIX2 fw	CACGGCGTTGTTCTCACCGTCAAGGTTTTATGTATCAATGGTGCTAGG
CLV1tmEIX2 rev	CCTAGCACCATTGATACATAAAACCTTGACGGTGAGAACAACGCCGTG
CLV1tmRLP23 fw	CACGGCGTTGTTCTCACCGTCAAGGGTGTTGAACGGGAGAGCAGTGGC
CLV1tmRLP23 rev	GCCACTGCTCTCCCGTTCAACACCCTTGACGGTGAGAACAACGCCGTG
CLV2 fw topo	CACCATGATAAAGATTGCAGATTTCAC
CLV2tmRLP23 fw	CAAAACGAATTGGTGGAAGGACCGGTGTTGAACGGGAGAGCAGTGGC
CLV2tmRLP23 rev	GCCACTGCTCTCCCGTTCAACACCGGTCCTTCCACCAATTCGTTTTG
COREΔkin rev	AGAAAATCTATCAGTTTCCC
CRN fw topo	CACCATGAAGCAAAGAAGAAGAAG
PEPR1Δkin rev	ATTTAGATTGTCAGTTGCTGC
CLV2 rev	TTAAGCTTTGGTCTGAAG
SOBIR rev	GTGCTTGATCTGGGACAAC
CLV2 rev no stop	AGCTTTGGTCTGAAGAATA
CRN rev	AAAGCTGTGCAGTTGTGTAAG
RLP23 topo fw	CACCATGTCAAAGGCGCTTTTGCATTTGC
RLP23_tmSOBIR_fw	GAAGAAGAAGAAGAAGAAGTAGCGGCATGGATCTTAG
RLP23_tmSOBIR_rev	CTAAGATCCATGCCGCTACTTCTTCTTCTTCTTC
EIX2_tmSOBIR fw	GTTCTCATCTCTGGAGGTAGCGGCATGGATCTTAG
EIX2_tmSOBIR rev	CTAAGATCCATGCCGCTACCTCCAGAGATGAGAAC
EFR_tmSOBIR fw	CTGTCAGTTAGAAAGAAAGTAGCGGCATGGATCTTAG
EFR_tmSOBIR rev	CTAAGATCCATGCCGCTACTTTCTTTCTAACTGACAG
tmSOBIR_RLP23_fw	GTCTTCTCGGTGTTGTTCAAACCGGAGTGGCTTGTC
tmSOBIR_RLP23_rev	GACAAGCCACTCCGGTTTGAACAACACCGAGAAGAC
tmSOBIR_EIX2_fw	GTCTTCTCGGTGTTGTTCAACCGTTCGTGGAGGAATG
tmSOBIR_EIX2_rev	CATTCCTCCACGAACGGTTGAACAACACCGAGAAGAC
tmSOBIR_EFR_fw	GTCTTCTCGGTGTTGTTCATGAAGAGGAAAAAGAAAAAC
tmSOBIR_EFR_rev	GTTTTTCTTTTTCCTCTTCATGAACAACACCGAGAAGAC
RLP23tmEFR_fw	GAAGAAGAAGAAGAAGAAGTTGTCAGTGGTATTTG

RLP23tmEFR_rev	CAAATACCACTGACAACTTCTTCTTCTTCTTC
tmEFR_RLP23_fw	GGCTTCTCTGTGTTGGTTCAAACCGGAGTGGCTTGTC
tmEFR_RLP23_rev	GACAAGCCACTCCGGTTTGAACCAACACAGAGAAGCC

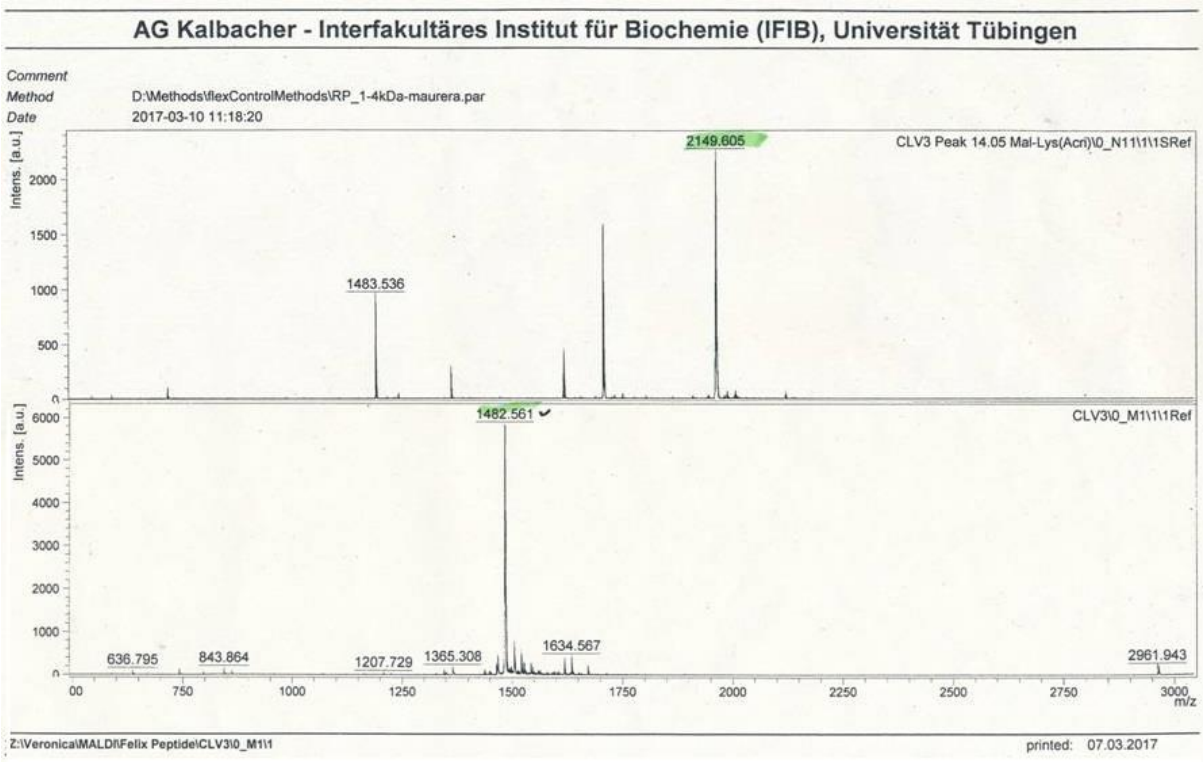

Annex Figure 1 - Synthesis of CLV3 and acri-CLV3

Quality control via HPLC shows that acridinium-labeled CLV3 (above) is heavier than unlabeled CLV3 (below).

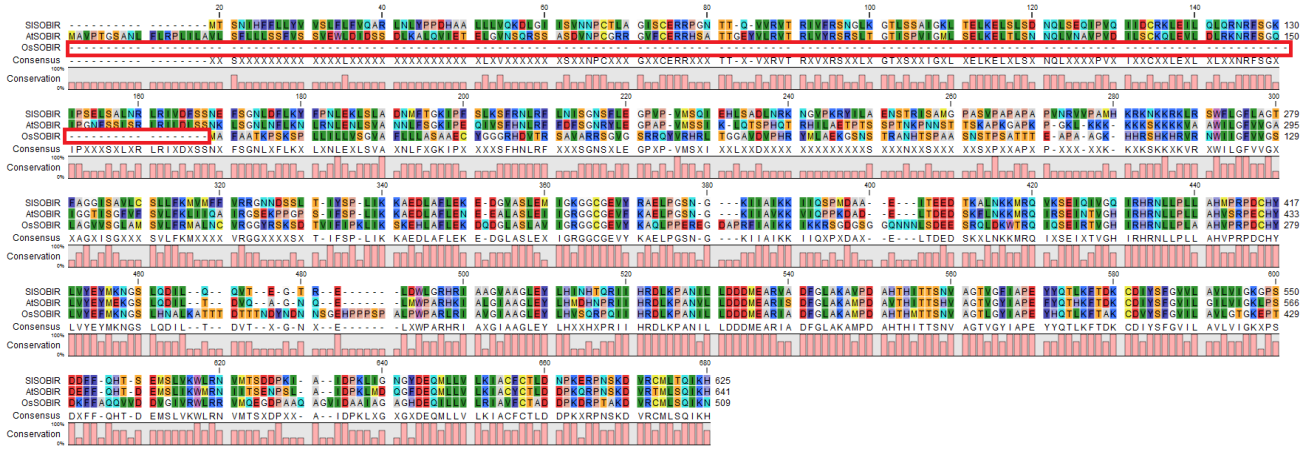

Annex Figure 2 - Alignment of At-, Sl- and OsSOBIR1

Alignment of AtSOBIR1, SlSOBIR1 and OsSOBIR1 reveals that OsSOBIR1 lost at least 3 complete LRRs. The same holds true for SOBIR1s from other grass species and thus these proteins did not show up in our CLANS analysis.

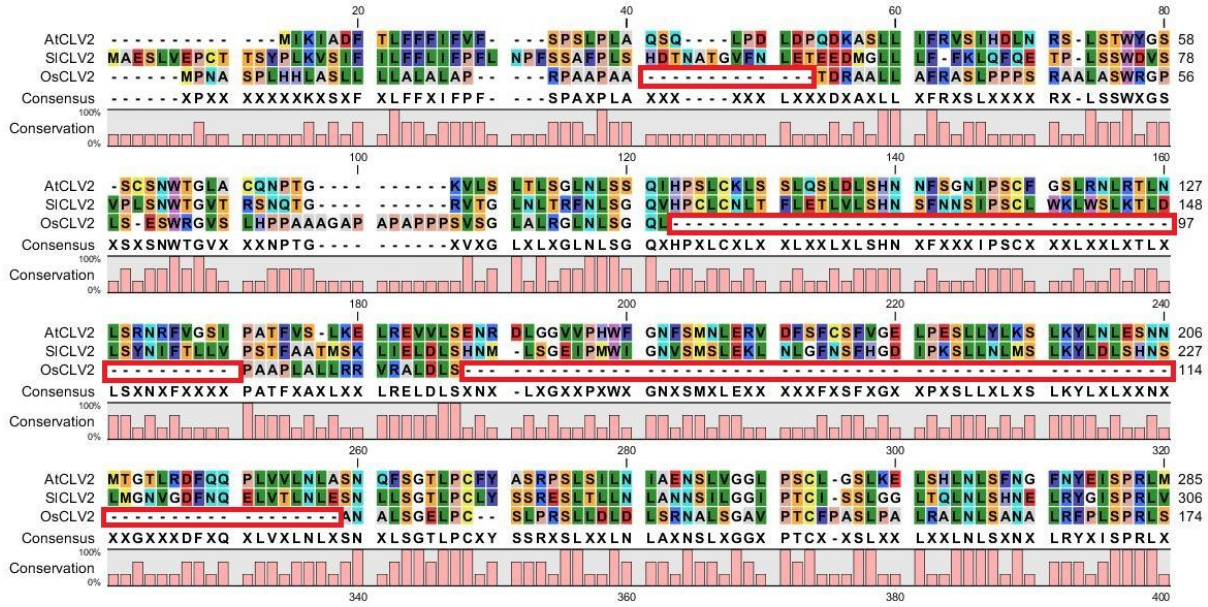

Annex Figure 3 - Alignment of the upper LRRs of At-, Sl-, and OsCLV2

Alignment of the first few LRRs of AtCLV2, SlCLV2 and OsCLV2 reveals that OsCLV2 lost at least 6 complete LRRs. The same holds true for CLV2s from other grass species and thus these proteins did not show up in our CLANS analysis.

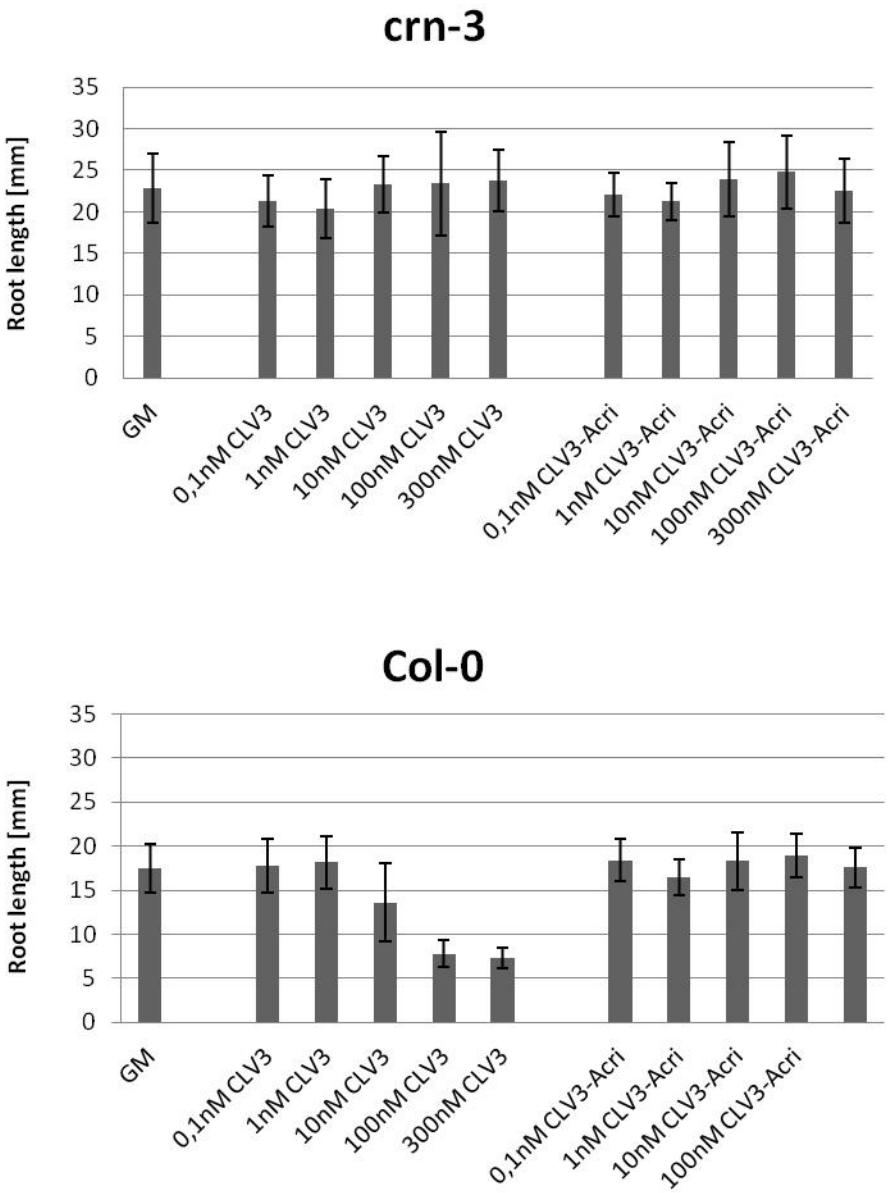

Annex Figure 4 – Root growth assay on *A. thaliana* 10 days old seedlings

Exposition to increasing concentrations of CLV3 reduce the root growth in Col-0 but not in the crn-3 mutant. In contrast, acri-CLV3 does not affect root growth in Col-0 nor crn-3, showing that this peptide cannot be sensed by CLV1/CLV2. Unpublished data from P. Schulz & R. Simon, Uni. Düsseldorf.

Curriculum vitae

Born in Lausanne (Switzerland) on the 23rd January 1989

Education

04.2014 – 12.2017	**PhD in Biochemistry** Uni. Tübingen, Germany
09.2010 – 02.2012	**M.Sc. Evolutionary Biology** Uni. Lausanne, Switzerland
09.2007 – 06.2010	**B.Sc. Biology** Uni. Lausanne, Switzerland & Uni. Aveiro, Portugal

Professonial experience

04.2014 – 12.2017	**Scientific collaborator** ZMBP, Uni. Tübingen, Germany
11.2016 – 05.2017	**Guest researcher** Max-Planck Institute, Tübingen, Germany
08.2013 – 02.2014	**Research assistant** Agroscope, Nyon, Switzerland
02.2013 – 07.2013	**Research assistant** Catholic Uni. Porto, Portugal
03.2012 – 12.2012	**Research assistant** Agroscope, Nyon, Switzerland
07.2010 – 08.2010	**Research assistant** Uni. Lausanne, Switzerland